

Chapter 8

Four-Wheel Autonomous Ground Vehicles



Abstract In the recent years there has been significant effort in the design of intelligent autonomous vehicles capable of operating in variable conditions. The precise modeling of the vehicles dynamics improves the efficiency of vehicles controllers in adverse cases, for example in high velocity, when performing abrupt maneuvers, under mass and loads changes or when moving on rough terrain. Using model-based control approaches it is possible to design a nonlinear controller that maintains the vehicle's motion characteristics according to given specifications. When the vehicle's dynamics is subject to modeling uncertainties or when there are unknown forces and torques exerted on the vehicle it is important to be in position to estimate in real-time disturbances and unknown dynamics so as to compensate for them. In this direction, estimation for the unknown dynamics of the vehicle and state estimation-based control schemes have been developed. Feedback control of robotic ground vehicles can be primarily based on (i) global linearization approaches, (ii) approximate linearization approaches and (iii) Lyapunov methods. The control is applied to (i) 4-wheel vehicles models, and (ii) articulated vehicles. At a second stage, to implement control under model uncertainty, estimation methods can be employed capable of identifying in real-time the vehicles' dynamics. The outcome of the estimation procedure can be used by the aforementioned feedback controllers thus implementing indirect adaptive control schemes. Finally to implement control of the ground vehicles through the measurement of a small number of its state variables, elaborated nonlinear filtering approaches are developed. The topics treated by the chapter are: (a) Nonlinear optimal control of four-wheel autonomous ground vehicles (b) Nonlinear optimal control for an autonomous truck and trailer system (c) Nonlinear optimal control of four-wheel steering autonomous vehicles and (d) Flatness-based control of autonomous four-wheel ground vehicles.

8.1 Chapter Overview

The topics treated by the chapter are: (a) Nonlinear optimal control of four-wheel autonomous ground vehicles (b) Nonlinear optimal control for an autonomous truck and trailer system (c) Nonlinear optimal control of four-wheel steering autonomous

vehicles and (d) Flatness-based control of autonomous four-wheel ground vehicles.

With reference to (a) the chapter proposes a new nonlinear optimal control method for solving the problem of path following for four-wheel non-holonomic Automatic Grounded Vehicles (AGVs). The dynamic model of the four-wheel AGVs undergoes first approximate linearization around a temporary operating point that is updated at each iteration of the control algorithm. The linearization takes place through first-order Taylor series expansion and through the computation of the Jacobian matrices of the state-space description of the vehicle. For the approximately linearized model of the four-wheel vehicle an H-infinity feedback controller is computed. Actually, the H-infinity controller stands for the solution of the optimal control problem for the vehicle's kinematics under model uncertainty and external perturbations. For the computation of the feedback gain of the H-infinity controller an algebraic Riccati equation is solved at each time-step of the control method.

With reference to (b) a nonlinear optimal control method is developed, this time for an autonomous truck and trailer system. The dynamic model of the autonomous vehicle undergoes linearization through Taylor series expansion. Adhering to the previously analyzed procedure, the linearization is computed at a temporary equilibrium that is defined at each time instant by the present value of the state vector and the last value of the control inputs vector. The linearization is based on the computation of Jacobian matrices. The modelling error due to approximate linearization is considered to be a perturbation that is compensated by the robustness of the control scheme. For the approximately linearized model of the truck and trailer autonomous vehicle an H-infinity feedback controller is designed. This requires again the solution of an algebraic Riccati equation at each iteration of the control algorithm.

With reference to (c) the chapter introduces a nonlinear optimal control method for feedback control of autonomous four-wheel steering (4WS) robotic vehicles. Comparing to two-wheel steering vehicles, four-wheel steering vehicles can exhibit improved maneuverability. The joint kinematic and dynamic model of such vehicles undergoes approximate linearization around a temporary operating point (equilibrium) which is updated at each iteration of the control method. This operating point comprises the present value of the vehicle's state vector and the last value of the control inputs vector exerted on it. As in previous applications of nonlinear optimal control, the linearization is performed using Taylor series expansion and the computation of the Jacobian matrices of the system's state-space description. For the approximately linearized model of the 4WS vehicle an optimal (H-infinity) feedback controller is designed. The controller's feedback gain requires the solution of an algebraic Riccati equation again at each time step of the control method. The concept of the control scheme is that at each time instant the state vector of the 4WS vehicle is made to converge to the temporary equilibrium, while the equilibrium is also shifted towards the reference setpoints. Thus asymptotically, the state vector of the 4WS vehicle reaches the targeted reference paths. For all cases (a) to (c) asymptotic stability of the control methods is proven through Lyapunov analysis.

With reference to (d) controller design for autonomous 4-wheel ground vehicles is performed with differential flatness theory. Using a 3-DOF nonlinear model of the vehicle's dynamics and through the application of differential flatness theory an

equivalent model in linear canonical (Brunovsky) form is obtained. For the latter model a state feedback controller is developed that enables accurate tracking of velocity setpoints. Moreover, it is shown that with the use of Kalman Filtering it is possible to dynamically estimate the disturbances due to unknown forces and torques exerted on the vehicle. The processing of velocity measurements (provided by a small number of on-board sensors) through a Kalman Filter which has been redesigned in the form of a disturbance observer results in accurate identification of external disturbances affecting the vehicle's dynamic model. By including in the vehicle's controller an additional term that compensates for the estimated disturbance forces, the desirable characteristics of the vehicle's motion are achieved. The global asymptotic stability for the AGV control scheme is assured.

8.2 Nonlinear Optimal Control of Four-Wheel Autonomous Ground Vehicles

8.2.1 Outline

Intelligent four-wheel autonomous vehicles are characterized by the capability to track precisely reference paths and to perform in a dexterous and accurate manner all designated maneuvers [40, 68–70, 392, 523]. The present section proposes a new nonlinear optimal (H-infinity) control method for the kinematic-dynamic model of a four-wheel autonomous vehicle. The considered model describes precisely the motion of four-wheel autonomous vehicles which receive as control inputs the engine's torque and the heading angle provided by the steering wheel, while also taking into account longitudinal and lateral forces exerted on the vehicle's front and rear wheels, as well as torques that result in a change of the vehicle's orientation [26, 72, 228, 622]. To accomplish precision in path following by autonomous vehicles several control approaches have been developed so far. One can primarily distinguish global linearization-based control schemes, requiring a change of state variables for the vehicle's model [317, 319, 332, 333, 419, 571]. Moreover, optimization-based control approaches have been a topic of significant research in autonomous four-wheel vehicles technology [66, 123, 284, 616, 641].

The present section's approach to the solution of the path tracking control problem for autonomous four-wheel land vehicles is based on a nonlinear optimal control concept and on the H-infinity control theory. To implement the considered control method the joint kinematic and dynamic model of the four-wheel vehicle undergoes first approximate linearization around a temporary operating point (equilibrium) which is updated at each iteration of the control method. The temporary equilibrium is defined by the present value of the vehicle's state vector and by the last value of the control inputs vector that was exerted on it [461, 466]. The linearization relies on first-order Taylor series expansion and on the computation of the Jacobian matrices of the vehicle's state-space description [33, 431, 463]. The modelling error which is due to the approximate linearization is considered to be a disturbance term

which is finally compensated by the robustness of the control algorithm. For the approximately linearized model of the four-wheel vehicle an H-infinity (optimal) feedback controller is designed.

The H-infinity feedback controller is the solution to the optimal control problem for the four-wheel vehicle, under model uncertainty and external perturbations [450, 457, 460]. It actually represents the solution to a min-max differential game in which the controller tries to minimize a cost function comprising a quadratic term of the state vector's tracking error, while at the same time the disturbances and model uncertainty terms try to maximize this cost function. The computation of the controller's feedback gain requires the solution of an algebraic Riccati equation taking place at each time step of the control method. The stability properties of the control scheme are analyzed with the use of the Lyapunov method. First, it is proven that the control loop satisfies the H-infinity tracking performance criterion which signifies elevated robustness against model uncertainty and external perturbations [305, 564]. Moreover, under moderate conditions it is proven that the control loop is also globally asymptotically stable. Finally, to implement state estimation-based control through the feedback of a small number of sensor measurements the H-infinity Kalman Filter is proposed as a robust state estimator [169, 511].

8.2.2 Dynamic and Kinematic Model of the Vehicle

8.2.2.1 Definition of Parameters in 4-Wheel Vehicle Dynamic Model

The dynamic model of the four-wheel vehicle has been analyzed in [332, 333, 457, 616]. With reference to Figs. 8.1 and 8.2 (where the lateral forces applied on the wheels are considered to define the vehicle's motion) one has the following parameters: β is the angle between the velocity and the vehicle's transversal angle, V is the velocity vector of the vehicle, ψ is the yaw angle (rotation round the z axis), f_x is the aggregate force along the x axis, f_y is the aggregate force along the y axis, T_z is the aggregate torque round the z axis and δ is the steering angle of the front wheels.

The motion of the vehicle is described by the following set of equations:

1. Longitudinal motion

$$-mV(\dot{\beta} + \dot{\psi})\sin(\beta) + m\dot{V}\cos(\beta) = f_x \quad (8.1)$$

2. Lateral motion

$$mV(\dot{\beta} + \dot{\psi})\cos(\beta) + m\dot{V}\sin(\beta) = f_y \quad (8.2)$$

3. yaw turn

$$I\ddot{\psi} = T_z \quad (8.3)$$

The above described dynamics of the four-wheel vehicle can be also written in matrix form

$$\begin{pmatrix} -\sin(\beta) & \cos(\beta) & 0 \\ \cos(\beta) & \sin(\beta) & 0 \\ 0 & 0 & 1 \end{pmatrix} \begin{pmatrix} mV(\dot{\beta} + \dot{\psi}) \\ m\dot{V} \\ I\dot{\psi} \end{pmatrix} = \begin{pmatrix} f_x \\ f_y \\ T_z \end{pmatrix} \tag{8.4}$$

Finally a matrix relation is provided about the transformation of forces on a tire into forces and torques along the vehicle’s axes:

$$\begin{pmatrix} f_x \\ f_y \\ T_z \end{pmatrix} = \begin{pmatrix} -\sin(\delta) & 0 \\ \cos(\delta) & 1 \\ L_1\cos(\delta) & -L_2 \end{pmatrix} \begin{pmatrix} F_f \\ F_r \end{pmatrix} \tag{8.5}$$

8.2.2.2 Vehicle Dynamic Model with Longitudinal and Lateral Forces

The previous model of Fig. 8.1 is reexamined considering that $\dot{\beta} = 0$ and that ψ is the yaw angle formed between the vehicle’s longitudinal axis and the horizontal axis of an inertial reference frame. Moreover, it is assumed that apart from the lateral forces there are traction torques transferred from the engine to the front wheels as well as braking torques on the rear and front wheels. Due to the distance between the wheels axes and the vehicle’s center of gravity, torques are also generated along the vehicle’s z -axis. With reference to Fig. 8.1 the model of the vehicle’s dynamics is formulated as follows [332, 333, 457]:

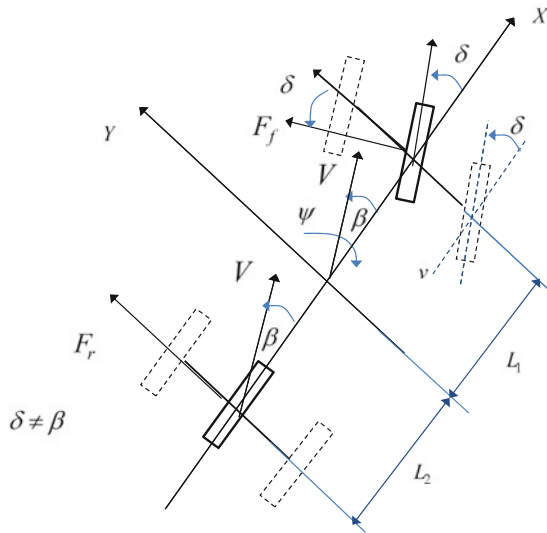
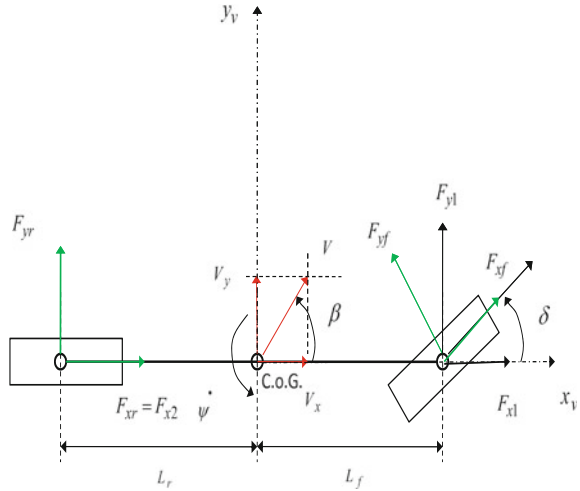


Fig. 8.1 Nonlinear 4-wheeled vehicle model

Fig. 8.2 Vehicle model with longitudinal and lateral forces



$$\begin{aligned}
 m\alpha_x &= m(\dot{V}_x - \dot{\psi} \dot{V}_y) = F_{x1} + F_{x2} \\
 m\alpha_y &= m(\dot{V}_y + \dot{\psi} \dot{V}_x) = F_{y1} + F_{y2} \\
 I_z \ddot{\psi} &= T_{z1} + T_{z2}
 \end{aligned} \tag{8.6}$$

where a_x and a_y are accelerations along the axes of the inertial reference frame and \dot{V}_x, \dot{V}_y in a reference frame that rotates with the yaw rate $\dot{\psi}$. The forces $F_{x_i}, i = 1, 2$ on the vehicle's longitudinal axis and $F_{y_i}, i = 1, 2$ on the vehicle's transversal axis are computed from the horizontal and vertical forces applied on the vehicle's wheels as follows:

$$\begin{aligned}
 F_{x1} &= F_{x_f} \cos(\delta) - F_{y_f} \sin(\delta) \\
 F_{x2} &= F_{x_r} \\
 F_{y1} &= F_{y_f} \sin(\delta) + F_{x_f} \cos(\delta) \\
 F_{y2} &= F_{y_r} \\
 T_{z1} &= L_f (F_{y_f} \cos(\delta) + F_{x_f} \sin(\delta)) \\
 T_{z2} &= -L_r F_{y_r}
 \end{aligned} \tag{8.7}$$

About the longitudinal and the lateral forces applied to the vehicle one has:

1. Longitudinal force on the front wheel

$$F_{x_f} = \left(\frac{1}{R} \right) (I_r \dot{\omega}_f + T_m - T_{b_f}) \tag{8.8}$$

2. Longitudinal force on the rear wheel

$$F_{x_r} = - \left(\frac{1}{R} \right) (T_{b_r} + I_r \dot{\omega}_r) \quad (8.9)$$

3. Lateral force on the front wheel (taking that the angle β between the vehicle's longitudinal axis and the wheel's velocity vector is approximated by $\beta = \frac{V_y + \dot{\psi} L_f}{V_x}$)

$$F_{y_f} = C_f \left(\delta - \frac{V_y + \dot{\psi} L_f}{V_x} \right) \quad (8.10)$$

4. Lateral force on the rear wheel (taking that for the rear wheel the steering angle is $\delta = 0$ and that the angle β between the vehicle's longitudinal axis and the wheel's velocity vector is approximated by $\beta = \frac{V_y - \dot{\psi} L_r}{V_x}$).

$$F_{y_r} = -C_r \frac{V_y - \dot{\psi} L_r}{V_x} \quad (8.11)$$

where C_f and C_r are the cornering stiffness coefficients for the front and rear tires respectively. Nominal values of these cornering stiffness coefficients can be estimated through identification procedures. The substitution of Eqs. (8.8)–(8.11) into (8.6) results into

$$\begin{aligned} m\dot{V}_x &= m\dot{\psi} V_y - \frac{I_r}{R}(\dot{\omega}_r + \dot{\omega}_f) + \frac{1}{R}(T_m - T_{b_f} - T_{b_r}) + C_f \left(\frac{V_y + \dot{\psi} L_f}{V_x} \right) \delta - C_f \delta^2 \\ m\dot{V}_y &= -m\dot{\psi} V_x - C_f \left(\frac{V_y + \dot{\psi} L_f}{V_x} \right) - C_r \left(\frac{V_y - \dot{\psi} L_r}{V_x} \right) + \left(\frac{1}{R} \right) (T_m - T_{b_f}) \delta + \left(C_f - \frac{I_r}{R} \dot{\omega}_f \right) \delta \\ I_z \ddot{\psi} &= -L_f C_f \left(\frac{V_y + \dot{\psi} L_f}{V_x} \right) + L_r C_r \left(\frac{V_y - \dot{\psi} L_r}{V_x} \right) + \frac{L_f}{R} (T_m - T_{b_f}) \delta + L_f \left(T_m - \frac{I_r}{R} \right) \delta \end{aligned} \quad (8.12)$$

The motion of the vehicle along its longitudinal axis is controlled by the traction or braking wheel torque $T_\omega = T_m - T_b$ with $T_b = T_{b_f} + T_{b_r}$ and the lateral movement via the steering angle δ . The two control inputs of the four wheel vehicle model are

$$\begin{aligned} u_1 &= T_\omega \\ u_2 &= \delta \end{aligned} \quad (8.13)$$

A first form of the vehicle's dynamic model is

$$\dot{x} = f(x, t) + g(x, t)u + g_1 u_1 u_2 + g_2 u_2^2 \quad (8.14)$$

where

$$f(x, t) = \begin{pmatrix} \frac{I_r}{mR}(\dot{\omega}_r + \dot{\omega}_f) \\ \dot{\psi}V_x + \frac{1}{m} \left(-C_f \frac{(V_y + L_f \dot{\psi})}{V_x} - C_r \frac{(V_y - L_f \dot{\psi})}{V_x} \right) \\ \frac{1}{I_z} \left(-L_f C_f \frac{(V_y + L_f \dot{\psi})}{V_x} + L_r C_r \frac{(V_y - L_f \dot{\psi})}{V_x} \right) \end{pmatrix} \quad (8.15)$$

$$g(x, t) = \begin{pmatrix} \frac{1}{mR} \frac{C_f}{m} \left(\frac{V_y + L_f \dot{\psi}}{V_x} \right) \\ 0 \quad \left(\frac{C_f R - L_f \dot{\omega}_f}{mR} \right) \\ 0 \quad \frac{(L_f C_f R - L_f I_r \dot{\omega}_f)}{I_z R} \end{pmatrix} \quad (8.16)$$

$$g_1 = \begin{pmatrix} 0 \\ \frac{1}{mR} \\ \frac{L_f}{I_z R} \end{pmatrix} \quad g_2 = \begin{pmatrix} -\frac{C_f}{m} \\ 0 \\ 0 \end{pmatrix} \quad x = \begin{pmatrix} V_x \\ V_y \\ \dot{\psi} \end{pmatrix} \quad u = \begin{pmatrix} u_1 \\ u_2 \end{pmatrix} \quad (8.17)$$

The previously analyzed nonlinear model of the vehicle's dynamics can be simplified if the control inputs $u_1 u_2$ and u_2^2 are not taken into account. In the latter case the dynamics of the vehicle takes the form

$$\dot{x} = f(x, t) + g(x, t)u \quad (8.18)$$

8.2.2.3 Joint Dynamic and Kinematic Model of the Vehicle

Using that the velocity variables of the vehicle V_x and V_y are expressed in a body-fixed orthogonal coordinates frame, and using that the heading angle of the vehicle is ψ one can express next the motion of the vehicle in an inertial reference frame as follows:

$$\begin{aligned} V_X &= \cos(\psi)V_x - \sin(\psi)V_y \Rightarrow \dot{X} = \cos(\psi)V_x - \sin(\psi)V_y \\ V_Y &= \sin(\psi)V_x + \cos(\psi)V_y \Rightarrow \dot{Y} = \sin(\psi)V_x + \cos(\psi)V_y \end{aligned} \quad (8.19)$$

Using the above, the state-space description of the four-wheel vehicle becomes

$$\begin{pmatrix} \dot{X} \\ \dot{Y} \\ \dot{V}_X \\ \dot{V}_Y \\ \dot{\psi} \\ \ddot{\psi} \end{pmatrix} \begin{pmatrix} \cos(\psi)V_x - \sin(\psi)V_y \\ \sin(\psi)V_x + \cos(\psi)V_y \\ \frac{I_r}{mR}(\dot{\omega}_R + \dot{\omega}_f) \\ \dot{\psi}V_x + \frac{1}{m} \left[-C_f \frac{(V_y + L_f \dot{\psi})}{V_x} - C_r \frac{(V_y - L_f \dot{\psi})}{V_x} \right] \\ \dot{\psi} \\ \frac{1}{I_z} \left[-L_f C_f \frac{(V_y + L_f \dot{\psi})}{V_x} + L_r C_r \frac{(V_y - L_f \dot{\psi})}{V_x} \right] \end{pmatrix} + \begin{pmatrix} 0 & 0 \\ 0 & 0 \\ \frac{1}{mR} & \frac{C_f}{m} \frac{V_y + L_f \dot{\psi}}{V_x} \\ 0 & \frac{C_f R - L_f \dot{\omega}_f}{mR} \\ 0 & 0 \\ 0 & \frac{L_f C_f R - L_f I_r \dot{\omega}_f}{I_z R} \end{pmatrix} \begin{pmatrix} T_\omega \\ \delta \end{pmatrix} \quad (8.20)$$

Next, by defining the following state variables $x_1 = X$, $x_2 = Y$, $x_3 = V_x$, $x_4 = V_y$, $x_5 = \psi$ and $x_6 = \dot{\psi}$ the state-space description of the system becomes:

$$\begin{pmatrix} \dot{x}_1 \\ \dot{x}_2 \\ \dot{x}_3 \\ \dot{x}_4 \\ \dot{x}_5 \\ \dot{x}_6 \end{pmatrix} \begin{pmatrix} \cos(x_5)x_3 - \sin(x_3)x_4 \\ \sin(x_5)x_3 + \cos(x_5)x_4 \\ \frac{I_r}{mR}(\dot{\omega}_R + \dot{\omega}_f) \\ x_6x_3 + \frac{1}{m} \left[-C_f \frac{(x_5+L_f x_6)}{x_3} - C_r \frac{(x_4-L_f x_6)}{x_3} \right] \\ x_6 \\ \frac{1}{I_z} \left[-L_f C_f \frac{(x_4+L_f x_6)}{x_3} + L_r C_r \frac{(x_4-L_f x_6)}{x_3} \right] \end{pmatrix} + \begin{pmatrix} 0 & 0 \\ 0 & 0 \\ \frac{1}{mR} & \frac{C_f}{m} \frac{x_4+L_f x_6}{x_3} \\ 0 & \frac{C_f R - I_r \dot{\omega}_f}{mR} \\ 0 & 0 \\ 0 & \frac{L_f C_f R - L_f I_r \dot{\omega}_f}{I_z R} \end{pmatrix} \begin{pmatrix} u_1 \\ u_2 \end{pmatrix} \quad (8.21)$$

In vector field form, one obtains the following state-space description about the vehicle's dynamics

$$\begin{aligned} \dot{x} &= f(x) + G(x)u \Rightarrow \\ \dot{x} &= f(x) + g_1(x)u_1 + g_2(x)u_2 \end{aligned} \quad (8.22)$$

where $f(x) \in R^{6 \times 1}$, $G(x) \in R^{6 \times 2}$ while its columns are defined as $g_1(x) \in R^{6 \times 1}$ and $g_2(x) \in R^{6 \times 1}$ with

$$\begin{aligned} f(x) &= \begin{pmatrix} \cos(x_5)x_3 - \sin(x_3)x_4 \\ \sin(x_5)x_3 + \cos(x_5)x_4 \\ \frac{I_r}{mR}(\dot{\omega}_R + \dot{\omega}_f) \\ x_6x_3 + \frac{1}{m} \left[-C_f \frac{(x_5+L_f x_6)}{x_3} - C_r \frac{(x_4-L_f x_6)}{x_3} \right] \\ x_6 \\ \frac{1}{I_z} \left[-L_f C_f \frac{(x_4+L_f x_6)}{x_3} + L_r C_r \frac{(x_4-L_f x_6)}{x_3} \right] \end{pmatrix} \\ g_1(x) &= \begin{pmatrix} 0 \\ 0 \\ \frac{1}{mR} \\ 0 \\ 0 \\ 0 \end{pmatrix} \quad g_2(x) = \begin{pmatrix} 0 \\ 0 \\ \frac{C_f}{m} \frac{x_4+L_f x_6}{x_3} \\ \frac{C_f R - I_r \dot{\omega}_f}{mR} \\ 0 \\ \frac{L_f C_f R - L_f I_r \dot{\omega}_f}{I_z R} \end{pmatrix} \end{aligned} \quad (8.23)$$

8.2.3 Approximate Linearization of the Four-Wheel Vehicle Dynamics

The dynamic model of the four-wheel vehicle undergoes approximate linearization around the temporary operating point (x^*, u^*) which is recomputed at each iteration of the control algorithm. The linearization point (equilibrium) consists of the present value of the vehicle's state vector x^* and of the last value of the control inputs vector u^* that was exerted on it. The linearization is based on first order Taylor

series expansion and on the computation of the Jacobian matrices of the state-space description of the vehicle. This gives:

$$\dot{x} = Ax + Bu + \tilde{d} \quad (8.24)$$

A and B are the system's Jacobian matrices to be defined in the following and \tilde{d} is a model uncertainty term denoting the modelling error due to the truncation of higher-order terms in the Taylor series expansion and the effects of external perturbations. About matrix A one has

$$\begin{aligned} A &= \nabla_x [f(x) + G(x)u]|_{(x^*, u^*)} \Rightarrow \\ A &= \nabla_x [f(x)]|_{(x^*, u^*)} + \nabla_x [g_1(x)]|_{(x^*, u^*)} + \nabla_x [g_2(x)]|_{(x^*, u^*)} \end{aligned} \quad (8.25)$$

About matrix B one has

$$\begin{aligned} B &= \nabla_u [f(x) + G(x)u]|_{(x^*, u^*)} \Rightarrow \\ B &= G(x)|_{(x^*, u^*)} \end{aligned} \quad (8.26)$$

The Jacobian matrix $\nabla_x f(x)$ of the state-space description of the system are computed as follows:

$$\nabla_x f(x) = \begin{pmatrix} \frac{\partial f_1}{\partial x_1} & \frac{\partial f_1}{\partial x_2} & \dots & \frac{\partial f_1}{\partial x_6} \\ \frac{\partial f_2}{\partial x_1} & \frac{\partial f_2}{\partial x_2} & \dots & \frac{\partial f_2}{\partial x_6} \\ \dots & \dots & \dots & \dots \\ \frac{\partial f_6}{\partial x_1} & \frac{\partial f_6}{\partial x_2} & \dots & \frac{\partial f_6}{\partial x_6} \end{pmatrix} |_{(x^*, u^*)} \quad (8.27)$$

The elements of the first row of the Jacobian matrix $\nabla_x f(x)$ are: $\frac{\partial f_1}{\partial x_1} = 0$, $\frac{\partial f_1}{\partial x_2} = 0$, $\frac{\partial f_1}{\partial x_3} = \cos(x_5)$, $\frac{\partial f_1}{\partial x_4} = -\sin(x_5)$, $\frac{\partial f_1}{\partial x_5} = -x_3 \sin(x_5) - x_4 \cos(x_5)$, $\frac{\partial f_1}{\partial x_6} = 0$.

The elements of the second row of the Jacobian matrix $\nabla_x f(x)$ are: $\frac{\partial f_2}{\partial x_1} = 0$, $\frac{\partial f_2}{\partial x_2} = 0$, $\frac{\partial f_2}{\partial x_3} = \sin(x_5)$, $\frac{\partial f_2}{\partial x_4} = \cos(x_5)$, $\frac{\partial f_2}{\partial x_5} = x_3 \cos(x_5) - x_4 \sin(x_5)$, $\frac{\partial f_2}{\partial x_6} = 0$.

The elements of the third row of the Jacobian matrix $\nabla_x f(x)$ are: $\frac{\partial f_3}{\partial x_1} = 0$, $\frac{\partial f_3}{\partial x_2} = 0$, $\frac{\partial f_3}{\partial x_3} = 0$, $\frac{\partial f_3}{\partial x_4} = 0$, $\frac{\partial f_3}{\partial x_5} = 0$, $\frac{\partial f_3}{\partial x_6} = 0$.

The elements of the fourth row of the Jacobian matrix $\nabla_x f(x)$ are: $\frac{\partial f_4}{\partial x_1} = 0$, $\frac{\partial f_4}{\partial x_2} = 0$, $\frac{\partial f_4}{\partial x_3} = x_6 + \frac{1}{m}[-C_f \frac{-(x_4 + L_f x_6)}{x_3^2} - C_r \frac{-(x_4 + L_f x_6)}{x_3^2}]$, $\frac{\partial f_4}{\partial x_4} = \frac{1}{m}[-C_f \frac{1}{x_3} - C_r \frac{1}{x_3}]$, $\frac{\partial f_4}{\partial x_5} = 0$, $\frac{\partial f_4}{\partial x_6} = x_3 + \frac{1}{m}[-C_f \frac{L_f}{x_3} - C_r \frac{-L_f}{x_3}]$.

The elements of the fifth row of the Jacobian matrix $\nabla_x f(x)$ are: $\frac{\partial f_5}{\partial x_1} = 0$, $\frac{\partial f_5}{\partial x_2} = 0$, $\frac{\partial f_5}{\partial x_3} = 0$, $\frac{\partial f_5}{\partial x_4} = 0$, $\frac{\partial f_5}{\partial x_5} = 0$, $\frac{\partial f_5}{\partial x_6} = 1$.

The elements of the sixth row of the Jacobian matrix $\nabla_x f(x)$ are: $\frac{\partial f_6}{\partial x_1} = 0$, $\frac{\partial f_6}{\partial x_2} = 0$, $\frac{\partial f_6}{\partial x_3} = 0$, $\frac{\partial f_6}{\partial x_4} = \frac{1}{I_z}[-L_f C_f \frac{1}{x_3} + L_f C_r \frac{1}{x_3}]$, $\frac{\partial f_6}{\partial x_5} = 0$, $\frac{\partial f_6}{\partial x_6} = \frac{1}{I_z}[-L_f C_f \frac{L_f}{x_3} + L_f C_r \frac{L_f}{x_3}]$.

The Jacobian matrix $\nabla_x g_1(x)$ of the state-space description of the system are computed as follows:

$$\nabla_x g_1(x) = \begin{pmatrix} \frac{\partial g_{11}}{\partial x_1} & \frac{\partial g_{11}}{\partial x_2} & \dots & \frac{\partial g_{11}}{\partial x_6} \\ \frac{\partial g_{12}}{\partial x_1} & \frac{\partial g_{12}}{\partial x_2} & \dots & \frac{\partial g_{12}}{\partial x_6} \\ \dots & \dots & \dots & \dots \\ \frac{\partial g_{16}}{\partial x_1} & \frac{\partial g_{16}}{\partial x_2} & \dots & \frac{\partial g_{16}}{\partial x_6} \end{pmatrix} \Big|_{(x^*, u^*)} \quad (8.28)$$

It holds that $\nabla_x g_1(x) = 0_{6 \times 6}$.

The Jacobian matrix $\nabla_x g_2(x)$ of the state-space description of the system are computed as follows:

$$\nabla_x g_2(x) = \begin{pmatrix} \frac{\partial g_{21}}{\partial x_1} & \frac{\partial g_{21}}{\partial x_2} & \dots & \frac{\partial g_{21}}{\partial x_6} \\ \frac{\partial g_{22}}{\partial x_1} & \frac{\partial g_{22}}{\partial x_2} & \dots & \frac{\partial g_{22}}{\partial x_6} \\ \dots & \dots & \dots & \dots \\ \frac{\partial g_{26}}{\partial x_1} & \frac{\partial g_{26}}{\partial x_2} & \dots & \frac{\partial g_{26}}{\partial x_6} \end{pmatrix} \Big|_{(x^*, u^*)} \quad (8.29)$$

The elements of 1st, 2nd, 4th, 5th and 6th row of the Jacobian matrix $\nabla_x g_2(x)$ are 0, while the elements of the third row of the Jacobian matrix $\nabla_x g_2(x)$ are: $\frac{\partial g_{32}}{\partial x_1} = 0$, $\frac{\partial g_{32}}{\partial x_2} = 0$, $\frac{\partial g_{32}}{\partial x_3} = \frac{C_f}{m}(-\frac{(x_4 + L_f x_6)}{x_3^2})$, $\frac{\partial g_{32}}{\partial x_4} = \frac{C_f}{m}(\frac{1}{x_3})$, $\frac{\partial g_{32}}{\partial x_5} = 0$, $\frac{\partial g_{32}}{\partial x_6} = \frac{C_f}{m}(\frac{L_f}{x_3})$.

8.2.4 The Nonlinear H-Infinity Control

8.2.4.1 Tracking Error Dynamics of the Four-Wheel Vehicle

The initial nonlinear model of the automatic ground vehicle is in the form

$$\dot{x} = f(x, u) \quad x \in R^n, \quad u \in R^m \quad (8.30)$$

Linearization of the system (four-wheel ground vehicle) is performed at each iteration of the control algorithm round its present operating point $(x^*, u^*) = (x(t), u(t - T_s))$. The linearized equivalent of the system is described by

$$\dot{x} = Ax + Bu + L\tilde{d} \quad x \in R^n, \quad u \in R^m, \quad \tilde{d} \in R^q \quad (8.31)$$

Thus, after linearization round its current operating point, the autonomous ground vehicle's dynamic model is written as

$$\dot{x} = Ax + Bu + d_1 \quad (8.32)$$

Parameter d_1 stands for the linearization error in the vehicle's dynamic model appearing in Eq. (8.32). The reference setpoints for the ground vehicle are denoted by $\mathbf{x}_d = [x_1^d, \dots, x_6^d]$. Tracking of this trajectory is achieved after applying the control input u^* . At every time instant the control input u^* is assumed to differ from the control input u appearing in Eq. (8.32) by an amount equal to Δu , that is $u^* = u + \Delta u$

$$\dot{x}_d = Ax_d + Bu^* + d_2 \quad (8.33)$$

The dynamics of the controlled system described in Eq. (8.32) can be also written as

$$\dot{x} = Ax + Bu + Bu^* - Bu^* + d_1 \quad (8.34)$$

and by denoting $d_3 = -Bu^* + d_1$ as an aggregate disturbance term one obtains

$$\dot{x} = Ax + Bu + Bu^* + d_3 \quad (8.35)$$

By subtracting Eq. (8.33) from (8.35) one has

$$\dot{x} - \dot{x}_d = A(x - x_d) + Bu + d_3 - d_2 \quad (8.36)$$

By denoting the tracking error as $e = x - x_d$ and the aggregate disturbance term as $\tilde{d} = d_3 - d_2$, the tracking error dynamics becomes

$$\dot{e} = Ae + Bu + \tilde{d} \quad (8.37)$$

The above linearized form of the four wheel vehicle's model can be efficiently controlled after applying an H-infinity feedback control scheme.

8.2.5 Min-Max Control and Disturbance Rejection

The initial nonlinear model of the four-wheel autonomous ground vehicle is in the form

$$\dot{x} = f(x, u) \quad x \in R^n, \quad u \in R^m \quad (8.38)$$

Linearization of the system (four-wheel vehicle) is performed at each iteration of the control algorithm round its present operating point $(x^*, u^*) = (x(t), u(t - T_s))$. The linearized equivalent of the system is described by

$$\dot{x} = Ax + Bu + L\tilde{d} \quad x \in R^n, \quad u \in R^m, \quad \tilde{d} \in R^q \quad (8.39)$$

where matrices A and B are obtained from the computation of the vehicle's Jacobians, according to Eqs. (8.25) and (8.26), and vector \tilde{d} denotes disturbance terms due to linearization errors. The problem of disturbance rejection for the linearized model that is described by

$$\begin{aligned}\dot{x} &= Ax + Bu + L\tilde{d} \\ y &= Cx\end{aligned}\tag{8.40}$$

where $x \in R^n$, $u \in R^m$, $\tilde{d} \in R^q$ and $y \in R^p$, cannot be handled efficiently if the classical LQR control scheme is applied. This is because of the existence of the perturbation term \tilde{d} . The disturbance term \tilde{d} apart from modeling (parametric) uncertainty and external perturbations can also represent noise terms of any distribution.

As already explained in the previous applications of the H_∞ control approach, a feedback control scheme is designed for trajectory tracking by the system's state vector and simultaneous disturbance rejection, considering that the disturbance affects the system in the worst possible manner. The disturbances' effect are incorporated in the following quadratic cost function:

$$J(t) = \frac{1}{2} \int_0^T [y^T(t)y(t) + ru^T(t)u(t) - \rho^2 \tilde{d}^T(t)\tilde{d}(t)]dt, \quad r, \rho > 0 \tag{8.41}$$

Once again, the significance of the negative sign in the cost function's term that is associated with the perturbation variable $\tilde{d}(t)$ is that the disturbance tries to maximize the cost function $J(t)$ while the control signal $u(t)$ tries to minimize it. The physical meaning of the relation given above is that the control signal and the disturbances compete to each other within a min-max differential game. This problem of min-max optimization can be written as

$$\min_u \max_{\tilde{d}} J(u, \tilde{d}) \tag{8.42}$$

The objective of the optimization procedure is to compute a control signal $u(t)$ which can compensate for the worst possible disturbance, that is externally imposed to the system of the four-wheel autonomous vehicle. However, the solution to the min-max optimization problem is directly related to the value of the parameter ρ . This means that there is an upper bound in the disturbances magnitude that can be annihilated by the control signal.

8.2.5.1 H-Infinity Feedback Control

For the linearized system given by Eq. (8.40) the cost function of Eq. (8.41) is defined, where the coefficient r determines the penalization of the control input and the weight coefficient ρ determines the reward of the disturbances' effects. Once more, it is assumed that (i) The energy that is transferred from the disturbances signal $\tilde{d}(t)$ is bounded, that is $\int_0^\infty \tilde{d}^T(t)\tilde{d}(t)dt < \infty$, (ii) matrices $[A, B]$ and $[A, L]$ are stabilizable, (iii) matrix $[A, C]$ is detectable. Then, the optimal feedback control law is given by

$$u(t) = -Kx(t) \tag{8.43}$$

with

$$K = \frac{1}{r} B^T P \tag{8.44}$$

where P is a positive semi-definite symmetric matrix which is obtained from the solution of the Riccati equation

$$A^T P + P A + Q - P \left(\frac{1}{r} B B^T - \frac{1}{2\rho^2} L L^T \right) P = 0 \tag{8.45}$$

where Q is also a positive definite symmetric matrix. The worst case disturbance is given by

$$\tilde{d}(t) = \frac{1}{\rho^2} L^T P x(t) \tag{8.46}$$

The diagram of the considered control loop is depicted in Fig. 8.3.

8.2.6 Lyapunov Stability Analysis

Through Lyapunov stability analysis it will be shown that the proposed nonlinear control scheme assures H_∞ tracking performance for the control loop of the four-

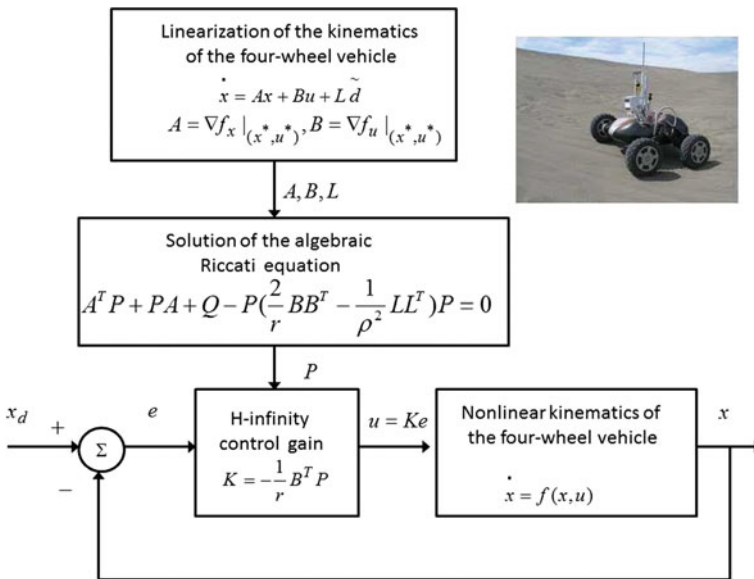


Fig. 8.3 Diagram of the nonlinear optimal control scheme for the four-wheel autonomous ground vehicle

wheel autonomous ground vehicle. Moreover, under moderate conditions asymptotic stability is proven and convergence to the reference setpoints is achieved. The tracking error dynamics for the automatic ground vehicle is written in the form

$$\dot{e} = Ae + Bu + L\tilde{d} \quad (8.47)$$

where in this autonomous vehicle's case $L = I \in \mathbb{R}^{6 \times 6}$ with I being the identity matrix. Variable \tilde{d} denotes model uncertainties and external disturbances of the vehicle's model. The following Lyapunov function is considered

$$V = \frac{1}{2}e^T P e \quad (8.48)$$

where $e = x - x_d$ is the tracking error. By differentiating with respect to time one obtains

$$\begin{aligned} \dot{V} &= \frac{1}{2}\dot{e}^T P e + \frac{1}{2}e^T P \dot{e} \Rightarrow \\ \dot{V} &= \frac{1}{2}[Ae + Bu + L\tilde{d}]^T P + \frac{1}{2}e^T P [Ae + Bu + L\tilde{d}] \Rightarrow \end{aligned} \quad (8.49)$$

$$\begin{aligned} \dot{V} &= \frac{1}{2}[e^T A^T + u^T B^T + \tilde{d}^T L^T] P e + \\ &+ \frac{1}{2}e^T P [Ae + Bu + L\tilde{d}] \Rightarrow \end{aligned} \quad (8.50)$$

$$\begin{aligned} \dot{V} &= \frac{1}{2}e^T A^T P e + \frac{1}{2}u^T B^T P e + \frac{1}{2}\tilde{d}^T L^T P e + \\ &\frac{1}{2}e^T P A e + \frac{1}{2}e^T P B u + \frac{1}{2}e^T P L \tilde{d} \end{aligned} \quad (8.51)$$

The previous equation is rewritten as

$$\begin{aligned} \dot{V} &= \frac{1}{2}e^T (A^T P + P A) e + \left(\frac{1}{2}u^T B^T P e + \frac{1}{2}e^T P B u \right) + \\ &+ \left(\frac{1}{2}\tilde{d}^T L^T P e + \frac{1}{2}e^T P L \tilde{d} \right) \end{aligned} \quad (8.52)$$

Assumption: For given positive definite matrix Q and coefficients r and ρ there exists a positive definite matrix P , which is the solution of the following matrix equation

$$A^T P + P A = -Q + P \left(\frac{2}{r} B B^T - \frac{1}{\rho^2} L L^T \right) P \quad (8.53)$$

Moreover, the following feedback control law is applied to the system

$$u = -\frac{1}{r} B^T P e \quad (8.54)$$

By substituting Eqs. (8.53) and (8.54) one obtains

$$\begin{aligned} \dot{V} = & \frac{1}{2} e^T \left[-Q + P \left(\frac{2}{r} B B^T - \frac{1}{2\rho^2} L L^T \right) P \right] e + \\ & + e^T P B \left(-\frac{1}{r} B^T P e \right) + e^T P L \tilde{d} \Rightarrow \end{aligned} \quad (8.55)$$

$$\begin{aligned} \dot{V} = & -\frac{1}{2} e^T Q e + \left(\frac{2}{r} P B B^T P e - \frac{1}{2\rho^2} e^T P L L^T \right) P e \\ & - \frac{1}{r} (e^T P B B^T P e) + e^T P L \tilde{d} \end{aligned} \quad (8.56)$$

which after intermediate operations gives

$$\dot{V} = -\frac{1}{2} e^T Q e - \frac{1}{2\rho^2} e^T P L L^T P e + e^T P L \tilde{d} \quad (8.57)$$

or, equivalently

$$\begin{aligned} \dot{V} = & -\frac{1}{2} e^T Q e - \frac{1}{2\rho^2} e^T P L L^T P e + \\ & + \frac{1}{2} e^T P L \tilde{d} + \frac{1}{2} \tilde{d}^T L^T P e \end{aligned} \quad (8.58)$$

Lemma: The following inequality holds

$$\frac{1}{2} e^T L \tilde{d} + \frac{1}{2} \tilde{d}^T L^T P e - \frac{1}{2\rho^2} e^T P L L^T P e \leq \frac{1}{2} \rho^2 \tilde{d}^T \tilde{d} \quad (8.59)$$

Proof: The binomial $(\rho\alpha - \frac{1}{\rho}b)^2$ is considered. Expanding the left part of the above inequality one gets

$$\begin{aligned} \rho^2 a^2 + \frac{1}{\rho^2} b^2 - 2ab \geq 0 & \Rightarrow \frac{1}{2} \rho^2 a^2 + \frac{1}{2\rho^2} b^2 - ab \geq 0 \Rightarrow \\ ab - \frac{1}{2\rho^2} b^2 \leq \frac{1}{2} \rho^2 a^2 & \Rightarrow \frac{1}{2} ab + \frac{1}{2} ab - \frac{1}{2\rho^2} b^2 \leq \frac{1}{2} \rho^2 a^2 \end{aligned} \quad (8.60)$$

The following substitutions are carried out: $a = \tilde{d}$ and $b = e^T PL$ and the previous relation becomes

$$\frac{1}{2}\tilde{d}^T L^T P e + \frac{1}{2}e^T PL\tilde{d} - \frac{1}{2\rho^2}e^T PLL^T P e \leq \frac{1}{2}\rho^2\tilde{d}^T \tilde{d} \quad (8.61)$$

Equation (8.61) is substituted in Eq. (8.58) and the inequality is enforced, thus giving

$$\dot{V} \leq -\frac{1}{2}e^T Q e + \frac{1}{2}\rho^2\tilde{d}^T \tilde{d} \quad (8.62)$$

Equation (8.62) shows that the H_∞ tracking performance criterion is satisfied. The integration of \dot{V} from 0 to T gives

$$\begin{aligned} \int_0^T \dot{V}(t)dt &\leq -\frac{1}{2}\int_0^T \|e\|_Q^2 dt + \frac{1}{2}\rho^2 \int_0^T \|\tilde{d}\|^2 dt \Rightarrow \\ 2V(T) + \int_0^T \|e\|_Q^2 dt &\leq 2V(0) + \rho^2 \int_0^T \|\tilde{d}\|^2 dt \end{aligned} \quad (8.63)$$

Moreover, if there exists a positive constant $M_d > 0$ such that

$$\int_0^\infty \|\tilde{d}\|^2 dt \leq M_d \quad (8.64)$$

then one gets

$$\int_0^\infty \|e\|_Q^2 dt \leq 2V(0) + \rho^2 M_d \quad (8.65)$$

Thus, the integral $\int_0^\infty \|e\|_Q^2 dt$ is bounded. Moreover, $V(T)$ is bounded and from the definition of the Lyapunov function V in Eq. (8.48) it becomes clear that $e(t)$ will be also bounded since $e(t) \in \Omega_e = \{e | e^T P e \leq 2V(0) + \rho^2 M_d\}$. According to the above and with the use of Barbalat's Lemma one obtains $\lim_{t \rightarrow \infty} e(t) = 0$.

8.2.7 Robust State Estimation with the Use of the H-Infinity Kalman Filter

The control loop for the four-wheel autonomous vehicle can be implemented with the feedback of a partially measurable state vector and by processing only a small number of state variables. To reconstruct the missing information about the state vector of the autonomous vehicle it is proposed to use a filtering scheme which allows to apply state estimation-based control [457]. The recursion of the H_∞ Kalman Filter, for the model of the distributed finance agents, can be formulated in terms of a *measurement update* and a *time update* part

Measurement update:

$$\begin{aligned}
 D(k) &= [I - \theta W(k)P^-(k) + C^T(k)R(k)^{-1}C(k)P^-(k)]^{-1} \\
 K(k) &= P^-(k)D(k)C^T(k)R(k)^{-1} \\
 \hat{x}(k) &= \hat{x}^-(k) + K(k)[y(k) - C\hat{x}^-(k)]
 \end{aligned} \tag{8.66}$$

Time update:

$$\begin{aligned}
 \hat{x}^-(k+1) &= A(k)x(k) + B(k)u(k) \\
 P^-(k+1) &= A(k)P^-(k)D(k)A^T(k) + Q(k)
 \end{aligned} \tag{8.67}$$

where it is assumed that parameter θ is sufficiently small to assure that the covariance matrix $P^-(k)^{-1} - \theta W(k) + C^T(k)R(k)^{-1}C(k)$ will be positive definite. When $\theta = 0$ the H_∞ Kalman Filter becomes equivalent to the standard Kalman Filter. One can measure only a part of the state vector of the system of the autonomous ground vehicle, such as the velocities V_x and V_y and the orientation angle ψ , and can estimate through filtering the rest of the state vector elements.

8.2.8 Simulation Tests

The performance of the proposed nonlinear optimal control scheme for the autonomous four-wheel vehicle has been tested in the case of tracking of different reference set-points (Figs. 8.4, 8.5, 8.6, 8.7, 8.8, 8.9, 8.10, 8.11, 8.12 and 8.13). The control scheme exhibited fast and accurate tracking of the reference paths. The computation of the feedback control gain required the solution of the algebraic Riccati equation given in Eq. (8.53), at each iteration of the control algorithm. The obtained results are depicted in Figs. 8.22, 8.23, 8.24, 8.25, 8.26, 8.27, 8.28, 8.29, 8.30, 8.31, 8.32 and 8.33. The measurement units for the state variables of the four-wheel vehicle's model were in the SI system (position coordinates measured in m and heading angle in rad). It can be noticed that the H-infinity controller achieved fast and accurate convergence to the reference setpoints for all elements of the four-wheel vehicle's state-vector. Moreover, the variations of the control inputs, that is of the autonomous vehicle's velocity and of its steering angle were smooth.

As noted, the proposed nonlinear optimal control method for the four-wheel autonomous vehicle was based on an approximate linearization of its joint kinematic and dynamic model. The advantages that the proposed control method exhibits are outlined as follows: (i) it is applied directly on the nonlinear dynamical model of the four-wheel vehicle and not on an equivalent linearized description of it, (ii) It avoids the elaborated linearizing transformations (diffeomorphisms) which can be

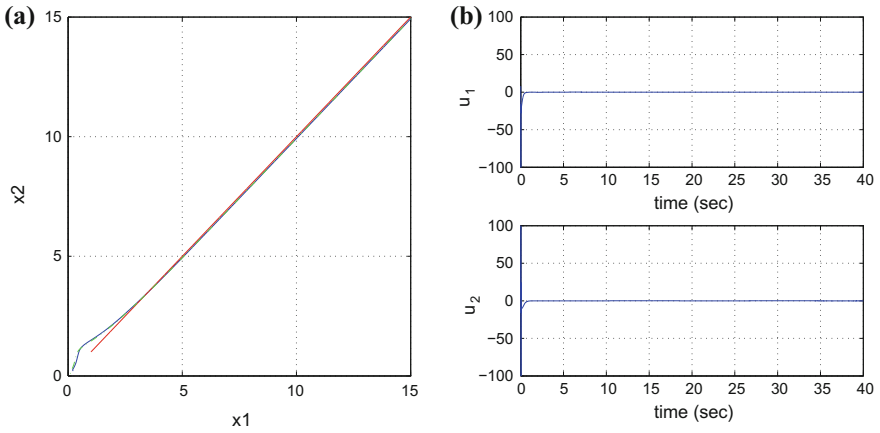


Fig. 8.4 **a** Tracking of reference path 1 (red-line) by the four-wheel autonomous vehicle (blue line) and trajectory estimated by the Kalman Filter (green line), **b** control inputs u_1 and u_2 applied to the vehicle

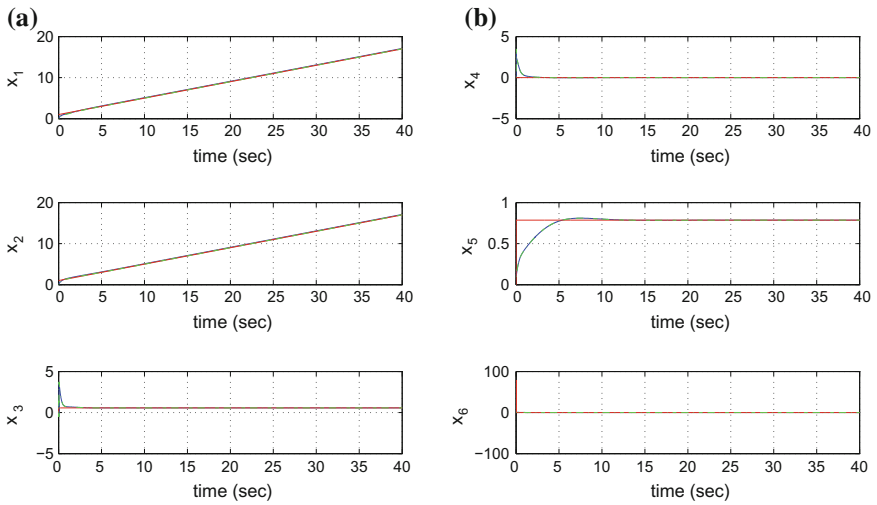


Fig. 8.5 Tracking of reference path 1: **a** convergence of state variables x_1 to x_3 of the four-wheel vehicle to their reference setpoints (red-lines) and estimated state variables provided by the Kalman Filter (green lines), **b** convergence of state variables x_4 to x_6 of the four-wheel vehicle to their reference setpoints (red-lines) and estimated state variables provided by the Kalman Filter (green lines)

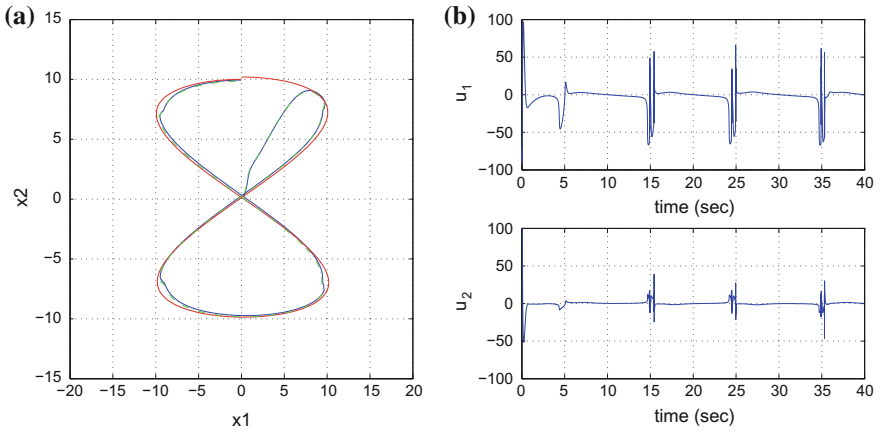


Fig. 8.6 **a** Tracking of reference path 2 (red-line) by the four-wheel autonomous vehicle (blue line) and trajectory estimated by the Kalman Filter (green line), **b** control inputs u_1 and u_2 applied to the vehicle

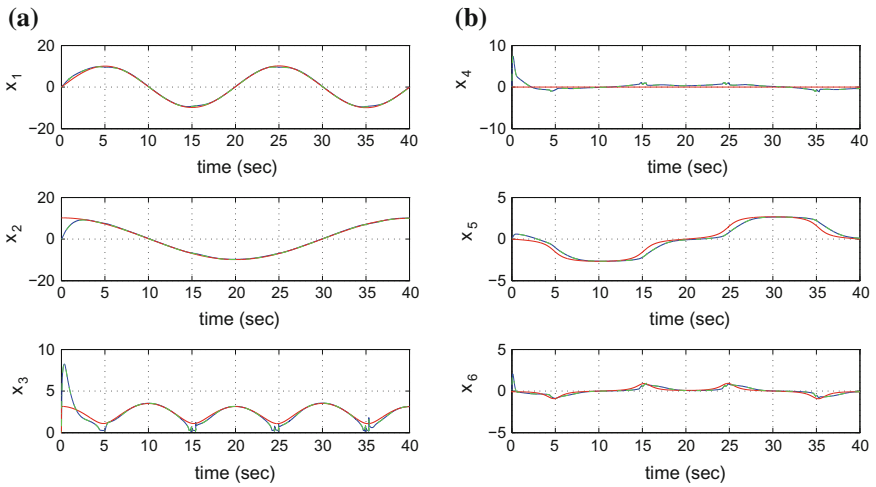


Fig. 8.7 Tracking of reference path 2: **a** convergence of state variables x_1 to x_3 of the four-wheel vehicle-to their reference setpoints (red-lines) and estimated state variables provided by the Kalman Filter (green lines), **b** convergence of state variables x_4 to x_6 of the four-wheel vehicle to their reference setpoints (red-lines) and estimated state variables provided by the Kalman Filter (green lines)

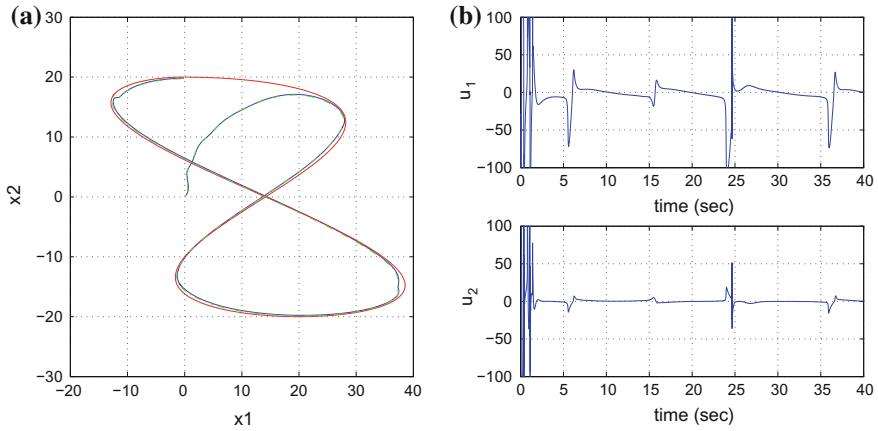


Fig. 8.8 **a** Tracking of reference path 3 (red-line) by the four-wheel autonomous vehicle (blue line) and trajectory estimated by the Kalman Filter (green line), **b** control inputs u_1 and u_2 applied to the vehicle

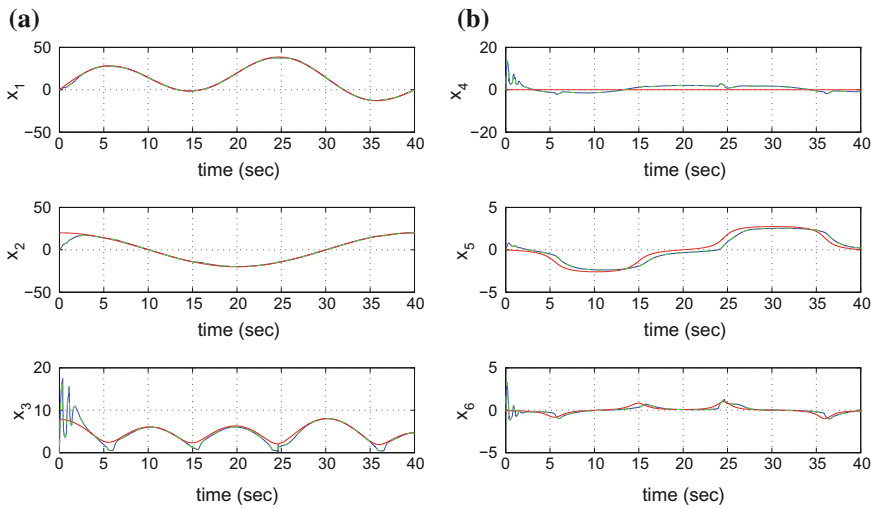


Fig. 8.9 Tracking of reference path 3: **a** convergence of state variables x_1 to x_3 of the four-wheel vehicle to their reference setpoints (red-lines) and estimated state variables provided by the Kalman Filter (green lines), **b** convergence of state variables x_4 to x_6 of the four-wheel vehicle to their reference setpoints (red-lines) and estimated state variables provided by the Kalman Filter (green lines)

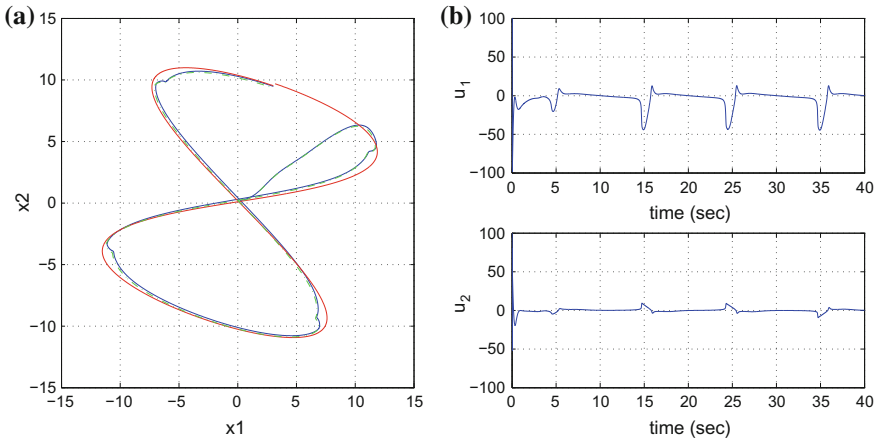


Fig. 8.10 **a** Tracking of reference path 1 (red-line) by the four-wheel autonomous vehicle (blue line) and trajectory estimated by the Kalman Filter (green line), **b** control inputs u_1 and u_2 applied to the vehicle

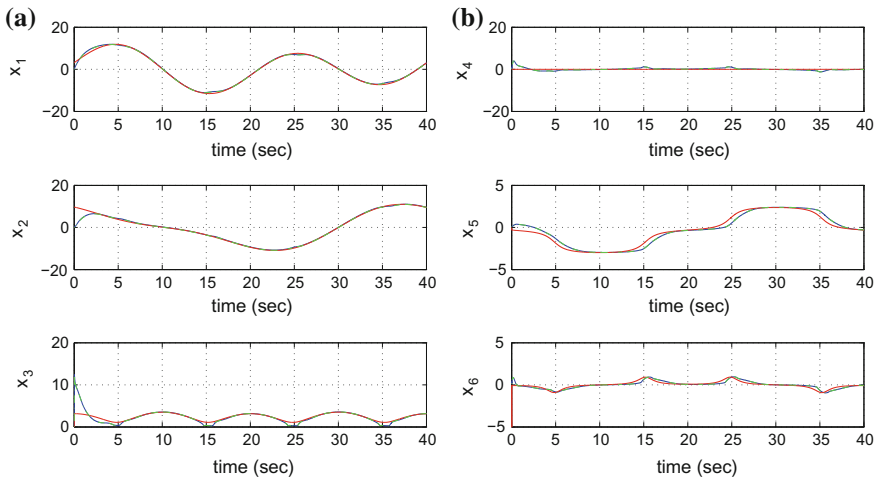


Fig. 8.11 Tracking of reference path 4: **a** convergence of state variables x_1 to x_3 of the four-wheel vehicle to their reference setpoints (red-lines) and estimated state variables provided by the Kalman Filter (green lines), **b** convergence of state variables x_4 to x_6 of the four-wheel vehicle to their reference setpoints (red-lines) and estimated state variables provided by the Kalman Filter (green lines)

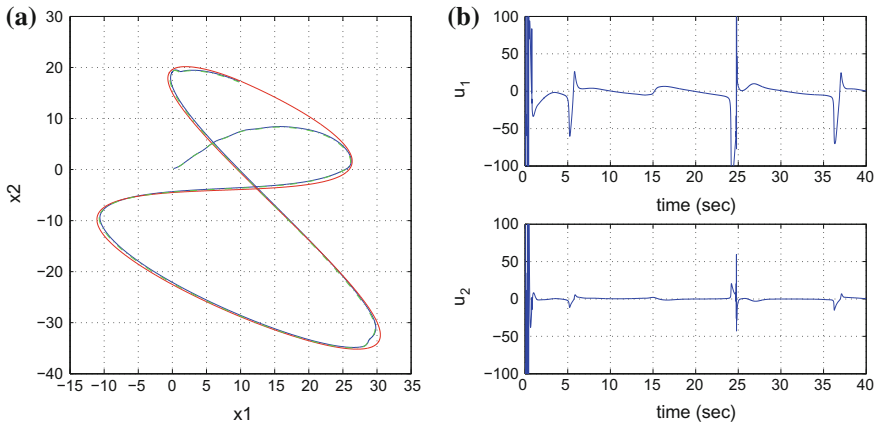


Fig. 8.12 **a** Tracking of reference path51 (red-line) by the four-wheel autonomous vehicle (blue line) and trajectory estimated by the Kalman Filter (green line), **b** control inputs u_1 and u_2 applied to the vehicle

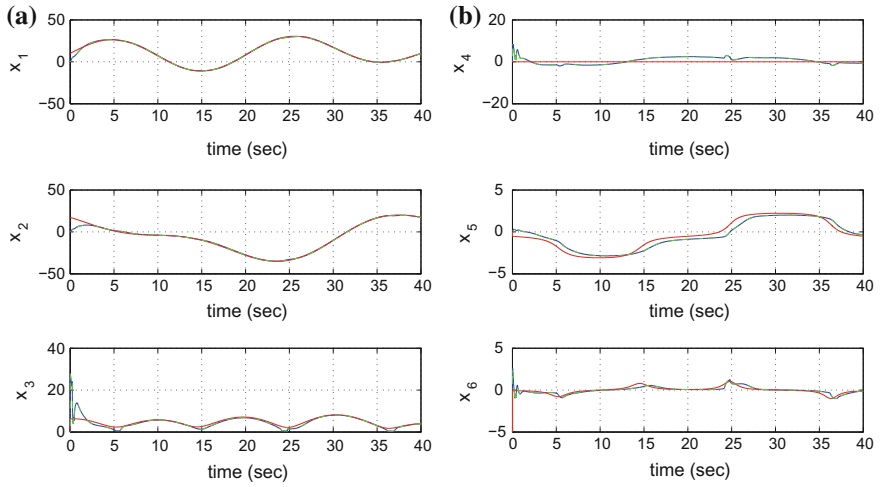


Fig. 8.13 Tracking of reference path 5: **a** convergence of state variables x_1 to x_3 of the four-wheel vehicle to their reference setpoints (red-lines) and estimated state variables provided by the Kalman Filter (green lines), **b** convergence of state variables x_4 to x_6 of the four-wheel vehicle to their reference setpoints (red-lines) and estimated state variables provided by the Kalman Filter (green lines)

met in global linearization-based control methods for autonomous vehicles (iii) the controller is designed according to optimal control principles which implies the best trade-off between precise tracking of the reference setpoints on the one side and moderate variations of the control inputs on the other side (iv) the control method exhibits significant robustness to parametric uncertainty, modelling errors as well as to external perturbations.

Yet computationally simple, the proposed H_∞ control scheme has an excellent performance. Comparing to the control of the automatic ground vehicles that can rely on global linearization methods the presented nonlinear H-infinity control scheme is equally efficient in setpoint tracking while also retaining optimal control features [457]. The tracking accuracy of the presented control method (H_∞) has been monitored in the case of several reference setpoints. By using the Kalman Filter as a robust observer estimates of the state vector of the vehicle were obtained and thus the implementation of state estimation-based control became possible. The measured state variables were $x_3 = V_x$, $x_4 = V_y$ and $x_5 = \psi$. The obtained results are given in Table 8.1.

The tracking performance of the nonlinear H-infinity control method for the model of the four-wheel vehicle was measured in the case of model uncertainty, imposing an imprecision equal to $\Delta a\%$ about the vehicle's moment of inertia I_z . The obtained results are outlined in Table 8.2. It can be noticed that despite model perturbations the tracking accuracy of the control method remained satisfactory.

Table 8.1 RMSE of the vehicle's state variables

Path	RMSE X (m)	RMSE Y (m)	RMSE ψ (rad)
1	$4.5 \cdot 10^{-3}$	$4.5 \cdot 10^{-3}$	$0.1 \cdot 10^{-3}$
2	$15.1 \cdot 10^{-3}$	$5.7 \cdot 10^{-3}$	$17.3 \cdot 10^{-3}$
3	$13.3 \cdot 10^{-3}$	$13.7 \cdot 10^{-3}$	$18.6 \cdot 10^{-3}$
4	$15.3 \cdot 10^{-3}$	$9.3 \cdot 10^{-3}$	$17.0 \cdot 10^{-3}$
5	$8.7 \cdot 10^{-3}$	$15.5 \cdot 10^{-3}$	$17.8 \cdot 10^{-3}$

Table 8.2 RMSE of state variables under disturbance

Δa (%)	RMSE X (m)	RMSE Y (m)	RMSE ψ (rad)
0	$8.7 \cdot 10^{-3}$	$15.5 \cdot 10^{-3}$	$17.8 \cdot 10^{-3}$
10	$9.0 \cdot 10^{-3}$	$16.2 \cdot 10^{-3}$	$16.3 \cdot 10^{-3}$
20	$9.5 \cdot 10^{-3}$	$17.2 \cdot 10^{-3}$	$14.8 \cdot 10^{-3}$
30	$10.1 \cdot 10^{-3}$	$18.3 \cdot 10^{-3}$	$13.4 \cdot 10^{-3}$
40	$10.8 \cdot 10^{-3}$	$19.3 \cdot 10^{-3}$	$12.0 \cdot 10^{-3}$
50	$11.6 \cdot 10^{-3}$	$20.3 \cdot 10^{-3}$	$10.7 \cdot 10^{-3}$
60	$12.7 \cdot 10^{-3}$	$20.9 \cdot 10^{-3}$	$9.5 \cdot 10^{-3}$

8.3 A Nonlinear H-Infinity Control Approach for an Autonomous Truck and Trailer System

8.3.1 Outline

Comparing to the previously analyzed unicycle-type and four-wheel vehicles there exist more complicated and difficult to control models, such as multi-body and articulated autonomous vehicles [202, 249, 508]. Due to their complicated kinematic and dynamic model the problems of path planning and path following for the aforementioned types of vehicles is of elevated difficulty [12, 109, 166, 218, 328, 394]. To achieve accurate tracking of reference paths and to assure stability for the vehicles' autonomous navigation system, nonlinear control approaches have been proposed [59, 344, 355, 366, 469]. In [248, 471] one can find results on global linearization-based control of multi-body and articulated vehicles, based on differential flatness theory. In [217] the controller's design for the above mentioned type of vehicles is based on approximate linearization and the description of their kinematics or dynamics with the use of local models. Moreover, in [24] Lyapunov theory-based control methods are developed for such complicated vehicles.

In this section the problems of nonlinear optimal control and the problem of autonomous navigation of a truck and trailer vehicle are considered. The kinematic model of the vehicle is formulated and the controller's design proceeds by carrying out an approximate linearization on this model around a time-varying equilibrium. The linearization procedure relies on Taylor series expansion for the articulated vehicle's kinematic model and on the computation of the associated Jacobian matrices [33, 431, 463]. The linearization point (equilibrium) is updated at each time instant and is defined by the present value of the vehicle's state vector and the last value of the vehicle's control inputs vector. The modelling error which is due to approximate linearization and the cut-off of higher order terms in the Taylor series expansion is considered as a perturbation that is compensated by the robustness of the H-infinity control scheme [461, 466].

For the linearized equivalent model of the truck and trailer vehicle an H-infinity feedback controller is designed. This is an optimal controller for the case of a system subject to model uncertainty and external perturbations [450, 452, 457, 459, 460]. H-infinity control stands for the solution of a min-max differential game. Actually, the control inputs try to minimize a quadratic cost function associated with the deviation of the vehicle's state vector from its reference values, while the perturbations and model uncertainty terms try to maximize this cost function [132, 305, 564]. The feedback gain of the controller is based on the solution of an algebraic Riccati equation that is performed at each iteration of the control algorithm. The stability of the control loop for the truck and trailer system is confirmed through Lyapunov analysis. First, it is shown that the H-infinity tracking performance criterion is satisfied. This signifies elevated robustness of the control loop against model uncertainty and

exogenous disturbances. Moreover, under moderate conditions the global asymptotic stability of the control loop is proven. Finally, to implement feedback control for the autonomous truck and trailer system when its state vector is only partially measurable, the H-infinity Kalman Filter is proposed [169, 511].

8.3.2 Kinematic Model of the Truck and Trailer

8.3.2.1 State-Space Description of the Truck and Trailer System

The kinematic model of the truck and trailer system is given by

$$\begin{pmatrix} \dot{x}^t \\ \dot{y}^t \\ \dot{\theta} \\ \dot{x}^i \\ \dot{y}^i \\ \dot{\psi} \end{pmatrix} = \begin{pmatrix} v \cos(\theta) \\ v \sin(\theta) \\ \omega \\ v \cos(\theta - \psi) \cos(\psi) \\ v \cos(\theta - \psi) \sin(\psi) \\ \frac{v}{L^i} \sin(\theta - \psi) \end{pmatrix} \quad (8.68)$$

where (x^t, y^t) are the cartesian coordinates of the truck in an inertial reference frame, θ is the heading angle of the truck formed by its transversal axis and the OX axis of the reference frame, ω is the turn rate of the truck (turn rate of the steering wheel), (x^i, y^i) are the cartesian coordinates of the trailer, ψ^i is the heading angle of the trailer, v is the longitudinal speed of the truck, and β is the hitch point angle between the truck and the drawbar that connects the truck with the trailer. The parameters of the truck and trailer system are shown in Fig. 8.14.

In the diagram of Fig. 8.14, the following distances are defined: L^t is the distance between the front and the rear axis of the truck, L^i is the distance between the hitch point RJ and the rear axis of the trailer. The state vector of the truck and trailer system is defined as $x = [x^t, y^t, \theta, x^i, y^i, \psi]^T$ while the control inputs vector is defined as $u = [v, \omega]^T$ and thus consists of the velocity of the truck and the turn rate of the steering wheel of the truck.

The kinematic model of the truck and trailer system is justified as follows: The velocity v of point RJ is first projected on the longitudinal axis of the trailer, thus giving $v \cos(\theta - \psi)$ and next (a) it is projected on the OX axis thus giving $v \cos(\theta - \psi) \cos(\psi)$. This variable is the velocity of the trailer along the OX axis (b) it is projected on the OY axis thus giving $v \cos(\theta - \psi) \sin(\psi)$. Moreover, the trailer performs a rotational motion round point RJ , with rotational speed denoted as $\dot{\psi}$. The linear velocity of point RJ that is parallel to the transversal axis of the vehicle is given by $v \sin(\theta - \psi)$. Thus, it holds: $\dot{\psi} = \frac{1}{L^i} v \sin(\theta - \psi)$.

The kinematic model of the truck and trailer system is also written in the vector form:

$$\dot{x} = f(x, u) \tag{8.69}$$

where $x \in R^{6 \times 1}$, $f \in R^{6 \times 1}$ and $u \in R^{2 \times 1}$. It also holds that $\beta = \theta - \psi$. With the previous definition of state variables one arrives at the following state-space description

$$\begin{pmatrix} \dot{x}_1 \\ \dot{x}_2 \\ \dot{x}_3 \\ \dot{x}_4 \\ \dot{x}_5 \\ \dot{x}_6 \end{pmatrix} = \begin{pmatrix} u_1 \cos(x_3) \\ u_1 \sin(x_3) \\ u_2 \\ u_1 \cos(x_3 - x_6) \cos(x_6) \\ u_1 \cos(x_3 - x_6) \sin(x_6) \\ \frac{u_1}{L_i} \sin(x_3 - x_6) \end{pmatrix} \tag{8.70}$$

8.3.2.2 Approximate Linearization of the Truck and Trailer Model

Approximate linearization is performed to the kinematic model of the truck and trailer system round a temporary equilibrium x^* which is re-computed at each iteration of the control algorithm. The method is based on Taylor series expansion and on the calculation of the associated Jacobian matrices, while the equilibrium consists of the present value of the system's state vector x^* and of the last value of the control inputs vector u^* that was exerted on it. Thus one has the linearization point (x^*, u^*) . Using that the kinematic model of the system is $\dot{x} = f(x, u)$ the following linearized description is obtained

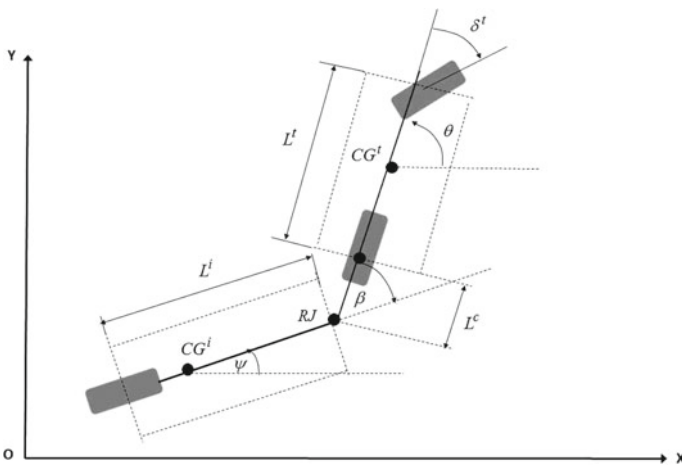


Fig. 8.14 Kinematic model of the truck and trailer

$$\dot{x} = Ax + Bu + \tilde{d} \quad (8.71)$$

where \tilde{d} is the linearization error and the associated Jacobian matrices are:

$$A = \nabla_x f(x, u) |_{(x^*, u^*)} \quad B = \nabla_u f(x, u) |_{(x^*, u^*)} \quad (8.72)$$

The elements of the Jacobian matrices are

$$A = \begin{pmatrix} \frac{\partial f_1}{\partial x_1} & \frac{\partial f_1}{\partial x_2} & \dots & \frac{\partial f_1}{\partial x_6} \\ \frac{\partial f_2}{\partial x_1} & \frac{\partial f_2}{\partial x_2} & \dots & \frac{\partial f_2}{\partial x_6} \\ \dots & \dots & \dots & \dots \\ \dots & \dots & \dots & \dots \\ \frac{\partial f_6}{\partial x_1} & \frac{\partial f_6}{\partial x_2} & \dots & \frac{\partial f_6}{\partial x_6} \end{pmatrix} \quad B = \begin{pmatrix} \frac{\partial f_1}{\partial u_1} & \frac{\partial f_1}{\partial u_2} \\ \frac{\partial f_2}{\partial u_1} & \frac{\partial f_2}{\partial u_2} \\ \dots & \dots \\ \dots & \dots \\ \frac{\partial f_6}{\partial u_1} & \frac{\partial f_6}{\partial u_2} \end{pmatrix} \quad (8.73)$$

With the previous definition of the Jacobian matrices one finds

The first row of the Jacobian matrix $A = \nabla_x f(x, u) |_{(x^*, u^*)}$ is $\frac{\partial f_1}{\partial x_1} = 0$, $\frac{\partial f_1}{\partial x_2} = 0$, $\frac{\partial f_1}{\partial x_3} = -u_1 \sin(x_3)$, $\frac{\partial f_1}{\partial x_4} = 0$, $\frac{\partial f_1}{\partial x_5} = 0$ and $\frac{\partial f_1}{\partial x_6} = 0$.

The second row of the Jacobian matrix $A = \nabla_x f(x, u) |_{(x^*, u^*)}$ is $\frac{\partial f_2}{\partial x_1} = 0$, $\frac{\partial f_2}{\partial x_2} = 0$, $\frac{\partial f_2}{\partial x_3} = u_1 \cos(x_3)$, $\frac{\partial f_2}{\partial x_4} = 0$, $\frac{\partial f_2}{\partial x_5} = 0$ and $\frac{\partial f_2}{\partial x_6} = 0$.

The third row of the Jacobian matrix $A = \nabla_x f(x, u) |_{(x^*, u^*)}$ is $\frac{\partial f_3}{\partial x_1} = 0$, $\frac{\partial f_3}{\partial x_2} = 0$, $\frac{\partial f_3}{\partial x_3} = 0$, $\frac{\partial f_3}{\partial x_4} = 0$, $\frac{\partial f_3}{\partial x_5} = 0$ and $\frac{\partial f_3}{\partial x_6} = 0$.

The fourth row of the Jacobian matrix $A = \nabla_x f(x, u) |_{(x^*, u^*)}$ is $\frac{\partial f_4}{\partial x_1} = 0$, $\frac{\partial f_4}{\partial x_2} = 0$, $\frac{\partial f_4}{\partial x_3} = -\sin(x_3 - x_6) \cos(x_6) u_1$, $\frac{\partial f_4}{\partial x_4} = 0$, $\frac{\partial f_4}{\partial x_5} = 0$ and $\frac{\partial f_4}{\partial x_6} = [\sin(x_3 - x_6) \cos(x_6) - \cos(x_3 - x_6) \sin(x_6)] u_1$.

The fifth row of the Jacobian matrix $A = \nabla_x f(x, u) |_{(x^*, u^*)}$ is $\frac{\partial f_5}{\partial x_1} = 0$, $\frac{\partial f_5}{\partial x_2} = 0$, $\frac{\partial f_5}{\partial x_3} = -\sin(x_3 - x_6) \sin(x_6) u_1$, $\frac{\partial f_5}{\partial x_4} = 0$, $\frac{\partial f_5}{\partial x_5} = 0$ and $\frac{\partial f_5}{\partial x_6} = [\sin(x_3 - x_6) \sin(x_6) + \cos(x_3 - x_6) \cos(x_6)] u_1$.

The sixth row of the Jacobian matrix $A = \nabla_x f(x, u) |_{(x^*, u^*)}$ is $\frac{\partial f_6}{\partial x_1} = 0$, $\frac{\partial f_6}{\partial x_2} = 0$, $\frac{\partial f_6}{\partial x_3} = \frac{1}{L_i} \cos(x_3 - x_6) u_1$, $\frac{\partial f_6}{\partial x_4} = 0$, $\frac{\partial f_6}{\partial x_5} = 0$ and $\frac{\partial f_6}{\partial x_6} = -\frac{1}{L_i} \cos(x_3 - x_6) u_1$.

In a similar manner one finds

The first row of the Jacobian matrix $B = \nabla_u f(x, u) |_{(x^*, u^*)}$ is $\frac{\partial f_1}{\partial u_1} = \cos(x_3)$, $\frac{\partial f_1}{\partial u_2} = 0$,

The second row of the Jacobian matrix $B = \nabla_u f(x, u) |_{(x^*, u^*)}$ is $\frac{\partial f_2}{\partial u_1} = \sin(x_3)$, $\frac{\partial f_2}{\partial u_2} = 0$,

The third row of the Jacobian matrix $B = \nabla_u f(x, u) |_{(x^*, u^*)}$ is $\frac{\partial f_3}{\partial u_1} = 0, \frac{\partial f_3}{\partial u_2} = 1,$

The fourth row of the Jacobian matrix $B = \nabla_u f(x, u) |_{(x^*, u^*)}$ is $\frac{\partial f_4}{\partial u_1} = \cos(x_3 - x_6)\cos(x_6), \frac{\partial f_4}{\partial u_2} = 0,$

The fifth row of the Jacobian matrix $B = \nabla_u f(x, u) |_{(x^*, u^*)}$ is $\frac{\partial f_5}{\partial u_1} = \cos(x_3 - x_6)\sin(x_6), \frac{\partial f_5}{\partial u_2} = 0,$

The sixth row of the Jacobian matrix $B = \nabla_u f(x, u) |_{(x^*, u^*)}$ is $\frac{\partial f_6}{\partial u_1} = \frac{1}{L^i}\sin(x_3 - x_6), \frac{\partial f_6}{\partial u_2} = 0,$

8.3.3 The Nonlinear H-Infinity Control

8.3.3.1 Mini-Max Control and Disturbance Rejection

The initial nonlinear model of the truck and trailer system is in the form

$$\dot{x} = f(x, u) \quad x \in R^n, \quad u \in R^m \quad (8.74)$$

Linearization of the system (truck and trailer) is performed at each iteration of the control algorithm round its present operating point $(x^*, u^*) = (x(t), u(t - T_s))$. The linearized equivalent model of the system is described by

$$\dot{x} = Ax + Bu + L\tilde{d} \quad x \in R^n, \quad u \in R^m, \quad \tilde{d} \in R^q \quad (8.75)$$

where matrices A and B are obtained from the computation of the Jacobians matrices of the truck and trailer's state-space model and vector \tilde{d} denotes disturbance terms due to linearization errors. The problem of disturbance rejection for the linearized model that is described by

$$\begin{aligned} \dot{x} &= Ax + Bu + L\tilde{d} \\ y &= Cx \end{aligned} \quad (8.76)$$

where $x \in R^n, u \in R^m, \tilde{d} \in R^q$ and $y \in R^p$, cannot be handled efficiently if the classical LQR control scheme is applied. This because of the existence of the perturbation term \tilde{d} . The disturbance term \tilde{d} apart from modeling (parametric) uncertainty and external perturbation terms can also represent noise terms of any distribution.

Adhering to the previous applications of the H_∞ control approach, a feedback control scheme is designed for trajectory tracking by the system's state vector and

simultaneous disturbance rejection, considering that the disturbance affects the system in the worst possible manner. The disturbances' effect are incorporated in the following quadratic cost function:

$$J(t) = \frac{1}{2} \int_0^T [y^T(t)y(t) + ru^T(t)u(t) - \rho^2 \tilde{d}^T(t)\tilde{d}(t)]dt, \quad r, \rho > 0 \quad (8.77)$$

According to the analysis of the previous sections, the significance of the negative sign in the cost function's term that is associated with the perturbation variable $\tilde{d}(t)$ is that the disturbance tries to maximize the cost function $J(t)$ while the control signal $u(t)$ tries to minimize it. The physical meaning of the relation given above is that the control signal and the disturbances compete to each other within a min-max differential game. This problem of min-max optimization can be written as

$$\min_u \max_{\tilde{d}} J(u, \tilde{d}) \quad (8.78)$$

As pointed out in previous cases, the objective of the optimization procedure is to compute a control signal $u(t)$ which can compensate for the worst possible disturbance, that is externally imposed to the system of the truck and trailer system. However, the solution to the min-max optimization problem is directly related to the value of the parameter ρ . This means that there is an upper bound in the disturbances magnitude that can be annihilated by the control signal.

8.3.3.2 H-Infinity Feedback Control

For the linearized system given by Eq. (8.76) the cost function of Eq. (8.77) is defined, where the coefficient r determines the penalization of the control input and the weight coefficient ρ determines the reward of the disturbances' effects. As in previous applications of the H-infinity control it is assumed that (i) The energy that is transferred from the disturbances signal $\tilde{d}(t)$ is bounded, that is $\int_0^\infty \tilde{d}^T(t)\tilde{d}(t)dt < \infty$, (ii) matrices $[A, B]$ and $[A, L]$ are stabilizable, (iii) matrix $[A, C]$ is detectable. Then, the optimal feedback control law is given by

$$u(t) = -Kx(t) \quad (8.79)$$

with

$$K = \frac{1}{r} B^T P \quad (8.80)$$

where P is a positive semi-definite symmetric matrix which is obtained from the solution of the Riccati equation

$$A^T P + PA + Q - P \left(\frac{1}{r} BB^T - \frac{1}{2\rho^2} LL^T \right) P = 0 \quad (8.81)$$

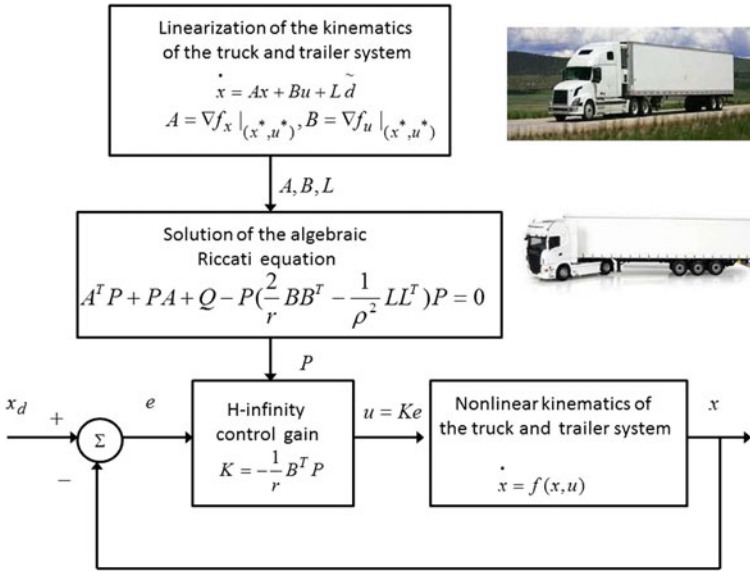


Fig. 8.15 Diagram of the nonlinear optimal control scheme for the truck and trailer system

where Q is also a positive definite symmetric matrix. The worst case disturbance is given by

$$\tilde{d}(t) = \frac{1}{\rho^2} L^T P x(t) \tag{8.82}$$

The diagram of the considered control loop is depicted in Fig. 8.15.

8.3.4 Lyapunov Stability Analysis

Through Lyapunov stability analysis it will be shown that the proposed nonlinear control scheme assures H_∞ tracking performance for the control loop of the truck and trailer system. Moreover, under moderate conditions asymptotic stability is proven and convergence to the reference setpoints is achieved. The tracking error dynamics for the truck and trailer system is written in the form

$$\dot{e} = Ae + Bu + L\tilde{d} \tag{8.83}$$

where in this autonomous vehicle's case $L = I \in R^{6 \times 6}$ with I being the identity matrix. Variable \tilde{d} denotes model uncertainties and external disturbances of the truck and trailer model. The following Lyapunov function is considered

$$V = \frac{1}{2}e^T P e \quad (8.84)$$

where $e = x - x_d$ is the tracking error. By differentiating with respect to time one obtains

$$\begin{aligned} \dot{V} &= \frac{1}{2}\dot{e}^T P e + \frac{1}{2}e^T P \dot{e} \Rightarrow \\ \dot{V} &= \frac{1}{2}[Ae + Bu + L\tilde{d}]^T P + \frac{1}{2}e^T P [Ae + Bu + L\tilde{d}] \Rightarrow \end{aligned} \quad (8.85)$$

$$\begin{aligned} \dot{V} &= \frac{1}{2}[e^T A^T + u^T B^T + \tilde{d}^T L^T] P e + \\ &+ \frac{1}{2}e^T P [Ae + Bu + L\tilde{d}] \Rightarrow \end{aligned} \quad (8.86)$$

$$\begin{aligned} \dot{V} &= \frac{1}{2}e^T A^T P e + \frac{1}{2}u^T B^T P e + \frac{1}{2}\tilde{d}^T L^T P e + \\ &\frac{1}{2}e^T P A e + \frac{1}{2}e^T P B u + \frac{1}{2}e^T P L \tilde{d} \end{aligned} \quad (8.87)$$

The previous equation is rewritten as

$$\begin{aligned} \dot{V} &= \frac{1}{2}e^T (A^T P + P A) e + \left(\frac{1}{2}u^T B^T P e + \frac{1}{2}e^T P B u \right) + \\ &+ \left(\frac{1}{2}\tilde{d}^T L^T P e + \frac{1}{2}e^T P L \tilde{d} \right) \end{aligned} \quad (8.88)$$

Assumption: For given positive definite matrix Q and coefficients r and ρ there exists a positive definite matrix P , which is the solution of the following matrix equation

$$A^T P + P A = -Q + P \left(\frac{2}{r} B B^T - \frac{1}{\rho^2} L L^T \right) P \quad (8.89)$$

Moreover, the following feedback control law is applied to the system

$$u = -\frac{1}{r} B^T P e \quad (8.90)$$

By substituting Eqs. (8.89) and (8.90) one obtains

$$\begin{aligned} \dot{V} &= \frac{1}{2}e^T \left[-Q + P \left(\frac{2}{r} B B^T - \frac{1}{2\rho^2} L L^T \right) P \right] e + \\ &+ e^T P B \left(-\frac{1}{r} B^T P e \right) + e^T P L \tilde{d} \Rightarrow \end{aligned} \quad (8.91)$$

$$\begin{aligned} \dot{V} = & -\frac{1}{2}e^T Qe + \left(\frac{2}{r}PBB^T Pe - \frac{1}{2\rho^2}e^T PLL^T \right) Pe \\ & - \frac{1}{r}(e^T PBB^T Pe) + e^T PL\tilde{d} \end{aligned} \quad (8.92)$$

which after intermediate operations gives

$$\dot{V} = -\frac{1}{2}e^T Qe - \frac{1}{2\rho^2}e^T PLL^T Pe + e^T PL\tilde{d} \quad (8.93)$$

or, equivalently

$$\begin{aligned} \dot{V} = & -\frac{1}{2}e^T Qe - \frac{1}{2\rho^2}e^T PLL^T Pe + \\ & + \frac{1}{2}e^T PL\tilde{d} + \frac{1}{2}\tilde{d}^T L^T Pe \end{aligned} \quad (8.94)$$

Lemma: The following inequality holds

$$\frac{1}{2}e^T L\tilde{d} + \frac{1}{2}\tilde{d}^T L^T Pe - \frac{1}{2\rho^2}e^T PLL^T Pe \leq \frac{1}{2}\rho^2\tilde{d}^T \tilde{d} \quad (8.95)$$

Proof: The binomial $(\rho a - \frac{1}{\rho}b)^2$ is considered. Expanding the left part of the above inequality one gets

$$\begin{aligned} \rho^2 a^2 + \frac{1}{\rho^2} b^2 - 2ab \geq 0 & \Rightarrow \frac{1}{2}\rho^2 a^2 + \frac{1}{2\rho^2} b^2 - ab \geq 0 \Rightarrow \\ ab - \frac{1}{2\rho^2} b^2 \leq \frac{1}{2}\rho^2 a^2 & \Rightarrow \frac{1}{2}ab + \frac{1}{2}ab - \frac{1}{2\rho^2} b^2 \leq \frac{1}{2}\rho^2 a^2 \end{aligned} \quad (8.96)$$

The following substitutions are carried out: $a = \tilde{d}$ and $b = e^T PL$ and the previous relation becomes

$$\frac{1}{2}\tilde{d}^T L^T Pe + \frac{1}{2}e^T PL\tilde{d} - \frac{1}{2\rho^2}e^T PLL^T Pe \leq \frac{1}{2}\rho^2\tilde{d}^T \tilde{d} \quad (8.97)$$

Equation (8.97) is substituted in Eq. (8.94) and the inequality is enforced, thus giving

$$\dot{V} \leq -\frac{1}{2}e^T Qe + \frac{1}{2}\rho^2\tilde{d}^T \tilde{d} \quad (8.98)$$

Equation (8.98) shows that the H_∞ tracking performance criterion is satisfied. The integration of \dot{V} from 0 to T gives

$$\begin{aligned} \int_0^T \dot{V}(t) dt &\leq -\frac{1}{2} \int_0^T \|e\|_Q^2 dt + \frac{1}{2} \rho^2 \int_0^T \|\tilde{d}\|^2 dt \Rightarrow \\ 2V(T) + \int_0^T \|e\|_Q^2 dt &\leq 2V(0) + \rho^2 \int_0^T \|\tilde{d}\|^2 dt \end{aligned} \quad (8.99)$$

Moreover, if there exists a positive constant $M_d > 0$ such that

$$\int_0^\infty \|\tilde{d}\|^2 dt \leq M_d \quad (8.100)$$

then one gets

$$\int_0^\infty \|e\|_Q^2 dt \leq 2V(0) + \rho^2 M_d \quad (8.101)$$

Thus, the integral $\int_0^\infty \|e\|_Q^2 dt$ is bounded. Moreover, $V(T)$ is bounded and from the definition of the Lyapunov function V in Eq. (8.84) it becomes clear that $e(t)$ will be also bounded since $e(t) \in \Omega_e = \{e | e^T P e \leq 2V(0) + \rho^2 M_d\}$. According to the above and with the use of Barbalat's Lemma one obtains $\lim_{t \rightarrow \infty} e(t) = 0$.

8.3.5 Robust State Estimation with the Use of the H-Infinity Kalman Filter

The control loop for the truck and trailer system can be implemented with the feedback of a partially measurable state vector and by processing only a small number of state variables. To reconstruct the missing information about the state vector of the autonomous vehicle it is proposed to use a filtering scheme which allows to apply state estimation-based control [457]. The recursion of the H_∞ Kalman Filter, can be formulated in terms of a *measurement update* and a *time update* part

Measurement update:

$$\begin{aligned} D(k) &= [I - \theta W(k)P^-(k) + C^T(k)R(k)^{-1}C(k)P^-(k)]^{-1} \\ K(k) &= P^-(k)D(k)C^T(k)R(k)^{-1} \\ \hat{x}(k) &= \hat{x}^-(k) + K(k)[y(k) - C\hat{x}^-(k)] \end{aligned} \quad (8.102)$$

Time update:

$$\begin{aligned} \hat{x}^-(k+1) &= A(k)x(k) + B(k)u(k) \\ P^-(k+1) &= A(k)P^-(k)D(k)A^T(k) + Q(k) \end{aligned} \tag{8.103}$$

where it is assumed that parameter θ is sufficiently small to assure that the covariance matrix $P^-(k)^{-1} - \theta W(k) + C^T(k)R(k)^{-1}C(k)$ will be positive definite. When $\theta = 0$ the H_∞ Kalman Filter becomes equivalent to the standard Kalman Filter. One can measure only a part of the state vector of the system of the truck and trailer system, such as state variables x_i $i = 1, 2$ (cartesian coordinates of the truck) and can estimate through filtering the rest of the state vector elements.

8.3.6 Simulation Tests

The performance of the proposed nonlinear optimal control scheme for the autonomous truck and trailer vehicle has been tested in the case of tracking of different reference setpoints. The control scheme exhibited fast and accurate tracking of the reference paths. The computation of the feedback control gain required the solution of the algebraic Riccati equation given in Eq. (8.89), at each iteration of the control algorithm. The obtained results are depicted in Figs. 8.16, 8.17 and 8.18. It can be noticed that the H-infinity controller achieved fast and accurate convergence to the reference setpoints for all elements of the vehicle’s state-vector. Moreover, the variations of the control inputs, that is of the truck’s velocity and of the truck’s steering angle were smooth.

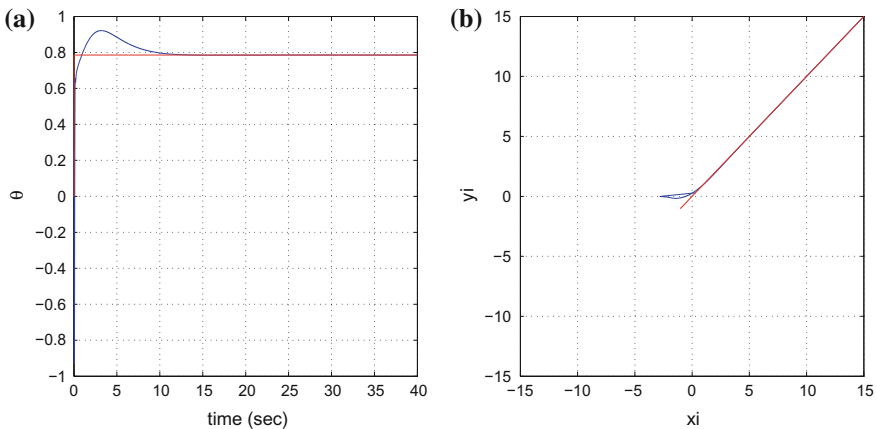


Fig. 8.16 **a** tracking of reference setpoint 1 (red-line) by the heading angle θ of the truck (blue line), **b** tracking of reference path (red line) on the xy -plane by the center of the rear wheel axis of the trailer (blue line)

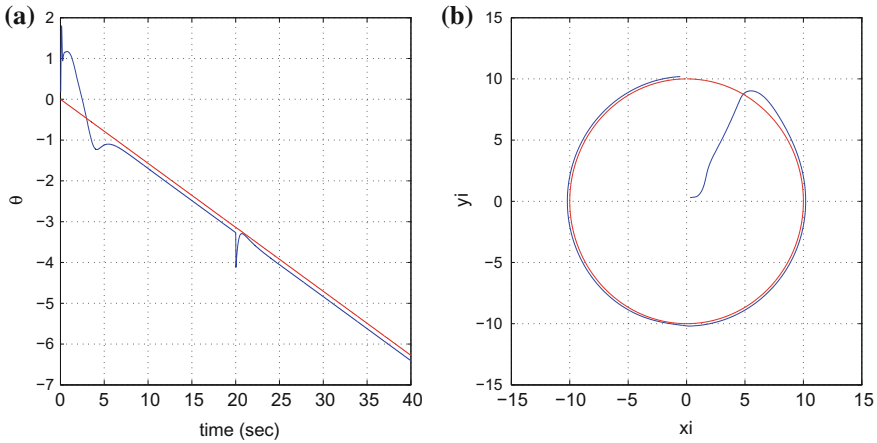


Fig. 8.17 **a** tracking of reference setpoint 2 (red-line) by the heading angle θ of the truck (blue line), **b** tracking of reference path (red line) on the xy -plane by the center of the rear wheel axis of the trailer (blue line)

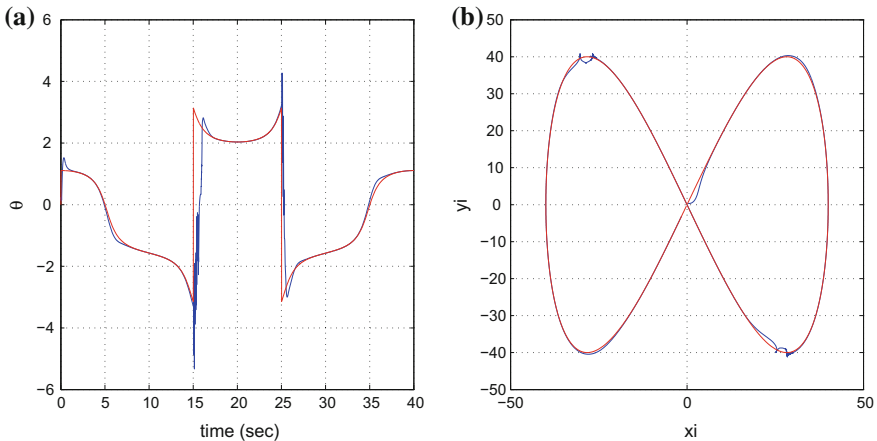


Fig. 8.18 **a** tracking of reference setpoint 3 (red-line) by the heading angle θ of the truck (blue line), **b** tracking of reference path (red line) on the xy -plane by the center of the rear wheel axis of the trailer (blue line)

As noted, the proposed nonlinear optimal control method for the truck and trailer model was based on an approximate linearization of the vehicle’s kinematics. Comparing to nonlinear feedback control approaches which are based on exact feedback linearization, the proposed H_∞ control scheme for the autonomous vehicle has the following features: (i) it uses an approximate linear description of the system’s kinematics which does not follow the elaborated transformations (diffeomorphisms) met in exact linearization methods, (ii) it is applied directly on the initial nonlinear

model of the vehicle. Thus, the computation of the control inputs which are applied to the vehicle does not require inverse transformations and avoids singularities, (iii) it retains the advantages of typical optimal control, that is accurate tracking of the reference trajectories through moderate variations of the control inputs.

8.4 Nonlinear Optimal Feedback Control of Four-Wheel Steering Autonomous Vehicles

8.4.1 Outline

Four-wheel steering (4WS) autonomous vehicles can exhibit improved maneuverability comparing to two-wheel steering vehicles. There are several examples of applications of 4WS autonomous vehicles in transportation, in security and defense tasks as well as in agriculture [7, 70, 213, 364]. In an aim to improve the steering capabilities of autonomous vehicles and mobile robots there have been several efforts to solve the problem of control of 4WS systems. The description of the kinematics and dynamics of 4WS vehicles typically takes the form of nonlinear models. However under specific assumptions such models can be locally simplified into a linear form and linear control methods can be considered. [67, 195, 381, 478, 586]. One can note also results on nonlinear model-based control for 4WS vehicles [216, 257, 306, 390]. In several approaches it is attempted to decouple the vehicle's multi-variable dynamics into simpler loops which are controlled independently [269, 270, 282, 317]. The efficiency of the aforementioned control methods depends on the proximity of the model considered for the controller's design to the real nonlinear dynamics of the vehicle [283, 578, 584].

In the present section, a nonlinear H-infinity (optimal) controller is introduced for the motion control problem of 4WS vehicles [419, 461]. The design of the controller remains consistent with the precise nonlinear dynamics of the four-wheel steering vehicle. As in previous applications of nonlinear optimal control the 4WS vehicle's kinematic and dynamic model undergoes first approximate linearization around a temporary operating point (equilibrium) which is recomputed at each iteration of the control algorithm. The equilibrium is defined by the present value of the system's state vector and the last value of the control inputs vector that was exerted on it. The linearization makes use of first order Taylor series expansion of the state-space description of the vehicle and requires the computation of the associated Jacobian matrices [33, 431, 463]. The modelling error due to truncation of higher order terms in the Taylor series expansion is considered as a perturbation which is asymptotically eliminated by the robustness of the control algorithm. Next, for the approximately linearized model of the 4WS vehicle an H-infinity feedback controller is designed.

The H-infinity controller stands for the solution to the optimal control problem for the 4WS vehicle under model uncertainty and external perturbations. As previously noted, it represents the solution to a min-max differential game in which the controller tries to minimize a cost function that comprises a quadratic term of the state vector's tracking error, whereas the model uncertainty and the external perturbations try to maximize this cost function. To compute the feedback gain of the H-infinity controller an algebraic Riccati equation has to be solved at each time step of the control method [450, 457, 460]. The stability properties of the control scheme are confirmed through Lyapunov analysis. First, it is shown that the control loop satisfies the H-infinity tracking performance criterion, which ascertains elevated robustness against model inconsistencies and external disturbances [305, 564]. Moreover, under moderate conditions the global asymptotic stability of the control scheme is proven. Finally, to implement state estimation-based control for the 4WS vehicle without the need to process measurements from a large number of on-board sensors the H-infinity Kalman Filter is used as a robust state estimator [169, 511].

Comparing to other control methods for the problem of motion control of autonomous vehicles and mobile robots the following can be noted [450, 457, 460]: (i) PID control which is widely used by practitioners in the area of robotics is finally an unreliable methodology because the tuning of such a controller is performed in a heuristic manner around local operating points where the unrealistic assumption is made that the dynamics of the 4WS vehicle remains linear. Such a control method lacks a global stability proof. (ii) On the other side the application of global linearization-based control methods to 4WS vehicles is hindered by the complexity of the associated state-space transformations that finally allow for describing the vehicle's dynamics into a linear canonical form. Besides this method may come against singularity problems because it requires inverse transformations for computing the control signal that will be finally applied to the initial nonlinear system of the 4WS vehicle. (iii) As far as optimal control methods for autonomous vehicles is concerned, the use of model predictive control is unsuccessful because this control method is addressed to linear dynamics and cannot compensate for the nonlinearities of the 4WS vehicle state-space model. On the other side the use of nonlinear model-predictive control for 4WS vehicles can be of questionable performance because its iterative search for an optimum is not of assured convergence and depends on initial parametrization, (iv) Finally, sliding mode control cannot be applied directly to the model of the 4WS vehicles because this is not inherently found into a canonical form. Additionally, the application of backstepping control approaches is hindered by the fact that the state-space description of 4WS vehicles is not found into a triangular form. For the aforementioned reasons, nonlinear optimal (H-infinity) control is one of the most efficient solutions one can have for the control problem of autonomous navigation of 4WS vehicles.

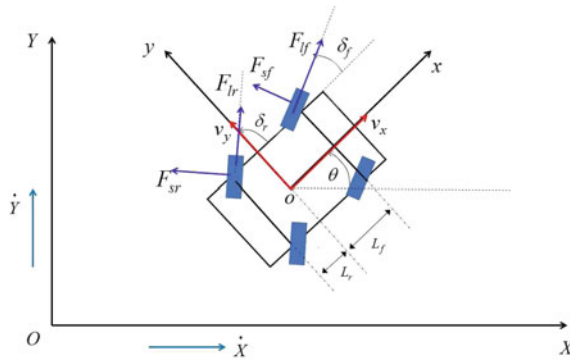


Fig. 8.19 Reference axes for the motion of the 4WS autonomous vehicle: the velocity of the vehicle is decomposed in two components in a body-fixed reference frame xOy . The control inputs for the 4WS vehicle are (i) the longitudinal force F_{lf} and F_{lr} at the wheels of the front and rear axes, provided by the vehicle’s engine or actuators, (ii) the turn angle of the front wheels δ_f , (iii) the turn angle of the rear wheels δ_r .

8.4.2 Modelling of the Kinematics and Dynamics of the 4WS Autonomous Vehicle

8.4.2.1 Outline of the Model of the 4WS Vehicle

Important parameters and variables in the 4WS vehicle model are: (i) the vehicle’s velocity v , which is a vector forming an angle β with the transversal axis of the vehicle. It can be decomposed in two components, a velocity V_x which is aligned with the horizontal axis Ox in a body-fixed reference frame and a velocity V_y which is aligned with the vertical axis Oy in such a body-fixed reference frame (Fig. 8.19), (ii) the vehicle’s mass m and its moment of inertia I for rotation around the Oz axis, (iii) the cornering stiffness coefficients c_f and c_r of the front and rear wheels of the vehicle.

The control inputs to the model of the 4WS vehicle are defined as follows: (i) the traction force that is exerted on the vehicle (ii) the turn angle of the front wheels (or the first derivative of this turn angle) (iii) the turn angle of the rear wheels (or the first derivative of this turn angle).

The difference between the turn angle of the vehicle’s wheels δ and the angle formed between the vehicle’s velocity and the vehicle’s transversal axis β , is the side-slip angle of the vehicle and is denoted by $a = \delta - \beta$.

The forces exerted on the 4WS vehicle are defined as follows: (i) the longitudinal force F_l which in turn is defined by the traction force of the vehicle’s engine or by the force developed by the vehicle’s breaking system, (ii) the side or transversal force F_s which depends on the vehicle’s side-slip angle a and on the reaction force F_z developed by the front and rear axle of the vehicle for compensating the vehicle’s weight or additional load.

About the X-axis forces, in the body-fixed reference frame for the vehicle one has that [216]:

$$\begin{aligned} F_{xf} &= F_{lf} \cos(\delta_f) - F_{sf} \sin(\delta_f) \\ F_{xr} &= F_{lr} \cos(\delta_r) - F_{sr} \sin(\delta_r) \end{aligned} \quad (8.104)$$

Under the assumption of a small turn angle of the vehicle's wheel, that is $\cos(\delta_f) \simeq 1$, $\sin(\delta_f) \simeq \delta_f$ and $\cos(\delta_r) \simeq 1$, $\sin(\delta_r) \simeq \delta_r$ one gets [216]:

$$\begin{aligned} F_{xf} &= F_{lf} - F_{sf} \delta_f \\ F_{xr} &= F_{lr} - F_{sr} \delta_r \end{aligned} \quad (8.105)$$

About the Y-axis forces, in the body-fixed reference frame for the vehicle one has that (Fig. 8.20):

$$\begin{aligned} F_{yf} &= F_{sf} \cos(\delta_f) + F_{lf} \sin(\delta_f) \\ F_{yr} &= F_{sr} \cos(\delta_r) + F_{lr} \sin(\delta_r) \end{aligned} \quad (8.106)$$

Again, under the assumption of a small turn angle of the vehicle's wheel, that is $\cos(\delta_f) \simeq 1$, $\sin(\delta_f) \simeq \delta_f$ and $\cos(\delta_r) \simeq 1$, $\sin(\delta_r) \simeq \delta_r$ one gets:

$$\begin{aligned} F_{yf} &= F_{sf} + F_{lf} \delta_f \\ F_{yr} &= F_{sr} + F_{lr} \delta_r \end{aligned} \quad (8.107)$$

Next, by considering that the vehicle's motion is expressed in a body-fixed frame and that Coriolis effects have to be taken into account, the equations of motion of the 4WS vehicle become

$$m(\dot{v}_x - rv_y) = F_{lf} + F_{lr} - F_{sf} \delta_f - F_{sr} \delta_r - c_a v_x^2 \quad (8.108)$$

$$m(\dot{v}_y + rv_x) = F_{lf} \delta_f + F_{lr} \delta_r + F_{sf} + F_{sr} \delta_r \quad (8.109)$$

$$I \dot{r} = l_f (F_{lf} \delta_f + F_{sf}) - l_r (F_{lr} \delta_r + F_{sr}) \quad (8.110)$$

8.4.2.2 Kinematic and Dynamic Model of the 4WS Vehicle

The dynamic model of the 4WS vehicle was shown to be given by Eqs. (8.108), (8.109) and (8.110). In this model F_{lf} and F_{lr} are the traction forces generated by the engine of the vehicle or by electric actuators and exerted on the wheels of the front rear axles respectively. The control inputs of the vehicle are (i) the traction forces u_1 , given by F_{lf} and F_{lr} (ii) the angle of the wheels of the front axle, that is $\delta_f = u_2$, (iii) the angle of the wheels of the rear axle, that is $\delta_r = u_3$.

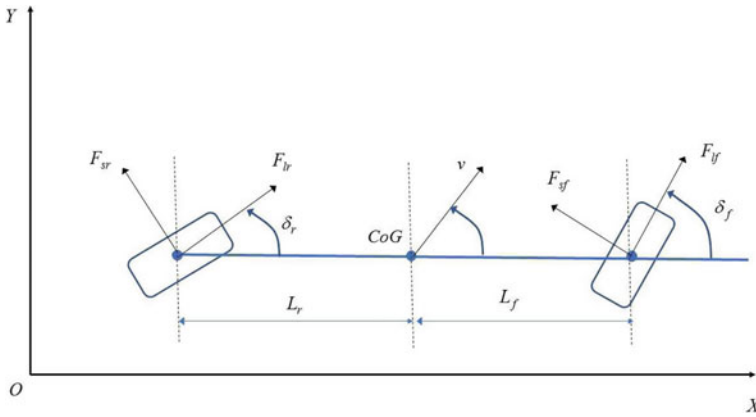


Fig. 8.20 Diagram of the 4 WS vehicle

About the side forces exerted on the front wheels of the vehicle one has

$$F_{s_f} = \frac{m}{l}(gl_r - \dot{v}_x h)c_f a_f \Rightarrow F_{s_f} = \frac{mgl_r}{l}c_f a_f - \frac{m\dot{v}_x h}{l}c_f a_f \tag{8.111}$$

and by considering that $\dot{v}_x \ll g$ and $h \ll l$ (h is the height of the center of gravity of the vehicle) one has that the term $\frac{m\dot{v}_x h}{l}c_f a_f$ can be considered as moderate disturbance which can be omitted. Thus, the model of the side force being exerted on the front wheels is given by

$$F_{s_f} = \frac{m}{l}(gl_r - \dot{v}_x h)c_f a_f \Rightarrow F_{s_f} = \frac{mgl_r}{l}c_f a_f \tag{8.112}$$

or equivalently

$$F_{s_f} = \frac{m}{l}(gl_r)c_f \left(u_2 - \frac{v_y + l_f r}{v_x} \right) \tag{8.113}$$

where it has been used that $a_f = \delta_f - \beta_f$ and $\beta_f = \frac{v_y + l_f r}{v_x}$

About the side forces exerted on the rear wheels of the vehicle one has

$$F_{s_r} = \frac{m}{l}(gl_f - \dot{v}_x h)c_r a_r \Rightarrow F_{s_r} = \frac{mgl_f}{l}c_r a_r - \frac{m\dot{v}_x h}{l}c_r a_r \tag{8.114}$$

and by considering that $\dot{v}_x \ll g$ and $h \ll l$ one has that the term $\frac{m\dot{v}_x h}{l}c_r a_r$ can be considered as moderate disturbance which can be omitted. Thus, the model of the force being exerted on the front wheels is given by

$$F_{s_r} = \frac{m}{l}(gl_f)c_r a_r \Rightarrow F_{s_r} = \frac{mgl_f}{l}c_r a_r, \tag{8.115}$$

or equivalently

$$F_{s_r} = \frac{m}{l}(gl_f)c_r \left(u_3 - \frac{v_y - l_r r}{v_x} \right) \quad (8.116)$$

where it has been used that $a_r = \delta_r - \beta_r$ and $\beta_r = \frac{v_y - l_r r}{v_x}$.

Consequently, the side forces exerted on the wheels of the vehicle are given by [216]

$$\begin{aligned} F_{s_f} &= \frac{m}{l}(gl_r)c_f \left(u_2 - \frac{v_y + l_r r}{v_x} \right) \\ F_{s_r} &= \frac{m}{l}(gl_f)c_r \left(u_3 - \frac{v_y - l_r r}{v_x} \right) \end{aligned} \quad (8.117)$$

Using Eq.(8.117) in (8.108)–(8.110) one obtains the following equations for the dynamic model of the 4WS autonomous vehicle:

$$\begin{aligned} m\dot{v}_x &= mr v_y + u_1 + u_1 - \frac{m}{l}(gl_r)c_f \left(u_2 - \frac{v_y + l_r r}{v_x} \right) u_2 - \\ &\quad - \frac{m}{l}(gl_f)c_r \left(u_3 - \frac{v_y - l_r r}{v_x} \right) u_3 - c_a v_x^2 \end{aligned} \quad (8.118)$$

$$\begin{aligned} m\dot{v}_y &= -mr v_x + u_1 u_2 + u_1 u_3 + \frac{m}{l}(gl_r)c_f \left(u_2 - \frac{v_y + l_r r}{v_x} \right) + \\ &\quad + \frac{m}{l}(gl_f)c_r \left(u_3 - \frac{v_y - l_r r}{v_x} \right) \end{aligned} \quad (8.119)$$

$$\begin{aligned} I\dot{r} &= l_f \left[(u_1 u_2) + \frac{m}{l}(gl_r)c_f \left(u_2 - \frac{v_y + l_r r}{v_x} \right) \right] - \\ &\quad - l_r \left[(u_1 u_3) + \frac{m}{l}(gl_f)c_r \left(u_3 - \frac{v_y - l_r r}{v_x} \right) \right] \end{aligned} \quad (8.120)$$

Moreover, taking that (x, y) are the cartesian coordinates and θ is the orientation angle of the vehicle, then the following equations about the 4WS vehicle kinematics are considered:

$$\dot{x} = v_x \cos(\theta) - v_y \sin(\theta) \quad (8.121)$$

$$\dot{y} = v_x \sin(\theta) + v_y \cos(\theta) \quad (8.122)$$

$$\dot{\theta} = r \quad (8.123)$$

After a re-arrangement of Eqs.(8.121)–(8.123) and (8.118)–(8.120), the state-space description of the 4WS is given as follows:

$$\dot{x} = v_x \cos(\theta) - v_y \sin(\theta) \quad (8.124)$$

$$\dot{y} = v_x \sin(\theta) + v_y \cos(\theta) \quad (8.125)$$

$$\begin{aligned} \dot{v}_x = & rv_y + \frac{2}{m}u_1 - \frac{1}{l}(gl_r)c_f \left(u_2 - \frac{v_y + l_r r}{v_x} \right) u_2 - \\ & - \frac{1}{l}(gl_f)c_r \left(u_3 - \frac{v_y - l_r r}{v_x} \right) u_3 - \frac{c_a}{m}v_x^2 \end{aligned} \quad (8.126)$$

$$\begin{aligned} \dot{v}_y = & -rv_x + \frac{1}{m}u_1u_2 + \frac{1}{m}u_1u_3 + \frac{1}{l}(gl_r)c_f \left(u_2 - \frac{v_y + l_r r}{v_x} \right) + \\ & + \frac{1}{l}(gl_f)c_r \left(u_3 - \frac{v_y - l_r r}{v_x} \right) \end{aligned} \quad (8.127)$$

$$\dot{\theta} = r \quad (8.128)$$

$$\begin{aligned} \dot{r} = & \frac{l_f}{I} \left[(u_1u_2) + \frac{m}{Il}(gl_r)c_f \left(u_2 - \frac{v_y + l_r r}{v_x} \right) \right] - \\ & - \frac{l_r}{I} \left[(u_1u_3) + \frac{m}{Il}(gl_f)c_r \left(u_3 - \frac{v_y - l_r r}{v_x} \right) \right] \end{aligned} \quad (8.129)$$

By defining the system's state vector as $X = [x, y, v_x, v_y, \theta, r]^T$ one obtains the following state-space description for the 4WS vehicle

$$\dot{x}_1 = x_3 \cos(x_5) - x_4 \sin(x_5) \quad (8.130)$$

$$\dot{x}_2 = x_3 \sin(x_5) + x_4 \cos(x_5) \quad (8.131)$$

$$\begin{aligned} \dot{x}_3 = & x_4x_6 + \frac{2}{m}u_1 - \frac{1}{l}(gl_r)c_f \left(u_2 - \frac{x_4 + l_r x_6}{x_3} \right) u_2 - \\ & - \frac{1}{l}(gl_f)c_r \left(u_3 - \frac{x_4 - l_r x_6}{x_3} \right) u_3 - \frac{c_a}{m}x_3^2 \end{aligned} \quad (8.132)$$

$$\begin{aligned} \dot{x}_4 = & -x_3x_6 + \frac{1}{m}u_1u_2 + \frac{1}{m}u_1u_3 + \frac{1}{l}(gl_r)c_f \left(u_2 - \frac{x_4 + l_r x_6}{x_3} \right) + \\ & + \frac{1}{l}(gl_f)c_r \left(u_3 - \frac{x_4 - l_r x_6}{x_3} \right) \end{aligned} \quad (8.133)$$

$$\dot{x}_5 = x_6 \quad (8.134)$$

$$\begin{aligned} \dot{x}_6 = & \frac{l_f}{I} \left[(u_1 u_2) + \frac{m}{Il} (gl_r) c_f \left(u_2 - \frac{x_4 + l_r x_6}{x_3} \right) \right] - \\ & - \frac{l_r}{I} \left[(u_1 u_3) + \frac{m}{Il} (gl_f) c_r \left(u_3 - \frac{x_4 - l_r x_6}{x_3} \right) \right] \end{aligned} \quad (8.135)$$

Thus, the joint kinematic-dynamic model of the 4WS vehicle is written in the form

$$\dot{x} = f(x, u) \quad (8.136)$$

where $x \in \mathbb{R}^{6 \times 1}$, $u \in \mathbb{R}^{3 \times 1}$, and $f \in \mathbb{R}^{6 \times 1}$.

8.4.3 Approximate Linearization of the Model of the 4WS Vehicle

8.4.3.1 1st Modelling and Linearization Approach

First, linearization of the complete kinematic-dynamic model of the 4WS vehicle is considered. The complete model has been given in Eqs. (8.130)–(8.135). The approximately linearized model of the vehicle is computed around the temporary operating point (equilibrium) (x^*, u^*) , where x^* is the present value of the system's state vector and u^* is the last value of the control input vector exerted on the 4WS vehicle. The linearized model is written as

$$\dot{x} = Ax + Bu + \tilde{d} \quad (8.137)$$

where

$$A = \begin{pmatrix} \frac{\partial f_1}{\partial x_1} & \frac{\partial f_1}{\partial x_2} & \dots & \frac{\partial f_1}{\partial x_6} \\ \frac{\partial f_2}{\partial x_1} & \frac{\partial f_2}{\partial x_2} & \dots & \frac{\partial f_2}{\partial x_6} \\ \dots & \dots & \dots & \dots \\ \frac{\partial f_6}{\partial x_1} & \frac{\partial f_6}{\partial x_2} & \dots & \frac{\partial f_6}{\partial x_6} \end{pmatrix} \Big|_{(x^*, u^*)} \quad B = \begin{pmatrix} \frac{\partial f_1}{\partial u_1} & \frac{\partial f_1}{\partial u_2} & \frac{\partial f_1}{\partial u_3} \\ \frac{\partial f_2}{\partial u_1} & \frac{\partial f_2}{\partial u_2} & \frac{\partial f_2}{\partial u_3} \\ \dots & \dots & \dots \\ \frac{\partial f_6}{\partial u_1} & \frac{\partial f_6}{\partial u_2} & \frac{\partial f_6}{\partial u_3} \end{pmatrix} \Big|_{(x^*, u^*)} \quad (8.138)$$

The computation of the Jacobian matrix $A = \nabla_x f(x, u) \Big|_{(x^*, u^*)}$ proceeds as follows:

For the first row of the Jacobian matrix $A = \nabla_x f(x, u)$ one has: $\frac{\partial f_1}{\partial x_1} = 0$, $\frac{\partial f_1}{\partial x_2} = 0$, $\frac{\partial f_1}{\partial x_3} = \cos(x_5)$, $\frac{\partial f_1}{\partial x_4} = -\sin(x_5)$, $\frac{\partial f_1}{\partial x_5} = -x_3 \sin(x_5) + x_4 \cos(x_5)$, $\frac{\partial f_1}{\partial x_6} = 0$.

For the second row of the Jacobian matrix $A = \nabla_x f(x, u)$ one has: $\frac{\partial f_2}{\partial x_1} = 0$, $\frac{\partial f_2}{\partial x_2} = 0$, $\frac{\partial f_2}{\partial x_3} = \sin(x_5)$, $\frac{\partial f_2}{\partial x_4} = \cos(x_5)$, $\frac{\partial f_2}{\partial x_5} = x_3 \cos(x_5) - x_5 \sin(x_5)$, $\frac{\partial f_2}{\partial x_6} = 0$,

For the third row of the Jacobian matrix $A = \nabla_x f(x, u)$ one has: $\frac{\partial f_3}{\partial x_1} = 0$, $\frac{\partial f_3}{\partial x_2} = 0$, $\frac{\partial f_3}{\partial x_3} = \frac{gl_r c_f}{l} \left(-\frac{x_4 + l_f x_6}{x_3^2} \right) u_2 - \frac{gl_f c_r}{l} \left(-\frac{x_4 - l_r x_6}{x_3^2} \right) u_3 - \frac{c_a}{m} 2x_3$, $\frac{\partial f_3}{\partial x_4} = x_6 + \frac{gl_r c_f}{l} \frac{1}{x_3} u_2$, $\frac{\partial f_3}{\partial x_5} = 0$, $\frac{\partial f_3}{\partial x_6} = x_4 + \frac{gl_r c_f}{l} \frac{l_f}{x_3} u_2 - \frac{gl_f c_r}{l} \frac{l_r}{x_3} u_3$

For the fourth row of the Jacobian matrix $A = \nabla_x f(x, u)$ one has: $\frac{\partial f_4}{\partial x_1} = 0$, $\frac{\partial f_4}{\partial x_2} = 0$, $\frac{\partial f_4}{\partial x_3} = -x_6 + \frac{gl_r c_f}{l} \frac{x_4 + l_f x_6}{x_3^2} + \frac{gl_f c_r}{l} \frac{x_4 - l_r x_6}{x_3^2}$, $\frac{\partial f_4}{\partial x_4} = \frac{gl_r c_f}{l} - \frac{1}{x_3} u_2 + \frac{gl_f c_r}{l} - \frac{1}{x_3} u_3$, $\frac{\partial f_4}{\partial x_5} = 0$, $\frac{\partial f_4}{\partial x_6} = -x_3 + \frac{gl_r c_f}{l} \left(-\frac{l_f}{x_3}\right) + \frac{gl_f c_r}{l} \left(\frac{l_r}{x_3}\right)$.

For the fifth row of the Jacobian matrix $A = \nabla_x f(x, u)$ one has: $\frac{\partial f_5}{\partial x_1} = 0$, $\frac{\partial f_5}{\partial x_2} = 0$, $\frac{\partial f_5}{\partial x_3} = 0$, $\frac{\partial f_5}{\partial x_4} = 0$, $\frac{\partial f_5}{\partial x_5} = 0$, $\frac{\partial f_5}{\partial x_6} = 1$.

For the sixth row of the Jacobian matrix $A = \nabla_x f(x, u)$ one has: $\frac{\partial f_6}{\partial x_1} = 0$, $\frac{\partial f_6}{\partial x_2} = 0$, $\frac{\partial f_6}{\partial x_3} = \frac{l_f m g l_r}{l l} c_f \frac{x_4 + l_f x_6}{x_3^2} - \frac{l_r m g l_f}{l l} c_r \frac{x_4 - l_r x_6}{x_3^2}$, $\frac{\partial f_6}{\partial x_4} = \frac{l_f m g l_r}{l l} c_f \left(-\frac{1}{x_3}\right) - \frac{l_r m g l_f}{l l} c_r \left(\frac{1}{x_3}\right)$, $\frac{\partial f_6}{\partial x_5} = 0$, $\frac{\partial f_6}{\partial x_6} = \frac{l_f m g l_r}{l l} c_f \left(-\frac{l_f}{x_3}\right) - \frac{l_r m g l_f}{l l} c_r \left(-\frac{l_r}{x_3}\right)$.

The computation of the Jacobian matrix $B = \nabla_u f(x, u) |_{(x^*, u^*)}$ proceeds as follows:

For the first row of the Jacobian matrix $B = \nabla_u f(x, u)$ one has: $\frac{\partial f_1}{\partial u_1} = 0$, $\frac{\partial f_1}{\partial u_2} = 0$, $\frac{\partial f_1}{\partial u_3} = 0$

For the second row of the Jacobian matrix $B = \nabla_u f(x, u)$ one has: $\frac{\partial f_2}{\partial u_1} = 0$, $\frac{\partial f_2}{\partial u_2} = 0$, $\frac{\partial f_2}{\partial u_3} = 0$

For the third row of the Jacobian matrix $B = \nabla_u f(x, u)$ one has: $\frac{\partial f_3}{\partial u_1} = \frac{2}{m}$, $\frac{\partial f_3}{\partial u_2} = -\frac{gl_r c_f}{l} \left(2u_2 - \frac{x_4 + l_f x_6}{x_3}\right)$, $\frac{\partial f_3}{\partial u_3} = -\frac{gl_f c_r}{l} \left(2u_3 - \frac{x_4 - l_r x_6}{x_3}\right)$.

For the fourth row of the Jacobian matrix $B = \nabla_u f(x, u)$ one has: $\frac{\partial f_4}{\partial u_1} = \frac{1}{m} u_2 + \frac{1}{m} u_3$, $\frac{\partial f_4}{\partial u_2} = \frac{1}{m} u_1 + \frac{gl_r c_f}{l}$, $\frac{\partial f_4}{\partial u_3} = \frac{1}{m} u_1 + \frac{gl_f c_r}{l}$.

For the fifth row of the Jacobian matrix $B = \nabla_u f(x, u)$ one has: $\frac{\partial f_5}{\partial u_1} = 0$, $\frac{\partial f_5}{\partial u_2} = 0$, $\frac{\partial f_5}{\partial u_3} = 0$.

For the sixth row of the Jacobian matrix $B = \nabla_u f(x, u)$ one has: $\frac{\partial f_6}{\partial u_1} = \frac{l_f}{l} u_2 - \frac{l_r}{l} u_3$, $\frac{\partial f_6}{\partial u_2} = \frac{l_f m g l_r}{l l} c_f + \frac{l_f}{l} u_1$, $\frac{\partial f_6}{\partial u_3} = -\frac{l_r m g l_f}{l l} c_r - \frac{l_r}{l} u_1$

8.4.3.2 2nd Modelling and Linearization Approach

Next, linearization of a simplified kinematic-dynamic model of the 4WS vehicle is considered. This model is obtained from the complete model given in Eqs. (8.130)–(8.135), after omitting terms comprising squares of the control inputs that is u_i^2 , or products between the control inputs, such as $u_i u_j$. Under such an approach the kinematic-dynamic model of the 4WS vehicle becomes:

$$\dot{x}_1 = x_3 \cos(x_5) - x_4 \sin(x_5) \quad (8.139)$$

$$\dot{x}_2 = x_3 \sin(x_5) + x_4 \cos(x_5) \quad (8.140)$$

$$\begin{aligned} \dot{x}_3 = & x_4 x_6 + \frac{2}{m} u_1 + \frac{1}{l} (gl_r) c_f \left(\frac{x_4 + l_r x_6}{x_3} \right) u_2 - \\ & + \frac{1}{l} (gl_f) c_r \left(\frac{x_4 - l_r x_6}{x_3} \right) u_3 - \frac{c_a}{m} x_3^2 \end{aligned} \quad (8.141)$$

$$\begin{aligned} \dot{x}_4 = & -x_3 x_6 + \frac{1}{l} (gl_r) c_f \left(u_2 - \frac{x_4 + l_r x_6}{x_3} \right) + \\ & + \frac{1}{l} (gl_f) c_r \left(u_3 - \frac{x_4 - l_r x_6}{x_3} \right) \end{aligned} \quad (8.142)$$

$$\dot{x}_5 = x_6 \quad (8.143)$$

$$\begin{aligned} \dot{x}_6 = & \frac{l_f}{I} \left[\frac{m}{Il} (gl_r) c_f \left(u_2 - \frac{x_4 + l_r x_6}{x_3} \right) \right] - \\ & - \frac{l_r}{I} \left[\frac{m}{Il} (gl_f) c_r \left(u_3 - \frac{x_4 - l_r x_6}{x_3} \right) \right] \end{aligned} \quad (8.144)$$

Then, the state-space model of the 4WS autonomous vehicle can be written as:

$$\begin{aligned} \begin{pmatrix} \dot{x}_1 \\ \dot{x}_2 \\ \dot{x}_3 \\ \dot{x}_4 \\ \dot{x}_5 \\ \dot{x}_6 \end{pmatrix} = & \begin{pmatrix} x_3 \cos(x_5) - x_4 \sin(x_5) \\ x_3 \sin(x_5) + x_4 \cos(x_5) \\ x_4 x_6 - \frac{c_a}{m} x_3^2 \\ -x_3 x_6 - \frac{1}{l} (gl_r) c_f \left(\frac{x_4 + l_r x_6}{x_3} \right) - \frac{1}{l} (gl_f) c_r \left(\frac{x_4 - l_r x_6}{x_3} \right) \\ x_6 \\ \frac{l_f}{I} \left[\frac{m}{Il} (gl_r) c_f \left(-\frac{x_4 + l_r x_6}{x_3} \right) \right] - \frac{l_r}{I} \left[\frac{m}{Il} (gl_f) c_r \left(-\frac{x_4 - l_r x_6}{x_3} \right) \right] \end{pmatrix} + \\ & + \begin{pmatrix} 0 & 0 & 0 \\ 0 & 0 & 0 \\ \frac{2}{m} \frac{1}{l} (gl_r) c_f \left(\frac{x_4 + l_r x_6}{x_3} \right) & \frac{1}{l} (gl_f) c_r \left(\frac{x_4 - l_r x_6}{x_3} \right) \\ 0 & \frac{1}{l} (gl_r) c_f & \frac{1}{l} (gl_f) c_r \\ 0 & 0 & 0 \\ 0 & \frac{l_f}{I} \frac{m}{Il} (gl_r) c_f & -\frac{l_r}{I} \frac{m}{Il} (gl_f) c_r \end{pmatrix} \begin{pmatrix} u_1 \\ u_2 \\ u_3 \end{pmatrix} \end{aligned} \quad (8.145)$$

Thus, the state-space model of the 4WS autonomous vehicle is written in the affine-in-the-input form:

$$\dot{x} = f(x) + g(x)u \quad (8.146)$$

with $x \in R^{6 \times 1}$, $f(x) \in R^{6 \times 1}$, $g(x) \in R^{6 \times 3}$ and $u \in R^{6 \times 3}$. For the state-space model of Eq. (8.146) linearization is performed around the temporary operating point (equi-

librium) (x^*, u^*) . This operating point which is updated at each iteration of the control method, consists of the present value of the 4WS vehicle state vector x^* and of the last value of the control inputs vector u^* that was exerted on it. By denoting the gain matrix $g(x) = [g_1(x), g_2(x), g_3(x)]$ the approximate linearization procedure gives

$$\dot{x} = Ax + Bu + \tilde{d} \quad (8.147)$$

where matrices A , B are associated with the system's Jacobians, as shown next:

$$A = \nabla_x f(x) |_{(x^*, u^*)} + \nabla_x g_2(x)u_2 |_{(x^*, u^*)} + \nabla_x g_3(x)u_3 |_{(x^*, u^*)} \quad (8.148)$$

$$B = \nabla_u [f(x) + g(x)u] |_{(x^*, u^*)} \Rightarrow B = g(x) |_{(x^*, u^*)} \quad (8.149)$$

The elements of the Jacobian matrix $\nabla_x f(x) |_{(x^*, u^*)}$ are computed as follows:

For the first row of the Jacobian matrix $\nabla_x f(x, u)$ one has: $\frac{\partial f_1}{\partial x_1} = 0$, $\frac{\partial f_1}{\partial x_2} = 0$, $\frac{\partial f_1}{\partial x_3} = \cos(x_5)$, $\frac{\partial f_1}{\partial x_4} = -\sin(x_5)$, $\frac{\partial f_1}{\partial x_5} = -x_3 \sin(x_5) + x_4 \cos(x_5)$, $\frac{\partial f_1}{\partial x_6} = 0$.

For the second row of the Jacobian matrix $\nabla_x f(x, u)$ one has: $\frac{\partial f_2}{\partial x_1} = 0$, $\frac{\partial f_2}{\partial x_2} = 0$, $\frac{\partial f_2}{\partial x_3} = \sin(x_5)$, $\frac{\partial f_2}{\partial x_4} = \cos(x_5)$, $\frac{\partial f_2}{\partial x_5} = x_3 \cos(x_5) - x_5 \sin(x_5)$, $\frac{\partial f_2}{\partial x_6} = 0$,

For the third row of the Jacobian matrix $\nabla_x f(x)$ one has: $\frac{\partial f_3}{\partial x_1} = 0$, $\frac{\partial f_3}{\partial x_2} = 0$, $\frac{\partial f_3}{\partial x_3} = -2c_a x_3$, $\frac{\partial f_3}{\partial x_4} = x_6$, $\frac{\partial f_3}{\partial x_5} = 0$, $\frac{\partial f_3}{\partial x_6} = x_4$

For the fourth row of the Jacobian matrix $\nabla_x f(x)$ one has: $\frac{\partial f_4}{\partial x_1} = 0$, $\frac{\partial f_4}{\partial x_2} = 0$, $\frac{\partial f_4}{\partial x_3} = -x_4 + \frac{g_{lr}c_f}{l} \frac{x_4 + l_f x_6}{x_3^2} + \frac{g_{lf}c_r}{l} \frac{x_4 - l_r x_6}{x_3^2}$, $\frac{\partial f_4}{\partial x_4} = -\frac{g_{lr}c_f}{l} \frac{1}{x_3} - \frac{g_{lf}c_r}{l} \frac{1}{x_3}$, $\frac{\partial f_4}{\partial x_5} = 0$, $\frac{\partial f_4}{\partial x_6} = -\frac{g_{lr}c_f}{l} \frac{l_f}{x_3} + \frac{g_{lf}c_r}{l} \frac{l_r}{x_3}$.

For the fifth row of the Jacobian matrix $\nabla_x f(x)$ one has: $\frac{\partial f_5}{\partial x_1} = 0$, $\frac{\partial f_5}{\partial x_2} = 0$, $\frac{\partial f_5}{\partial x_3} = 0$, $\frac{\partial f_5}{\partial x_4} = 0$, $\frac{\partial f_5}{\partial x_5} = 0$, $\frac{\partial f_5}{\partial x_6} = 0$.

For the sixth row of the Jacobian matrix $\nabla_x f(x)$ one has: $\frac{\partial f_6}{\partial x_1} = 0$, $\frac{\partial f_6}{\partial x_2} = 0$, $\frac{\partial f_6}{\partial x_3} = \frac{l_f m g_{lr}}{\Pi} c_f \frac{x_4 + l_f x_6}{x_3^2} - \frac{l_r m g_{lf}}{\Pi} c_r \frac{x_4 - l_r x_6}{x_3^2}$, $\frac{\partial f_6}{\partial x_4} = \frac{l_f m g_{lr}}{\Pi} c_f \frac{1}{x_3} + \frac{l_r m g_{lf}}{\Pi} c_r \frac{1}{x_3}$, $\frac{\partial f_6}{\partial x_5} = 0$, $\frac{\partial f_6}{\partial x_6} = -\frac{l_f m g_{lr}}{\Pi} c_f \frac{l_f}{x_3} - \frac{l_r m g_{lf}}{\Pi} c_r \frac{l_r}{x_3}$.

The elements of the Jacobian matrix $\nabla_x g_2(x) |_{(x^*, u^*)}$ are computed as follows:

$$\nabla_x g_2(x) |_{(x^*, u^*)} = \begin{pmatrix} 0 & 0 & 0 & 0 & 0 \\ 0 & 0 & 0 & 0 & 0 \\ 0 & -\frac{g_{lr}c_f}{l} \frac{x_4 + l_f x_6}{x_3^2} & \frac{g_{lf}c_r}{l} \frac{1}{x_3} & 0 & \frac{g_{lr}c_f}{l} \frac{l_f}{x_3} \\ 0 & 0 & 0 & 0 & 0 \\ 0 & 0 & 0 & 0 & 0 \\ 0 & 0 & 0 & 0 & 0 \end{pmatrix} \quad (8.150)$$

The elements of the Jacobian matrix $\nabla_x g_3(x) |_{(x^*, u^*)}$ are computed as follows:

$$\nabla_x g_3(x) |_{(x^*, u^*)} = \begin{pmatrix} 0 & 0 & 0 & 0 & 0 & 0 \\ 0 & 0 & 0 & 0 & 0 & 0 \\ 0 & 0 & -\frac{gl_f c_r}{l} \frac{x_4 - l_f x_6}{x_3^2} & \frac{gl_f c_r}{l} \frac{1}{x_3} & 0 & \frac{gl_f c_r}{l} - \frac{l_f}{x_3} \\ 0 & 0 & 0 & 0 & 0 & 0 \\ 0 & 0 & 0 & 0 & 0 & 0 \\ 0 & 0 & 0 & 0 & 0 & 0 \end{pmatrix} \quad (8.151)$$

8.4.4 The Nonlinear H-Infinity Control

8.4.4.1 Tracking Error Dynamics for the 4WS Vehicle

The initial nonlinear model of the 4WS automatic ground vehicle is in the form

$$\dot{x} = f(x, u) \quad x \in R^n, \quad u \in R^m \quad (8.152)$$

Linearization of the model of the 4WS ground vehicle is performed at each iteration of the control algorithm round its present operating point $(x^*, u^*) = (x(t), u(t - T_s))$. The linearized equivalent model of the 4WS vehicle is described by

$$\dot{x} = Ax + Bu + L\tilde{d} \quad x \in R^n, \quad u \in R^m, \quad \tilde{d} \in R^q \quad (8.153)$$

Thus, after linearization round its current operating point, the 4WS autonomous ground vehicle's kinematic-dynamic model is written as

$$\dot{x} = Ax + Bu + d_1 \quad (8.154)$$

Parameter d_1 stands for the linearization error in the 4WS vehicle's dynamic model appearing in Eq. (8.154). The reference setpoints for the 4WS ground vehicle are denoted by $\mathbf{x}_d = [x_1^d, \dots, x_6^d]$. Tracking of this trajectory is achieved after applying the control input u^* . At every time instant the control input u^* is assumed to differ from the control input u appearing in Eq. (8.154) by an amount equal to Δu , that is $u^* = u + \Delta u$

$$\dot{x}_d = Ax_d + Bu^* + d_2 \quad (8.155)$$

The joint kinematics and dynamics of the controlled 4WS vehicle described in Eq. (8.154) can be also written as

$$\dot{x} = Ax + Bu + Bu^* - Bu^* + d_1 \quad (8.156)$$

and by denoting $d_3 = -Bu^* + d_1$ as an aggregate disturbance term one obtains

$$\dot{x} = Ax + Bu + Bu^* + d_3 \quad (8.157)$$

By subtracting Eq. (8.155) from (8.157) one has

$$\dot{x} - \dot{x}_d = A(x - x_d) + Bu + d_3 - d_2 \quad (8.158)$$

By denoting the tracking error as $e = x - x_d$ and the aggregate disturbance term as $\tilde{d} = d_3 - d_2$, the tracking error dynamics becomes

$$\dot{e} = Ae + Bu + \tilde{d} \quad (8.159)$$

The above linearized form of the 4WS vehicle's model can be efficiently controlled after applying an H-infinity feedback control scheme.

8.4.4.2 Min-Max Control and Disturbance Rejection

The initial nonlinear model of the 4WS autonomous ground vehicle is in the form

$$\dot{x} = f(x, u) \quad x \in R^n, \quad u \in R^m \quad (8.160)$$

Linearization of the joint kinematic and dynamic model of the 4WS ground vehicle is performed at each iteration of the control algorithm round its present operating point $(x^*, u^*) = (x(t), u(t - T_s))$. The linearized equivalent of the system is described by

$$\dot{x} = Ax + Bu + L\tilde{d} \quad x \in R^n, \quad u \in R^m, \quad \tilde{d} \in R^q \quad (8.161)$$

where matrices A and B are obtained from the computation of the 4WS vehicle's Jacobians, according to Eq. (8.138), and vector \tilde{d} denotes disturbance terms due to linearization errors. The problem of disturbance rejection for the linearized model that is described by

$$\begin{aligned} \dot{x} &= Ax + Bu + L\tilde{d} \\ y &= Cx \end{aligned} \quad (8.162)$$

where $x \in R^n$, $u \in R^m$, $\tilde{d} \in R^q$ and $y \in R^p$, cannot be handled efficiently if the classical LQR control scheme is applied. This is because of the existence of the perturbation term \tilde{d} . The disturbance term \tilde{d} apart from modeling (parametric) uncertainty and external perturbation terms can also represent noise terms of any distribution.

As pointed out in previous applications of the H_∞ control approach, a feedback control scheme is designed for trajectory tracking by the 4WS vehicle's state vector and simultaneous disturbance rejection, considering that the disturbance affects the system in the worst possible manner. The disturbances' effect are incorporated in the following quadratic cost function:

$$J(t) = \frac{1}{2} \int_0^T [y^T(t)y(t) + ru^T(t)u(t) - \rho^2 \tilde{d}^T(t)\tilde{d}(t)]dt, \quad r, \rho > 0 \quad (8.163)$$

The significance of the negative sign in the cost function's term that is associated with the perturbation variable $\tilde{d}(t)$ is that the disturbance tries to maximize the cost function $J(t)$ while the control signal $u(t)$ tries to minimize it. The physical meaning of the relation given above is that the control signal and the disturbances compete to each other within a min-max differential game. This problem of min-max optimization can be written as

$$\min_u \max_{\tilde{d}} J(u, \tilde{d}) \quad (8.164)$$

As in previously examined ground vehicles, the objective of the optimization procedure for the 4WS vehicle is to compute a control signal $u(t)$ which can compensate for the worst possible disturbance, that is externally imposed to the system of the 4WS autonomous vehicle. However, the solution to the min-max optimization problem is directly related to the value of the parameter ρ . This means that there is an upper bound in the disturbances magnitude that can be annihilated by the control signal.

8.4.4.3 H-Infinity Feedback Control

Following previous applications of the H-infinity control, for the linearized system given by Eq.(8.162) the cost function of Eq.(8.163) is defined, where the coefficient r determines the penalization of the control input and the weight coefficient ρ determines the reward of the disturbances' effects. It is assumed that (i) The energy that is transferred from the disturbances signal $\tilde{d}(t)$ is bounded, that is $\int_0^\infty \tilde{d}^T(t)\tilde{d}(t)dt < \infty$, (ii) the matrices $[A, B]$ and $[A, L]$ are stabilizable, (iii) the matrix $[A, C]$ is detectable. Then, the optimal feedback control law is given by

$$u(t) = -Kx(t) \quad (8.165)$$

with

$$K = \frac{1}{r} B^T P \quad (8.166)$$

where P is a positive semi-definite symmetric matrix which is obtained from the solution of the Riccati equation

$$A^T P + PA + Q - P \left(\frac{1}{r} BB^T - \frac{1}{2\rho^2} LL^T \right) P = 0 \quad (8.167)$$

where Q is also a positive definite symmetric matrix. The worst case disturbance is given by

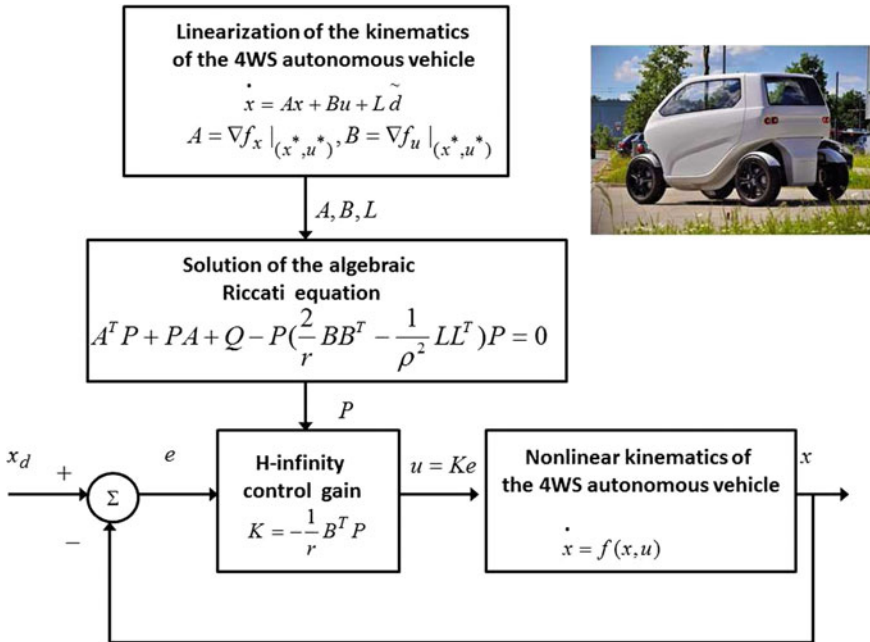


Fig. 8.21 Diagram of the nonlinear optimal control scheme for the 4WS autonomous ground vehicle

$$\tilde{d}(t) = \frac{1}{\rho^2} L^T P x(t) \tag{8.168}$$

The diagram of the considered control loop is depicted in Fig. 8.21.

8.4.5 Lyapunov Stability Analysis

Through Lyapunov stability analysis it will be shown that the proposed nonlinear control scheme assures H_∞ tracking performance for the control loop of the 4WS autonomous ground vehicle. Moreover, under moderate conditions asymptotic stability is proven and convergence to the reference setpoints is achieved. The tracking error dynamics for the 4WS automatic ground vehicle is written in the form

$$\dot{e} = Ae + Bu + L\tilde{d} \tag{8.169}$$

where in this 4WS autonomous vehicle's case $L = I \in R^{6 \times 6}$ with I being the identity matrix. Variable \tilde{d} denotes model uncertainties and external disturbances of the vehicle's model. The following Lyapunov function is considered

$$V = \frac{1}{2}e^T P e \quad (8.170)$$

where $e = x - x_d$ is the tracking error. By differentiating with respect to time one obtains

$$\begin{aligned} \dot{V} &= \frac{1}{2}\dot{e}^T P e + \frac{1}{2}e^T P \dot{e} \Rightarrow \\ \dot{V} &= \frac{1}{2}[Ae + Bu + L\tilde{d}]^T P + \frac{1}{2}e^T P [Ae + Bu + L\tilde{d}] \Rightarrow \end{aligned} \quad (8.171)$$

$$\begin{aligned} \dot{V} &= \frac{1}{2}[e^T A^T + u^T B^T + \tilde{d}^T L^T] P e + \\ &+ \frac{1}{2}e^T P [Ae + Bu + L\tilde{d}] \Rightarrow \end{aligned} \quad (8.172)$$

$$\begin{aligned} \dot{V} &= \frac{1}{2}e^T A^T P e + \frac{1}{2}u^T B^T P e + \frac{1}{2}\tilde{d}^T L^T P e + \\ &\frac{1}{2}e^T P A e + \frac{1}{2}e^T P B u + \frac{1}{2}e^T P L \tilde{d} \end{aligned} \quad (8.173)$$

The previous equation is rewritten as

$$\begin{aligned} \dot{V} &= \frac{1}{2}e^T (A^T P + P A) e + \left(\frac{1}{2}u^T B^T P e + \frac{1}{2}e^T P B u \right) + \\ &+ \left(\frac{1}{2}\tilde{d}^T L^T P e + \frac{1}{2}e^T P L \tilde{d} \right) \end{aligned} \quad (8.174)$$

Assumption: For given positive definite matrix Q and coefficients r and ρ there exists a positive definite matrix P , which is the solution of the following matrix equation

$$A^T P + P A = -Q + P \left(\frac{2}{r} B B^T - \frac{1}{\rho^2} L L^T \right) P \quad (8.175)$$

Moreover, the following feedback control law is applied to the system

$$u = -\frac{1}{r} B^T P e \quad (8.176)$$

By substituting Eqs. (2.89) and (2.90) one obtains

$$\begin{aligned} \dot{V} &= \frac{1}{2}e^T \left[-Q + P \left(\frac{2}{r} B B^T - \frac{1}{2\rho^2} L L^T \right) P \right] e + \\ &+ e^T P B \left(-\frac{1}{r} B^T P e \right) + e^T P L \tilde{d} \Rightarrow \end{aligned} \quad (8.177)$$

$$\begin{aligned} \dot{V} = & -\frac{1}{2}e^T Qe + \left(\frac{2}{r}PBB^T Pe - \frac{1}{2\rho^2}e^T PLL^T \right) Pe \\ & - \frac{1}{r}(e^T PBB^T Pe) + e^T PL\tilde{d} \end{aligned} \quad (8.178)$$

which after intermediate operations gives

$$\dot{V} = -\frac{1}{2}e^T Qe - \frac{1}{2\rho^2}e^T PLL^T Pe + e^T PL\tilde{d} \quad (8.179)$$

or, equivalently

$$\begin{aligned} \dot{V} = & -\frac{1}{2}e^T Qe - \frac{1}{2\rho^2}e^T PLL^T Pe + \\ & + \frac{1}{2}e^T PL\tilde{d} + \frac{1}{2}\tilde{d}^T L^T Pe \end{aligned} \quad (8.180)$$

Lemma: The following inequality holds

$$\frac{1}{2}e^T L\tilde{d} + \frac{1}{2}\tilde{d}^T L^T Pe - \frac{1}{2\rho^2}e^T PLL^T Pe \leq \frac{1}{2}\rho^2\tilde{d}^T \tilde{d} \quad (8.181)$$

Proof: The binomial $(\rho a - \frac{1}{\rho}b)^2$ is considered. Expanding the left part of the above inequality one gets

$$\begin{aligned} \rho^2 a^2 + \frac{1}{\rho^2} b^2 - 2ab \geq 0 & \Rightarrow \frac{1}{2}\rho^2 a^2 + \frac{1}{2\rho^2} b^2 - ab \geq 0 \Rightarrow \\ ab - \frac{1}{2\rho^2} b^2 \leq \frac{1}{2}\rho^2 a^2 & \Rightarrow \frac{1}{2}ab + \frac{1}{2}ab - \frac{1}{2\rho^2} b^2 \leq \frac{1}{2}\rho^2 a^2 \end{aligned} \quad (8.182)$$

The following substitutions are carried out: $a = \tilde{d}$ and $b = e^T PL$ and the previous relation becomes

$$\frac{1}{2}\tilde{d}^T L^T Pe + \frac{1}{2}e^T PL\tilde{d} - \frac{1}{2\rho^2}e^T PLL^T Pe \leq \frac{1}{2}\rho^2\tilde{d}^T \tilde{d} \quad (8.183)$$

Equation (8.183) is substituted in Eq. (8.180) and the inequality is enforced, thus giving

$$\dot{V} \leq -\frac{1}{2}e^T Qe + \frac{1}{2}\rho^2\tilde{d}^T \tilde{d} \quad (8.184)$$

Equation (8.184) shows that the H_∞ tracking performance criterion is satisfied. The integration of \dot{V} from 0 to T gives

$$\begin{aligned} \int_0^T \dot{V}(t) dt &\leq -\frac{1}{2} \int_0^T \|e\|_Q^2 dt + \frac{1}{2} \rho^2 \int_0^T \|\tilde{d}\|^2 dt \Rightarrow \\ 2V(T) + \int_0^T \|e\|_Q^2 dt &\leq 2V(0) + \rho^2 \int_0^T \|\tilde{d}\|^2 dt \end{aligned} \quad (8.185)$$

Moreover, if there exists a positive constant $M_d > 0$ such that

$$\int_0^\infty \|\tilde{d}\|^2 dt \leq M_d \quad (8.186)$$

then one gets

$$\int_0^\infty \|e\|_Q^2 dt \leq 2V(0) + \rho^2 M_d \quad (8.187)$$

Thus, the integral $\int_0^\infty \|e\|_Q^2 dt$ is bounded. Moreover, $V(T)$ is bounded and from the definition of the Lyapunov function V in Eq. (8.170) it becomes clear that $e(t)$ will be also bounded since $e(t) \in \Omega_e = \{e | e^T P e \leq 2V(0) + \rho^2 M_d\}$. According to the above and with the use of Barbalat's Lemma one obtains $\lim_{t \rightarrow \infty} e(t) = 0$.

Elaborating on the above, it can be noted that the proof of global asymptotic stability for the control loop of the 4WS vehicle's model is based on Eq. (8.184) and on the application of Barbalat's Lemma. It uses the condition of Eq. (8.186) about the boundedness of the square of the aggregate disturbance and modelling error term \tilde{d} that affects the model. However, as explained above the proof of global asymptotic stability is not restricted by this condition. By selecting the attenuation coefficient ρ to be sufficiently small and in particular to satisfy $\rho^2 < \|e\|_Q^2 / \|\tilde{d}\|^2$ one has that the first derivative of the Lyapunov function is upper bounded by 0. Therefore for the i th time interval it is proven that the Lyapunov function defined in Eq. (8.170) is a decreasing one. This also assures the Lyapunov function of the system defined in Eq. (8.170) will always have a negative first-order derivative.

8.4.6 Robust State Estimation Using the H-Infinity Kalman Filter

The control loop for the 4WS autonomous vehicle can be implemented with the feedback of a partially measurable state vector and by processing only a small number of state variables. To reconstruct the missing information about the state vector of the 4WS autonomous vehicle it is proposed to use a filtering scheme and based on it to apply state estimation-based control [457]. The recursion of the H_∞ Kalman Filter, can be formulated in terms of a *measurement update* and a *time update* part

Measurement update:

$$\begin{aligned}
 D(k) &= [I - \theta W(k)P^-(k) + C^T(k)R(k)^{-1}C(k)P^-(k)]^{-1} \\
 K(k) &= P^-(k)D(k)C^T(k)R(k)^{-1} \\
 \hat{x}(k) &= \hat{x}^-(k) + K(k)[y(k) - C\hat{x}^-(k)]
 \end{aligned} \tag{8.188}$$

Time update:

$$\begin{aligned}
 \hat{x}^-(k+1) &= A(k)x(k) + B(k)u(k) \\
 P^-(k+1) &= A(k)P^-(k)D(k)A^T(k) + Q(k)
 \end{aligned} \tag{8.189}$$

where it is assumed that parameter θ is sufficiently small to assure that the covariance matrix $P^-(k)^{-1} - \theta W(k) + C^T(k)R(k)^{-1}C(k)$ will be positive definite. When $\theta = 0$ the H_∞ Kalman Filter becomes equivalent to the standard Kalman Filter. One can measure only a part of the state vector of the system of the 4WS autonomous vehicle, such as the velocities V_x and V_y and the orientation angle θ , and can estimate through filtering the rest of the state vector elements.

8.4.7 Simulation Tests

The performance of the proposed nonlinear optimal control scheme for the autonomous 4WS vehicle has been tested in the case of tracking of different reference setpoints. The control scheme exhibited fast and accurate tracking of the reference paths. The computation of the feedback control gain required the solution of the algebraic Riccati equation given in Eq. (8.175), at each iteration of the control algorithm. The obtained results are depicted in Figs. 8.22, 8.23, 8.24, 8.25, 8.26, 8.27, 8.28, 8.29, 8.30, 8.31, 8.32 and 8.33. The measurement units for the state variables of the 4WS vehicle's model were in the SI system (position coordinates measured in m and heading angle in rad). It can be noticed that the H-infinity controller achieved fast and accurate convergence to the reference setpoints for all elements of the 4WS vehicle's state-vector. Moreover, the variations of the control inputs, that is of the 4WS autonomous vehicle's velocity and of its steering angle were smooth.

As noted, the proposed nonlinear optimal control method for the 4WS autonomous vehicle was based on an approximate linearization of its joint kinematic and dynamic model. The advantages that the proposed control method exhibits are outlined as follows: (i) it is applied directly on the nonlinear dynamical model of the 4WS vehicle and not on an equivalent linearized description of it, (ii) It avoids the elaborated linearizing transformations (diffeomorphisms) which can be met in global linearization-based control methods for autonomous vehicles (iii) the controller is

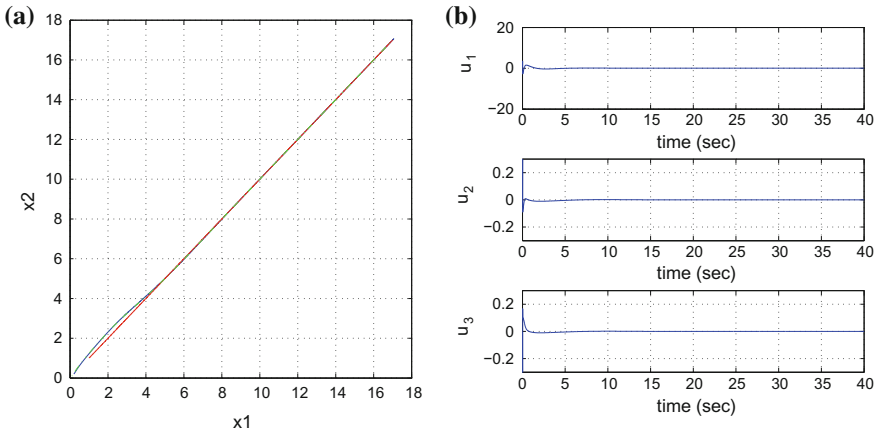


Fig. 8.22 **a** Tracking of reference path 1 (red-line) by the 4WS autonomous vehicle (blue line) and trajectory estimated by the Kalman Filter (green line), **b** control inputs u_1 to u_3 applied to the 4WS vehicle

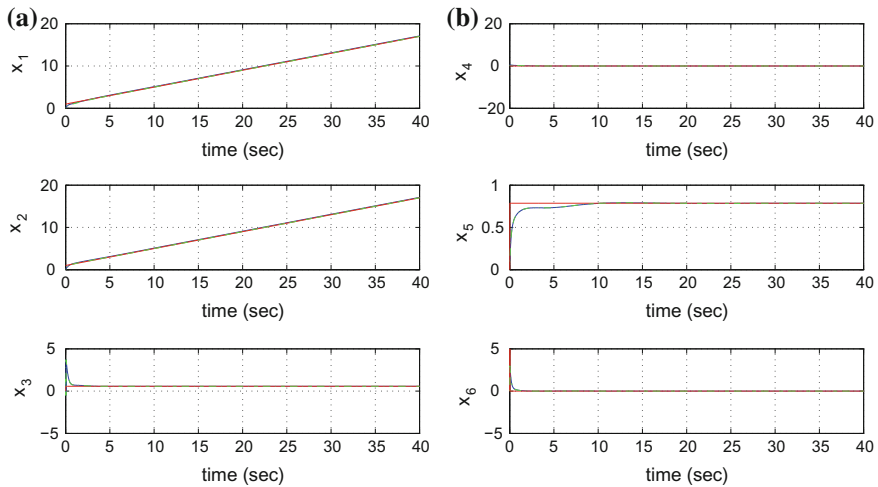


Fig. 8.23 Tracking of reference path 1: **a** convergence of state variables x_1 to x_3 of the 4WS vehicle to their reference setpoints (red-lines) and estimated state variables provided by the Kalman Filter (green lines), **b** convergence of state variables x_4 to x_6 of the 4WS vehicle to their reference setpoints (red-lines) and estimated state variables provided by the Kalman Filter (green lines)

designed according to optimal control principles which implies the best trade-off between precise tracking of the reference setpoints on the one side and moderate variations of the control inputs on the other side (iv) the control method exhibits significant robustness to parametric uncertainty, modelling errors as well as to external perturbations.

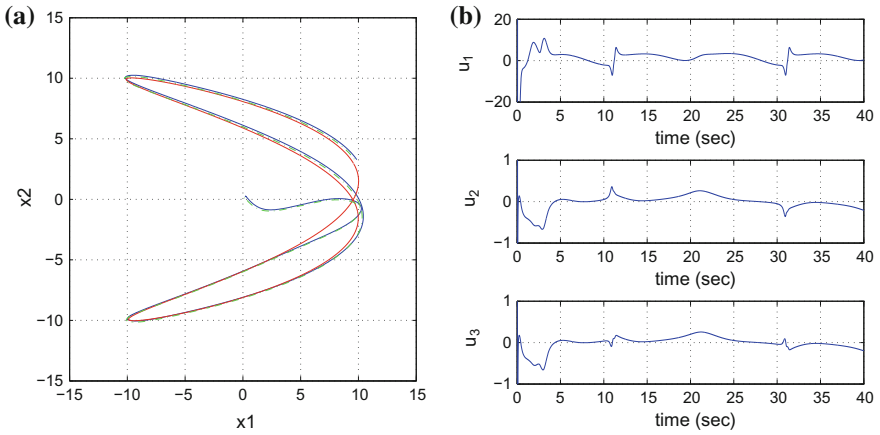


Fig. 8.24 **a** Tracking of reference path 2 (red-line) by the 4WS autonomous vehicle (blue line) and trajectory estimated by the Kalman Filter (green line), **b** control inputs u_1 to u_3 applied to the 4WS vehicle

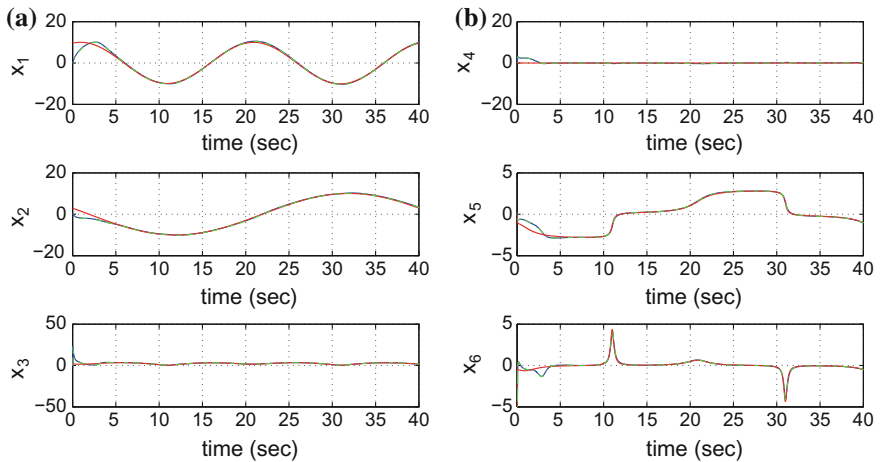


Fig. 8.25 Tracking of reference path 2: **a** convergence of state variables x_1 to x_3 of the 4WS vehicle to their reference setpoints (red-lines) and estimated state variables provided by the Kalman Filter (green lines), **b** convergence of state variables x_4 to x_6 of the 4WS vehicle to their reference setpoints (red-lines) and estimated state variables provided by the Kalman Filter (green lines)

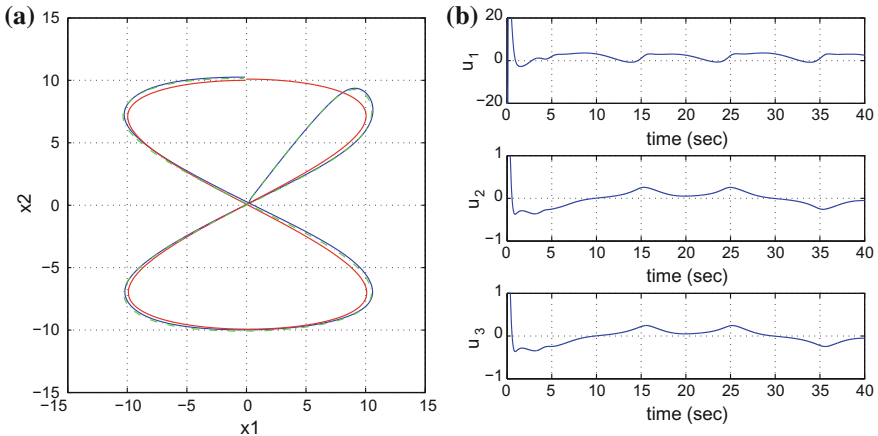


Fig. 8.26 **a** Tracking of reference path 3 (red-line) by the 4WS autonomous vehicle (blue line) and trajectory estimated by the Kalman Filter (green line), **b** control inputs u_1 to u_3 applied to the 4WS vehicle

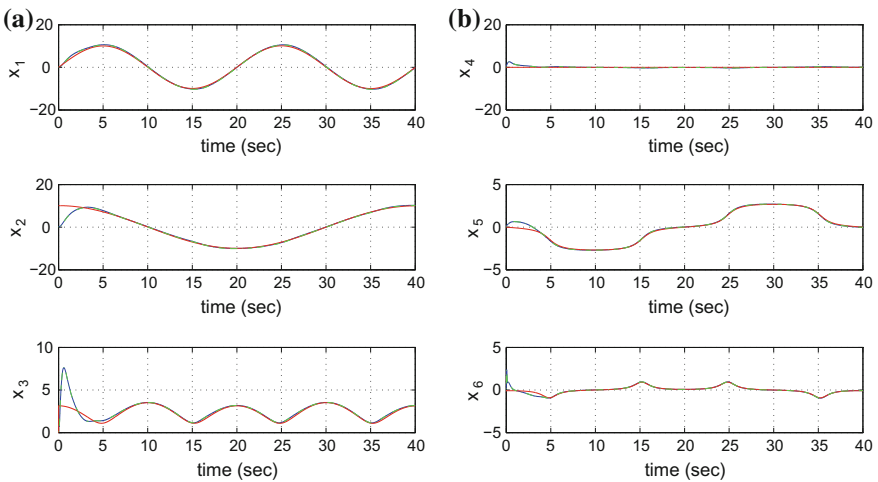


Fig. 8.27 Tracking of reference path 3: **a** convergence of state variables x_1 to x_3 of the 4WS vehicle to their reference setpoints (red-lines) and estimated state variables provided by the Kalman Filter (green lines), **b** convergence of state variables x_4 to x_6 of the 4WS vehicle to their reference setpoints (red-lines) and estimated state variables provided by the Kalman Filter (green lines)

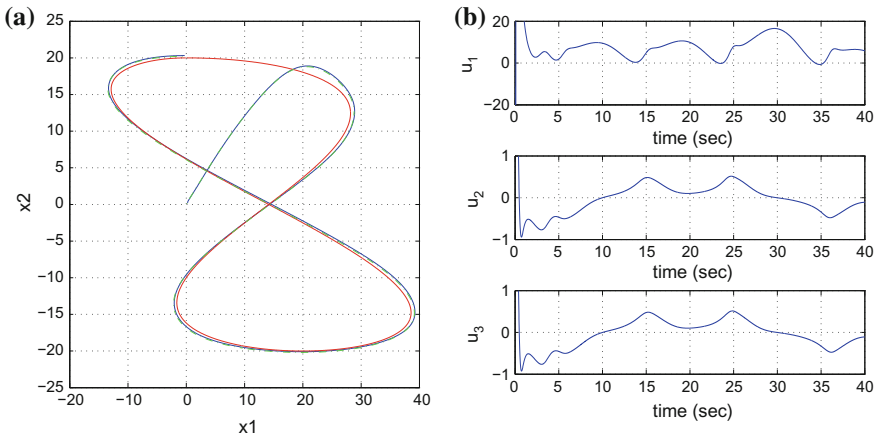


Fig. 8.28 **a** Tracking of reference path 4 (red-line) by the 4WS autonomous vehicle (blue line) and trajectory estimated by the Kalman Filter (green line), **b** control inputs u_1 to u_3 applied to the 4WS vehicle

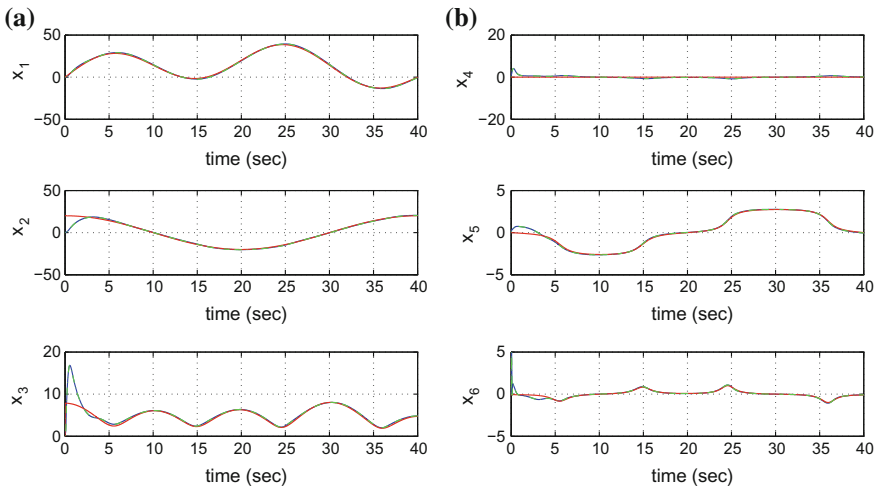


Fig. 8.29 Tracking of reference path 4: **a** convergence of state variables x_1 to x_3 of the 4WS vehicle to their reference setpoints (red-lines) and estimated state variables provided by the Kalman Filter (green lines), **b** convergence of state variables x_4 to x_6 of the 4WS vehicle to their reference setpoints (red-lines) and estimated state variables provided by the Kalman Filter (green lines)

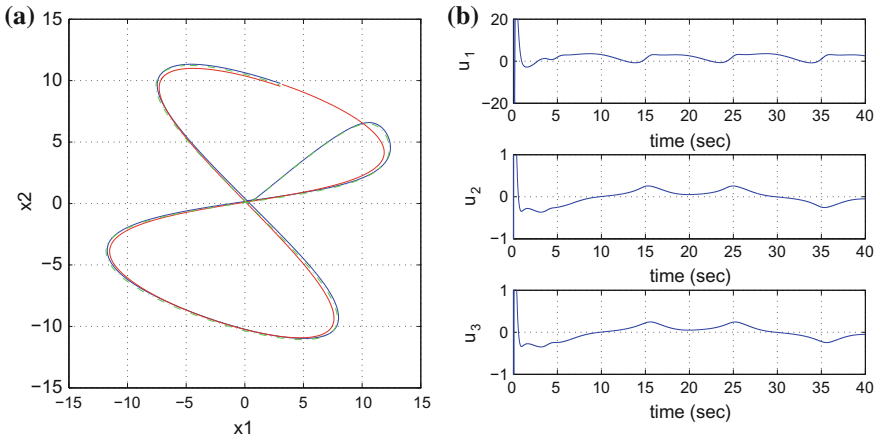


Fig. 8.30 **a** Tracking of reference path 5: (red-line) by the 4WS autonomous vehicle (blue line) and trajectory estimated by the Kalman Filter (green line), **b** control inputs u_1 to u_3 applied to the 4WS vehicle

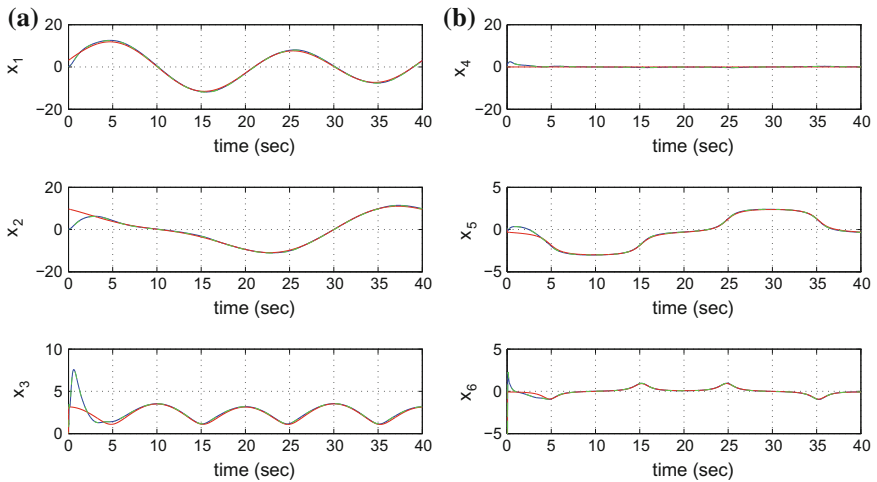


Fig. 8.31 Tracking of reference path 5: **a** convergence of state variables x_1 to x_3 of the 4WS vehicle to their reference setpoints (red-lines) and estimated state variables provided by the Kalman Filter (green lines), **b** convergence of state variables x_4 to x_6 of the 4WS vehicle to their reference setpoints (red-lines) and estimated state variables provided by the Kalman Filter (green lines)

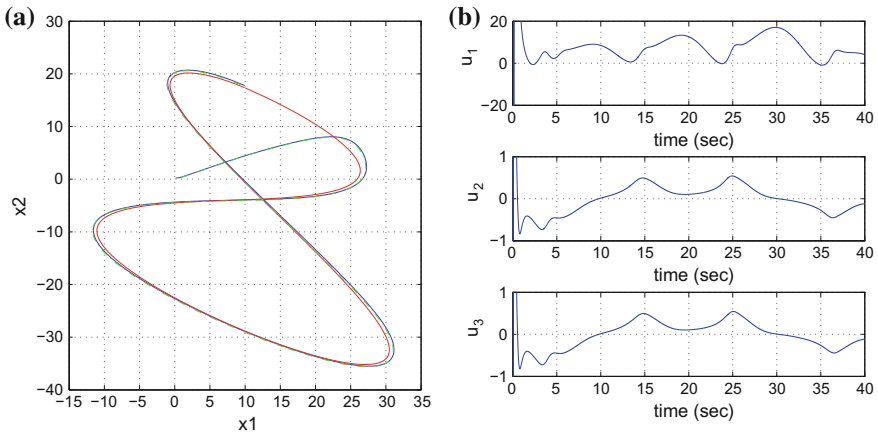


Fig. 8.32 **a** Tracking of reference path 6: (red-line) by the 4WS autonomous vehicle (blue line) and trajectory estimated by the Kalman Filter (green line), **b** control inputs u_1 to u_3 applied to the 4WS vehicle

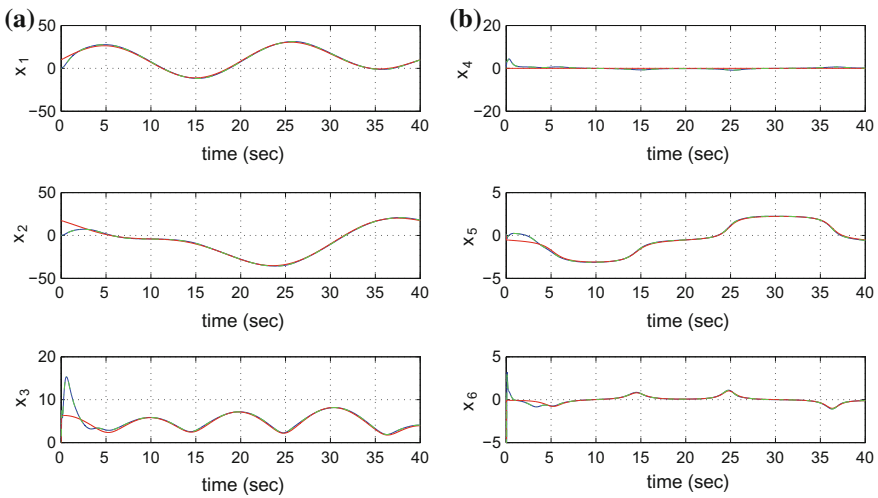


Fig. 8.33 Tracking of reference path 6: **a** convergence of state variables x_1 to x_3 of the 4WS vehicle to their reference setpoints (red-lines) and estimated state variables provided by the Kalman Filter (green lines), **b** convergence of state variables x_4 to x_6 of the 4WS vehicle to their reference setpoints (red-lines) and estimated state variables provided by the Kalman Filter (green lines)

Table 8.3 RMSE of the 4WS vehicle's state variables

Path	RMSE X (m)	RMSE Y (m)	RMSE θ (rad)
1	$3.3 \cdot 10^{-3}$	$3.3 \cdot 10^{-3}$	$0.1 \cdot 10^{-3}$
2	$6.0 \cdot 10^{-3}$	$13.0 \cdot 10^{-3}$	$0.7 \cdot 10^{-3}$
3	$8.2 \cdot 10^{-3}$	$6.0 \cdot 10^{-3}$	$1.1 \cdot 10^{-3}$
4	$13.3 \cdot 10^{-3}$	$11.6 \cdot 10^{-3}$	$2.4 \cdot 10^{-3}$
5	$5.0 \cdot 10^{-3}$	$4.2 \cdot 10^{-3}$	$1.0 \cdot 10^{-3}$
6	$12.2 \cdot 10^{-3}$	$12.6 \cdot 10^{-3}$	$1.2 \cdot 10^{-3}$

Table 8.4 RMSE of the 4WS state variables under disturbance

Δa (%)	RMSE X (m)	RMSE Y (m)	RMSE θ (rad)
0	$8.2 \cdot 10^{-3}$	$6.0 \cdot 10^{-3}$	$1.1 \cdot 10^{-3}$
10	$8.2 \cdot 10^{-3}$	$6.2 \cdot 10^{-3}$	$0.6 \cdot 10^{-3}$
20	$8.2 \cdot 10^{-3}$	$6.3 \cdot 10^{-3}$	$0.8 \cdot 10^{-3}$
30	$8.0 \cdot 10^{-3}$	$6.4 \cdot 10^{-3}$	$1.3 \cdot 10^{-3}$
40	$7.9 \cdot 10^{-3}$	$6.5 \cdot 10^{-3}$	$1.8 \cdot 10^{-3}$
50	$7.9 \cdot 10^{-3}$	$6.6 \cdot 10^{-3}$	$2.3 \cdot 10^{-3}$
60	$7.8 \cdot 10^{-3}$	$6.6 \cdot 10^{-3}$	$2.8 \cdot 10^{-3}$

Yet computationally simple, the proposed H_∞ control scheme has an excellent performance. Comparing to the control of 4WS automatic ground vehicles that rely on global linearization methods the presented nonlinear H-infinity control scheme is equally efficient in setpoint tracking while also retaining optimal control features [457]. The tracking accuracy of the presented control method (H_∞) has been evaluated in the case of several reference setpoints. By using the Kalman Filter as a robust observer estimates of the state vector of the vehicle were obtained, and thus the implementation of state estimation-based control became possible. The measured state variables were $x_3 = V_x$, $x_4 = V_y$ and $x_5 = \theta$. The obtained results are given in Table 8.3.

The tracking performance of the nonlinear H-infinity control method for the model of the 4WS vehicle was measured in the case of model uncertainty, imposing an imprecision equal to $\Delta a\%$ about the vehicle's moment of inertia I . The obtained results are outlined in Table 8.4. It can be noticed that despite model perturbations the tracking accuracy of the control method remained satisfactory.

8.5 Flatness-Based Control for AGVs and Kalman Filter-Based Compensation of Disturbance Forces and Torques

8.5.1 *Outline*

The present section analyzes the use of a global linearization-based control approach that is based on differential flatness theory to the problem of autonomous navigation of four-wheel robotic vehicles. As previously noted, the precise modeling of the vehicles' dynamics improves the efficiency of vehicles controllers in adverse cases, for example in high velocity, when performing abrupt maneuvers, under mass and loads changes or when moving on rough terrain. Using model-based control approaches it is possible to design a nonlinear controller that maintains the vehicle's motion characteristics within desirable ranges [45, 319, 332, 333, 348, 616]. When the vehicle's dynamics is subject to modeling uncertainties or when there are unknown forces and torques exerted on the vehicle it is important to be in position to estimate in real-time disturbances and unknown dynamics so as to compensate them through the control input and to maintain the satisfactory performance of the vehicle's automated steering system. In this direction, estimation for the unknown dynamics of the vehicle and state estimation-based control schemes have been developed [201, 312, 350, 580].

The objective of the present section is two-fold. On the one side it analyzes the design of a controller for autonomous navigation of automatic ground vehicles (AGVs). On the other side it proposes a solution to the problem of four-wheel vehicle control under model uncertainties and external disturbances. Considering, that only under ideal conditions the dynamic model of the vehicle is precisely known (e.g. there may be variations in the transported mass, or in the cornering stiffness coefficients characterizing the interaction of the tires with the ground, or in the position of the vehicle's center of gravity) and that in several cases there is uncertainty about the forces and torques developed on the vehicle (e.g. traction and braking torques on the wheels, forces due to traction of implements, or lateral forces which generate torques affecting the yaw stability of the vehicle) the need for designing robust controllers of the autonomous vehicles becomes obvious [49, 510, 521, 590]. By compensating efficiently such disturbances forces and torques safety features of the vehicle are improved and its autonomous functioning remains reliable even under adverse road conditions.

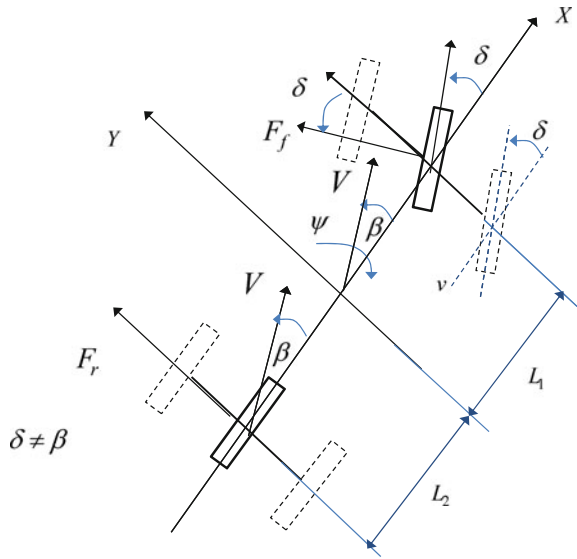
Dynamic analysis for the 4-wheel vehicle provided, as in the case of Sect. 8.2. A 3-DOF model is introduced having as elements the vehicle's velocity along the horizontal and vertical axis of an inertial reference frame as well as the rate of change of its orientation angle (this is the angle defined by the vehicle's longitudinal axis and the horizontal axis of the frame). Lateral forces are shown to affect the vehicle's motion and to be dependent on the longitudinal and lateral velocity of the vehicle, on the yaw rate and on the cornering stiffness coefficients for the front and rear tires. The control inputs to the vehicles' dynamic model are the traction/braking

wheel torque and the turn angle of the steering wheel. Since the parameters of the dynamic model of the vehicle cannot always be known with precision or may be time-varying (e.g. cornering stiffness coefficients, transported mass) and since there may be unmodelled external forces and torques exerted on the vehicle (e.g. due to road condition, disturbances in traction forces) it is important to design a control loop with robustness to the aforementioned sources of uncertainty and disturbances, as well as to be in position to estimate in real-time such disturbances through the processing of measurements from a small number of on-board sensors.

Next, it is shown how a nonlinear controller for the aforementioned vehicle's model can be obtained through the application of differential flatness theory [145, 476, 546, 572]. The flat output for the vehicle's model is a vector comprising the x -axis velocity and a second variable based on a linear relation between the y -axis velocity and the rate of change of the orientation angle [332, 333]. By expressing all state variables and the control input of the four-wheel vehicle model as functions of the flat output and its derivatives the system's dynamic model is transformed into the linear Brunovsky (canonical) form [303, 495]. For the latter model it is possible to design a state feedback controller that enables accurate tracking of the vehicle's velocity set-points.

By exploiting the vehicle's exactly linearized model and its transformation into a canonical form it is possible to design a state estimator for approximating the system's state vector through the processing of measurements coming from a small number of on-board sensors. To this end the concept of *Derivative-free nonlinear Kalman Filtering* is used once again. Unlike the Extended Kalman Filter, the proposed filtering method provides estimates of the state vector of the nonlinear system without the need for derivatives and Jacobians calculation [439, 445, 450]. By avoiding linearization approximations, the proposed filtering method improves the accuracy of estimation of the system's state variables. Moreover, it is shown that it is possible to redesign the Kalman Filter in the form of a disturbance observer and using the estimation of the disturbance to develop an auxiliary control input that compensates for their effects. In this way the vehicle's control and autonomous navigation system can become robust with respect to uncertainties in the model's parameters or uncertainties about external forces and torques. It is also noted that in terms of computation speed the proposed Kalman Filter-based disturbance estimator for the vehicle is faster than disturbance estimators that may be based on other nonlinear filtering approaches (e.g. Extended Kalman Filter, Unscented Kalman Filter or Particle Filter) thus becoming advantageous for the real-time estimation of the unknown vehicle dynamics [438, 457]. The efficiency of the proposed nonlinear control and Kalman Filter-based disturbances estimation scheme is evaluated through numerical simulation tests. It has been shown that by accurately estimating disturbance forces and torques the control loop achieves elimination of the tracking error for all state variables of the vehicle.

Fig. 8.34 Nonlinear 4-wheeled vehicle model



8.5.2 Dynamic Model of the Vehicle

8.5.2.1 Definition of Parameters in 4-Wheel Vehicle Dynamic Model

The dynamic model of the four-wheel vehicle that was analyzed in a previous section is now re-examined. With reference to Fig. 8.34 (where the lateral forces applied on the wheels are considered to define the vehicle’s motion) one has the following parameters: β is the angle between the velocity and the vehicle’s transversal angle, V is the velocity vector of the vehicle, ψ is the yaw angle (rotation round the z axis), f_x is the aggregate force along the x axis, f_y is the aggregate force along the y axis, T_z is the aggregate torque round the z axis and δ is the steering angle of the front wheels [332, 348, 572].

The motion of the vehicle along its longitudinal axis is controlled by the traction or braking wheel torque $T_\omega = T_m - T_b$ with $T_b = T_{bf} + T_{br}$ and the lateral movement via the steering angle δ . The two control inputs of the four wheel vehicle model are

$$\begin{aligned} u_1 &= T_\omega \\ u_2 &= \delta \end{aligned} \tag{8.190}$$

As explained in Sect. 8.2, a first form of the vehicle’s dynamic model is

$$\dot{x} = f(x, t) + g(x, t)u + g_1u_1u_2 + g_2u_2^2 \tag{8.191}$$

where

$$f(x, t) = \begin{pmatrix} \frac{I_r}{mR}(\dot{\omega}_r + \dot{\omega}_f) \\ \dot{\psi} V_x + \frac{1}{m} \left(-C_f \frac{(V_y + L_f \dot{\psi})}{V_x} - C_r \frac{(V_y - L_f \dot{\psi})}{V_x} \right) \\ \frac{1}{I_z} \left(-L_f C_f \frac{(V_y + L_f \dot{\psi})}{V_x} + L_r C_r \frac{(V_y - L_f \dot{\psi})}{V_x} \right) \end{pmatrix} \quad (8.192)$$

$$g(x, t) = \begin{pmatrix} \frac{1}{mR} \frac{C_f}{m} \left(\frac{V_y + L_f \dot{\psi}}{V_x} \right) \\ 0 \\ 0 \end{pmatrix} \begin{pmatrix} \left(\frac{C_f R - I_r \dot{\omega}_f}{mR} \right) \\ \left(\frac{L_f C_f R - L_f I_r \dot{\omega}_f}{I_z R} \right) \end{pmatrix} \quad (8.193)$$

$$g_1 = \begin{pmatrix} 0 \\ \frac{1}{mR} \\ \frac{L_f}{I_z R} \end{pmatrix} g_2 = \begin{pmatrix} -\frac{C_f}{m} \\ 0 \\ 0 \end{pmatrix} x = \begin{pmatrix} V_x \\ V_y \\ \dot{\psi} \end{pmatrix} u = \begin{pmatrix} u_1 \\ u_2 \end{pmatrix} \quad (8.194)$$

The previously analyzed nonlinear model of the vehicle's dynamics can be simplified if the control inputs $u_1 u_2$ and u_2^2 are not taken into account. In the latter case the dynamics of the vehicle takes the form

$$\dot{x} = f(x, t) + g(x, t)u \quad (8.195)$$

8.5.3 Flatness-Based Controller for the 3-DOF Vehicle Model

8.5.3.1 Flatness-Based Controller for the 4-Wheel Vehicle

To show that the four-wheel vehicle is differentially flat the following flat outputs are defined [332, 333]:

$$\begin{aligned} y_1 &= V_x \\ y_2 &= L_f m V_y - I_z \dot{\psi} \end{aligned} \quad (8.196)$$

Then it holds that all elements of the system's state vector can be written as functions of the flat outputs and their derivatives. Indeed, for $x = [V_x, V_y, \dot{\psi}]^T$ it holds

$$V_x = y_1 \quad (8.197)$$

$$V_y = \frac{y_2}{L_f m} - \left(\frac{I_z}{L_f m} \right) \left(\frac{L_f m y_1 \dot{y}_2 + C_r (L_f + L_r) y_2}{C_r (L_f + L_r) (I_z - L_f L_r m) + (L_f m y_1)^2} \right) \quad (8.198)$$

$$\dot{\psi} = \frac{L_f m y_1 \dot{y}_2 + C_r (L_f + L_r) y_2}{C_r (L_f + L_r) (I_z - L_f L_r m) + (L_f m y_1)^2} \quad (8.199)$$

Expressing the system's state variables as functions of the flat outputs one has the following state-space description for the system

$$\begin{pmatrix} \dot{y}_1 \\ \ddot{y}_2 \end{pmatrix} = \Delta(y_1, y_2, \dot{y}_2) \begin{pmatrix} u_1 \\ u_2 \end{pmatrix} + \Phi(y_1, y_2, \dot{y}_2) \quad (8.200)$$

where

$$\Delta(y_1, y_2, \dot{y}_2) = \begin{pmatrix} \Delta_{11}(y_1, y_2, \dot{y}_2) & \Delta_{12}(y_1, y_2, \dot{y}_2) \\ \Delta_{21}(y_1, y_2, \dot{y}_2) & \Delta_{22}(y_1, y_2, \dot{y}_2) \end{pmatrix} \quad (8.201)$$

with

$$\Delta_{11}(y_1, y_2, \dot{y}_2) = \frac{1}{mR} \quad (8.202)$$

$$\Delta_{12}(y_1, y_2, \dot{y}_2) = \frac{C_f}{m} \left(\frac{V_y + L_f \dot{\psi}}{y_1} \right) \quad (8.203)$$

$$\Delta_{21}(y_1, y_2, \dot{y}_2) = \frac{C_r(L_f + L_r)(V_y - L_r \dot{\psi}) - L_f m \dot{\psi} y_1^2}{mR y_1^2} \quad (8.204)$$

$$\begin{aligned} \Delta_{22}(y_1, y_2, \dot{y}_2) = & \left(-L_f m y_1 + \frac{L_r C_r (L_f + L_r)}{y_1} \right) \frac{(L_f C_f R - L_f I_r \dot{\omega}_f)}{I_z R} + \\ & + \frac{((C_r(L_f + L_r))(V_y - L_r \dot{\psi}) - L_f m \dot{\psi} y_1^2)}{y_1^2} \cdot \frac{C_f (V_y + L_f \dot{\psi})}{m y_1} - \frac{C_r (L_f + L_r)}{y_1} \frac{R C_f - I_r \dot{\omega}_f}{mR} \end{aligned} \quad (8.205)$$

Moreover about matrix $\Phi(y_1, y_2, \dot{y}_2)$ it holds

$$\Phi(y_1, y_2, \dot{y}_2) = \begin{pmatrix} \Phi_1(y_1, y_2, \dot{y}_2) \\ \Phi_2(y_1, y_2, \dot{y}_2) \end{pmatrix} \quad (8.206)$$

with elements

$$\Phi_1(y_1, y_2, \dot{y}_2) = \dot{\psi} V_y - \frac{I_r}{mR} (\dot{\omega}_r + \dot{\omega}_f) \quad (8.207)$$

$$\begin{aligned} \Phi_2(y_1, y_2, \dot{y}_2) = & -L_f m y_1 f_3(x, t) - \frac{C_r(L_f + L_r)}{y_1} f_2(x, t) + \\ & + \frac{C_f(L_f + L_r)(V_y - L_r \dot{\psi}) - L_f m \dot{\psi} y_1^2}{y_1^2} f_1(x, t) + \frac{L_r C_r(L_f + L_r)}{y_1} f_3(x, t) \end{aligned} \quad (8.208)$$

According to the above the system's control input can be also written as a function of the flat output and its derivatives. Thus one has

$$\begin{pmatrix} \dot{y}_1 \\ \ddot{y}_2 \end{pmatrix} = \Delta(y_1, y_2, \dot{y}_2) \begin{pmatrix} u_1 \\ u_2 \end{pmatrix} + \Phi(y_1, y_2, \dot{y}_2) \quad (8.209)$$

i.e.

$$\begin{pmatrix} u_1 \\ u_2 \end{pmatrix} = \Delta^{-1}(y_1, y_2, \dot{y}_2) \left(\begin{pmatrix} \dot{y}_1 \\ \ddot{y}_2 \end{pmatrix} - \Phi(y_1, y_2, \dot{y}_2) \right) \quad (8.210)$$

which means that provided that matrix $\Delta(y_1, y_2, \dot{y}_2)$ is invertible, the control input $u = [u_1, u_2]^T$ can be written as a function of the flat output and its derivatives. The non-singularity of matrix $\Delta(y_1, y_2, \dot{y}_2)$ depends on the determinant

$$\det(\Delta(y_1, y_2, \dot{y}_2)) = \frac{(I_r \dot{\omega}_f - C_f R)(L_f^2 y_1^2 m^2 - C_r(L_f + L_r)L_r L_f m + C_r I_z L_r)}{I_z R^2 y_1 m^2} \quad (8.211)$$

This determinant has non-zero values because it holds:

(i) $(I_r \dot{\omega}_f - C_f R) \neq 0$ since for the wheels rotational acceleration one has $\dot{\omega}_f < \frac{C_f R}{I_r}$, and also

(ii) $(L_f^2 y_1^2 m^2 - C_r(L_f + L_r)L_r L_f m + C_r I_z L_r) \neq 0$ when $I_z > L_f m$.

The differentially flat model of the vehicle can be also written in a canonical form after defining the new control input vector

$$\begin{pmatrix} v_1 \\ v_2 \end{pmatrix} = \Delta(y_1, y_2, \dot{y}_2) \begin{pmatrix} u_1 \\ u_2 \end{pmatrix} + \Phi(y_1, y_2, \dot{y}_2) \quad (8.212)$$

thus one obtains a MIMO system description into canonical form, i.e.

$$\begin{pmatrix} \dot{y}_1 \\ \dot{y}_2 \\ \ddot{y}_2 \end{pmatrix} = \begin{pmatrix} 0 & 0 & 0 \\ 0 & 0 & 1 \\ 0 & 0 & 0 \end{pmatrix} \begin{pmatrix} y_1 \\ y_2 \\ \dot{y}_2 \end{pmatrix} + \begin{pmatrix} 1 & 0 \\ 0 & 0 \\ 0 & 1 \end{pmatrix} \begin{pmatrix} v_1 \\ v_2 \end{pmatrix} \quad (8.213)$$

Once the vehicle's model is written in the differentially flat form the controller that enables tracking of a desirable trajectory defined by y_1^{ref} , y_2^{ref} , \dot{y}_2^{ref} is given by

$$\begin{aligned} v_1 &= \dot{y}_1^{ref} - k_{p1}(y_1 - y_1^{ref}) \\ v_2 &= \ddot{y}_2^{ref} - k_{d2}(\dot{y}_2 - \dot{y}_2^{ref}) - k_{p2}(y_2 - y_2^{ref}) \end{aligned} \quad (8.214)$$

and defining the error variables $e_1 = y_1 - y_1^{ref}$ and $e_2 = y_2 - y_2^{ref}$ one has the following tracking error dynamics for the closed-loop system

$$\begin{aligned} \dot{e}_1 + k_{p1}e_1 &= 0 \\ \ddot{e}_2 + k_{d2}\dot{e}_2 + k_{p2}e_2 &= 0 \end{aligned} \quad (8.215)$$

Therefore, the suitable selection of gains $k_{p_1 > 0}$ and $k_{p_2} > 0, k_{d_2} > 0$ assures the asymptotic elimination of the tracking errors, i.e. $\lim_{t \rightarrow \infty} e_1(t) = 0$ and $\lim_{t \rightarrow \infty} e_2(t) = 0$.

The control input that is finally applied for the vehicle's steering is given by

$$\begin{pmatrix} u_1 \\ u_2 \end{pmatrix} = \Delta(y_1, y_2, \dot{y}_2)^{-1} \left(\begin{pmatrix} v_1 \\ v_2 \end{pmatrix} - \Phi(y_1, y_2, \dot{y}_2) \right) \quad (8.216)$$

or equivalently

$$\begin{pmatrix} u_1 \\ u_2 \end{pmatrix} = \Delta(y_1, y_2, \dot{y}_2)^{-1} \left[\begin{pmatrix} \dot{y}_1^{ref} - k_{p_1}(y_1 - y_1^{ref}) \\ \dot{y}_2^{ref} - k_{d_2}(\dot{y}_2 - \dot{y}_2^{ref}) - k_{p_2}(y_2 - y_2^{ref}) \end{pmatrix} - \Phi(y_1, y_2, \dot{y}_2) \right] \quad (8.217)$$

The transformation of the vehicle's model into a canonical form, through the application of the differential flatness theory, facilitates not only the design of a feedback controller for trajectory tracking but also the design of filters for the estimation of the state vector of the vehicle out of a limited number of sensor measurements.

8.5.4 Estimation of Vehicle Disturbance Forces with the Derivative-Free Nonlinear Kalman Filter

8.5.4.1 State Estimation with the Derivative-Free Nonlinear Kalman Filter

It was shown that the initial nonlinear model of the vehicle can be written in the MIMO canonical form

$$\begin{pmatrix} \dot{y}_1 \\ \dot{y}_2 \\ \ddot{y}_2 \end{pmatrix} = \begin{pmatrix} 0 & 0 & 0 \\ 0 & 0 & 1 \\ 0 & 0 & 0 \end{pmatrix} \begin{pmatrix} y_1 \\ y_2 \\ \dot{y}_2 \end{pmatrix} + \begin{pmatrix} 1 & 0 \\ 0 & 0 \\ 0 & 1 \end{pmatrix} \begin{pmatrix} v_1 \\ v_2 \end{pmatrix} \quad (8.218)$$

Thus one has a MIMO linear model of the form

$$\begin{aligned} \dot{y}_f &= A_f y_f + B_f v \\ z_f &= C_f y_f \end{aligned} \quad (8.219)$$

where $y_f = [y_1, y_2, \dot{y}_2]^T$ and matrices A_f, B_f, C_f are in the MIMO canonical form

$$A_f = \begin{pmatrix} 0 & 0 & 0 \\ 0 & 0 & 1 \\ 0 & 0 & 0 \end{pmatrix} \quad B_f = \begin{pmatrix} 1 & 0 \\ 0 & 0 \\ 0 & 1 \end{pmatrix} \quad C_f^T = \begin{pmatrix} 1 & 0 \\ 0 & 1 \\ 0 & 0 \end{pmatrix} \quad (8.220)$$

where the measurable variables $y_1 = V_x$, $y_2 = L_f m V_y - I_z \dot{\psi}$ are associated with the linear velocity of the vehicle V_x , V_y and with its angular velocity $\dot{\psi}$. For the aforementioned model, and after carrying out discretization of matrices A_f , B_f and C_f with common discretization methods one can perform linear Kalman filtering using Eqs. (8.229) and (8.230). This is *Derivative-free nonlinear Kalman filtering* for the model of the vehicle which, unlike EKF, is performed without the need to compute Jacobian matrices and does not introduce numerical errors.

8.5.4.2 Kalman Filter-Based Estimation of Disturbances

It is assumed that disturbance forces affect the nonlinear vehicle model along its longitudinal and transversal axis and that disturbance torques affect the nonlinear vehicle model on its z axis. For example disturbance forces can be due to a force vector that coincides with the vehicle's longitudinal axis (e.g. traction disturbance) or disturbance torques can be due to unmodelled lateral forces. These disturbance forces and torques change dynamically in time and their dynamics is given by

$$\begin{aligned}\tilde{d}_x &= f_{d_x}(V_x, V_y, \dot{\psi}) \\ \tilde{d}_y &= f_{d_y}(V_x, V_y, \dot{\psi}) \\ \tilde{d}_\psi &= T_{d_\psi}(V_x, V_y, \dot{\psi})\end{aligned}\quad (8.221)$$

Since the state variables of the vehicle's dynamic model can be written as functions of the flat outputs y_1 and y_2 and of their derivatives it also holds

$$\begin{aligned}\tilde{d}_x^{(i)} &= f_{d_x}^{(i)}(y_1, y_2, \dot{y}_2) \\ \tilde{d}_y^{(i)} &= f_{d_y}^{(i)}(y_1, y_2, \dot{y}_2) \\ \tilde{d}_\psi^{(i)} &= T_{d_\psi}^{(i)}(y_1, y_2, \dot{y}_2)\end{aligned}\quad (8.222)$$

where $i = 1, 2, \dots$ stands for the i th order derivative of the disturbance variable.

Considering the effect of disturbance functions on the initial nonlinear state equation of the vehicle and the linear relation between the initial state variables $[V_x, V_y]$ and the state variables of the flat system description $[y_1, y_2]$ one has the appearance of the disturbance terms in the canonical form model of Eq. (8.213)

$$\begin{pmatrix} \dot{y}_1 \\ \dot{y}_2 \\ \dot{y}_2 \end{pmatrix} = \begin{pmatrix} 0 & 0 & 0 \\ 0 & 0 & 1 \\ 0 & 0 & 0 \end{pmatrix} \begin{pmatrix} y_1 \\ y_2 \\ \dot{y}_2 \end{pmatrix} + \begin{pmatrix} 1 & 0 \\ 0 & 0 \\ 0 & 1 \end{pmatrix} \begin{pmatrix} v_1 \\ v_2 \end{pmatrix} + \begin{pmatrix} \frac{1}{m} \tilde{d}_x \\ 0 \\ L_f \dot{\tilde{d}}_y - \dot{\tilde{d}}_\psi \end{pmatrix}\quad (8.223)$$

Next, the state vector of the model of Eq. (8.223) is extended to include as additional state variables the disturbance forces \tilde{d}_x , \tilde{d}_y and \tilde{d}_ψ . Then, in the new state-space

description one has $z_1 = y_1, z_2 = y_2, z_3 = \dot{y}_2, z_4 = \tilde{f}_a = \frac{1}{m}\tilde{d}_x, z_5 = \dot{\tilde{f}}_a, z_6 = \dot{\tilde{f}}_b = L_f\dot{\tilde{d}}_y - \dot{\tilde{d}}_\psi, z_7 = \ddot{\tilde{f}}_b$, which takes the form of matrix equations

$$\dot{z} = \tilde{A} \cdot z + \tilde{B} \cdot \tilde{v} \quad (8.224)$$

where the control input is

$$\begin{aligned} \tilde{v} &= \left(v_1 \ v_2 \ \frac{1}{m}\ddot{\tilde{d}}_x \ L_f\ddot{\tilde{d}}_y^{(3)} - \ddot{\tilde{d}}_\psi^{(3)} \right)^T \text{ or} \\ \tilde{v} &= \left(v_1 \ v_2 \ \ddot{\tilde{f}}_a \ \ddot{\tilde{f}}_b^{(3)} \right)^T \end{aligned} \quad (8.225)$$

with

$$\tilde{A} = \begin{pmatrix} 0 & 0 & 0 & 1 & 0 & 0 & 0 \\ 0 & 0 & 1 & 0 & 0 & 0 & 0 \\ 0 & 0 & 0 & 0 & 0 & 1 & 0 \\ 0 & 0 & 0 & 0 & 1 & 0 & 0 \\ 0 & 0 & 0 & 0 & 0 & 0 & 0 \\ 0 & 0 & 0 & 0 & 0 & 0 & 1 \\ 0 & 0 & 0 & 0 & 0 & 0 & 0 \end{pmatrix} \quad \tilde{B} = \begin{pmatrix} 1 & 0 & 0 & 0 \\ 0 & 0 & 0 & 0 \\ 0 & 1 & 0 & 0 \\ 0 & 0 & 0 & 0 \\ 0 & 0 & 1 & 0 \\ 0 & 0 & 0 & 0 \\ 0 & 0 & 0 & 1 \end{pmatrix} \quad \tilde{C}^T = \begin{pmatrix} 1 & 0 \\ 0 & 1 \\ 0 & 0 \\ 0 & 0 \\ 0 & 0 \\ 0 & 0 \\ 0 & 0 \end{pmatrix} \quad (8.226)$$

where the measurable state variables are z_1 and z_2 . Since the dynamics of the disturbance terms \tilde{f}_a and \tilde{f}_b are taken to be unknown in the design of the associated disturbances' estimator one has the following dynamics:

$$\dot{z}_o = \tilde{A}_o \cdot z + \tilde{B}_o \cdot \tilde{v} + K(C_o z - C_o \hat{z}) \quad (8.227)$$

where $K \in R^{7 \times 2}$ is the state estimator's gain and

$$\tilde{A}_o = \begin{pmatrix} 0 & 0 & 0 & 1 & 0 & 0 & 0 \\ 0 & 0 & 1 & 0 & 0 & 0 & 0 \\ 0 & 0 & 0 & 0 & 0 & 1 & 0 \\ 0 & 0 & 0 & 0 & 1 & 0 & 0 \\ 0 & 0 & 0 & 0 & 0 & 0 & 0 \\ 0 & 0 & 0 & 0 & 0 & 0 & 1 \\ 0 & 0 & 0 & 0 & 0 & 0 & 0 \end{pmatrix} \quad \tilde{B}_o = \begin{pmatrix} 1 & 0 & 0 & 0 \\ 0 & 0 & 0 & 0 \\ 0 & 1 & 0 & 0 \\ 0 & 0 & 0 & 0 \\ 0 & 0 & 0 & 0 \\ 0 & 0 & 0 & 0 \\ 0 & 0 & 0 & 0 \end{pmatrix} \quad \tilde{C}_o^T = \begin{pmatrix} 1 & 0 \\ 0 & 1 \\ 0 & 0 \\ 0 & 0 \\ 0 & 0 \\ 0 & 0 \\ 0 & 0 \end{pmatrix} \quad (8.228)$$

Defining as \tilde{A}_d , \tilde{B}_d , and \tilde{C}_d , the discrete-time equivalents of matrices \tilde{A}_o , \tilde{B}_o and \tilde{C}_o respectively, a Derivative-free nonlinear Kalman Filter can be designed for the aforementioned representation of the system dynamics [438, 459]. The associated Kalman Filter-based disturbance estimator is given by

measurement update:

$$\begin{aligned} K(k) &= P^-(k) \tilde{C}_d^T [\tilde{C}_d P^-(k) \tilde{C}_d^T + R]^{-1} \\ \hat{x}(k) &= \hat{x}^-(k) + K(k) [z(k) - \tilde{C}_d \hat{x}^-(k)] \\ P(k) &= P^-(k) - K(k) \tilde{C}_d P^-(k) \end{aligned} \quad (8.229)$$

time update:

$$\begin{aligned} P^-(k+1) &= \tilde{A}_d(k) P(k) \tilde{A}_d^T(k) + Q(k) \\ \hat{x}^-(k+1) &= \tilde{A}_d(k) \hat{x}(k) + \tilde{B}_d(k) \tilde{v}(k) \end{aligned} \quad (8.230)$$

To compensate for the effects of the disturbance forces it suffices to use in the control loop the modified control input vector

$$v = \begin{pmatrix} v_1 - \hat{\tilde{f}}_a \\ v_2 - \hat{\tilde{f}}_b \end{pmatrix} \text{ or } v = \begin{pmatrix} v_1 - \hat{\tilde{z}}_4 \\ v_2 - \hat{\tilde{z}}_6 \end{pmatrix} \quad (8.231)$$

8.5.5 Simulation Tests

To evaluate for the performance of the proposed nonlinear control scheme, as well as about the performance of the Kalman Filter-based disturbances estimator simulation experiments have been carried out. Different velocity setpoints had been assumed (for velocity along the horizontal and vertical axis of the inertial reference frame, as well as for angular velocity round the vehicle's z axis). Moreover, different disturbances forces and torques have been assumed to affect the vehicles' dynamic model. Using the representation of the vehicle's dynamics given in Eq. (8.223) two generalized disturbance forces/torques have been considered: the first denoted as \tilde{f}_a was associated with state variable y_1 , while the second one denoted as \tilde{f}_b was associated with the state variable y_2 . It was also assumed that the change in time of the generalized forces and torques was defined by the second derivative of the associated variable, i.e. $\ddot{\tilde{f}}_a$ and $\ddot{\tilde{f}}_b$. The disturbances dynamics was completely unknown to the controller and their identification was performed in real time by the disturbance estimator. The control loop used in the vehicle's autonomous navigation is given in Fig. 8.35.

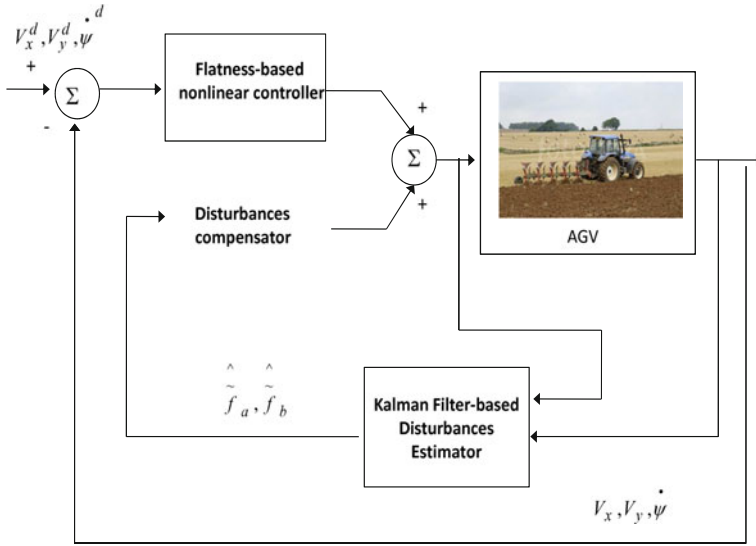


Fig. 8.35 Control loop for the autonomous vehicle comprising a flatness-based nonlinear controller and a Kalman Filter-based disturbances estimator

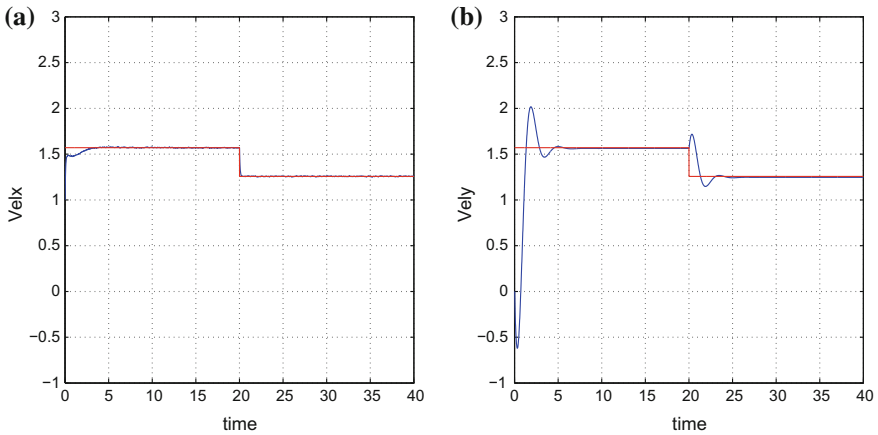


Fig. 8.36 Vehicle control under disturbances profile 1: **a** Convergence of x-axis velocity V_x (blue line) to the desirable setpoint (red line), **b** Convergence of the y-axis velocity V_y (blue line) to the desirable setpoint (red line)

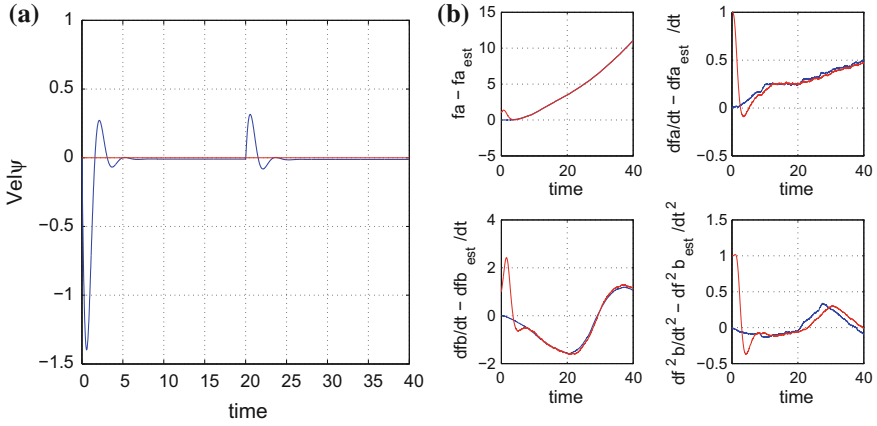


Fig. 8.37 Vehicle control under disturbances profile 1: **a** Convergence of yaw rate $\dot{\psi}$ (blue line) to the desirable setpoint (red line), **b** Estimation of the disturbance terms and of their rate of change (red line) and the associated real values (blue line)

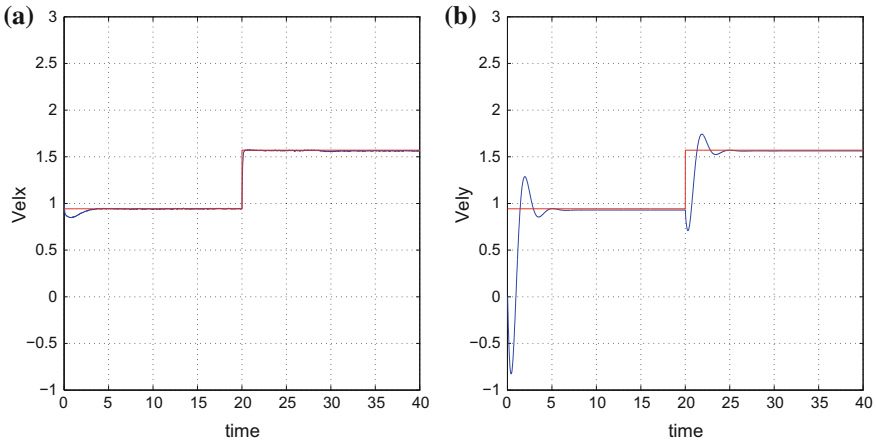


Fig. 8.38 Vehicle control under disturbances profile 2: **a** Convergence of x-axis velocity V_x (blue line) to the desirable setpoint (red line), **b** Convergence of the y-axis velocity V_y (blue line) to the desirable setpoint (red line)

The measurable variables used by the control and disturbances’ estimation scheme were the vehicle’s velocity V_x along the longitudinal axis, the vehicle’s velocity V_y along the lateral axis and the vehicle’s yaw rate $\dot{\psi}$. The first two variables can be obtained with the use of onboard accelerometers while the third variable can be

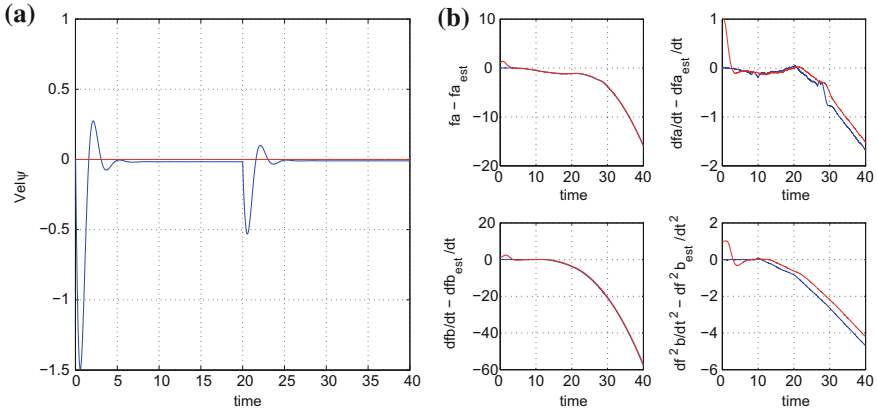


Fig. 8.39 Vehicle control under disturbances profile 2: **a** Convergence of yaw rate $\dot{\psi}$ (blue line) to the desirable setpoint (red line), **b** Estimation of the disturbance terms and of their rate of change (red line) and the associated real values (blue line)

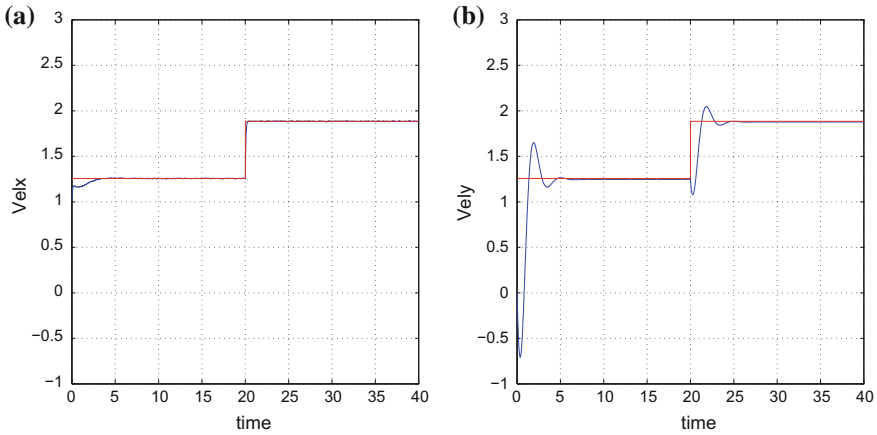


Fig. 8.40 Vehicle control under disturbances profile 3: **a** Convergence of x-axis velocity V_x (blue line) to the desirable setpoint (red line), **b** Convergence of the y-axis velocity V_y to the desirable setpoint (blue line) and the associated real values (red line)

obtained with the use of a gyrocompass. The longitudinal axis of the vehicle is denoted as x -axis, while the lateral axis of the vehicle is denoted as y -axis. As it can be seen in Figs. 8.36, 8.37, 8.38, 8.39, 8.40, 8.41, 8.42 and 8.43 the proposed nonlinear controller achieved accurate tracking of velocity setpoints. Moreover, the efficient

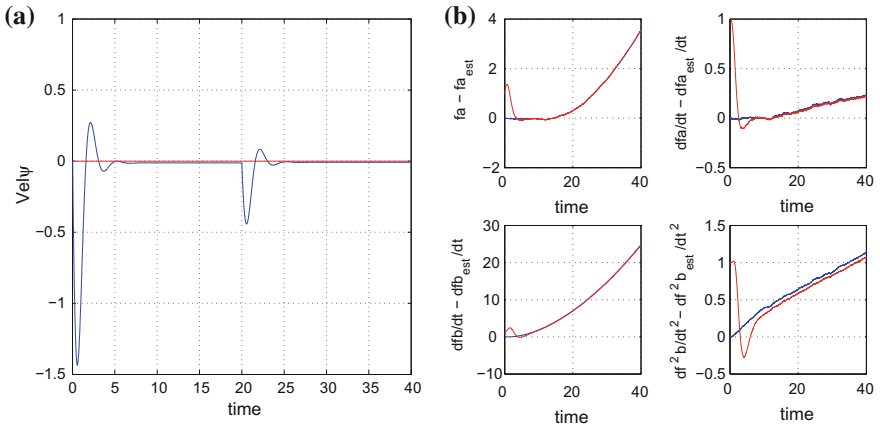


Fig. 8.41 Vehicle control under disturbances profile 3: **a** Convergence of yaw rate $\dot{\psi}$ (blue line) to the desirable setpoint (red line), **b** Estimation of the disturbance terms and of their rate of change (red line) and the associated real values (blue line)

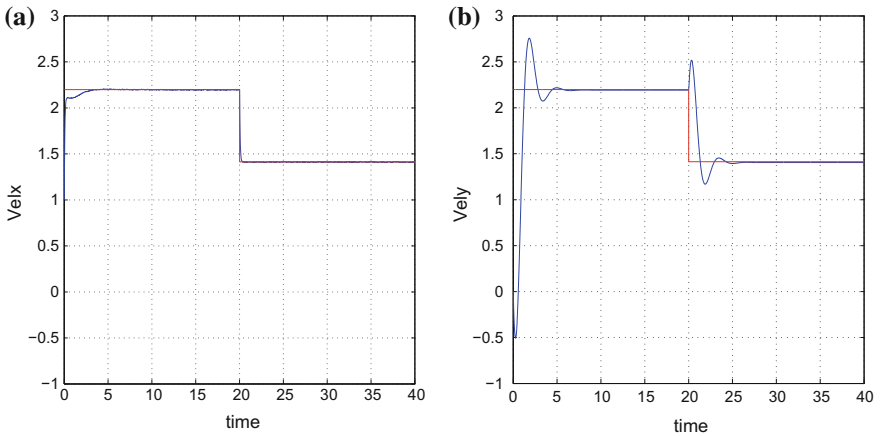


Fig. 8.42 Vehicle control under disturbances profile 4: **a** Convergence of x-axis velocity V_x (blue line) to the desirable setpoint (red line), **b** Convergence of the y-axis velocity V_y (blue line) to the desirable setpoint (red line)

estimation of disturbance forces and torques that was achieved by the Kalman Filter-based disturbance estimator enabled their compensation through the inclusion of an additional control term in the loop.

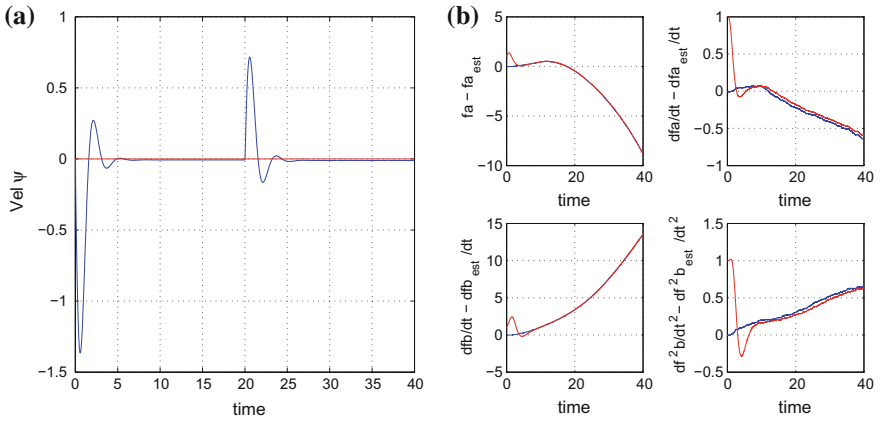


Fig. 8.43 Vehicle control under disturbances profile 4: **a** Convergence of yaw rate $\dot{\psi}$ (blue line) to the desirable setpoint (red line), **b** Estimation of the disturbance terms and of their rate of change (red line) and the associated real values (blue line)